INFORMATION TO USERS

This manuscript has been reproduced from the microfilm master. UMI films the text directly from the original or copy submitted. Thus, some thesis and dissertation copies are in typewriter face, while others may be from any type of computer printer.

The quality of this reproduction is dependent upon the quality of the copy submitted. Broken or indistinct print, colored or poor quality illustrations and photographs, print bleedthrough, substandard margins, and improper alignment can adversely affect reproduction.

In the unlikely event that the author did not send UMI a complete manuscript and there are missing pages, these will be noted. Also, if unauthorized copyright material had to be removed, a note will indicate the deletion.

Oversize materials (e.g., maps, drawings, charts) are reproduced by sectioning the original, beginning at the upper left-hand corner and continuing from left to right in equal sections with small overlaps. Each original is also photographed in one exposure and is included in reduced form at the back of the book.

Photographs included in the original manuscript have been reproduced xerographically in this copy. Higher quality 6" x 9" black and white photographic prints are available for any photographs or illustrations appearing in this copy for an additional charge. Contact UMI directly to order.
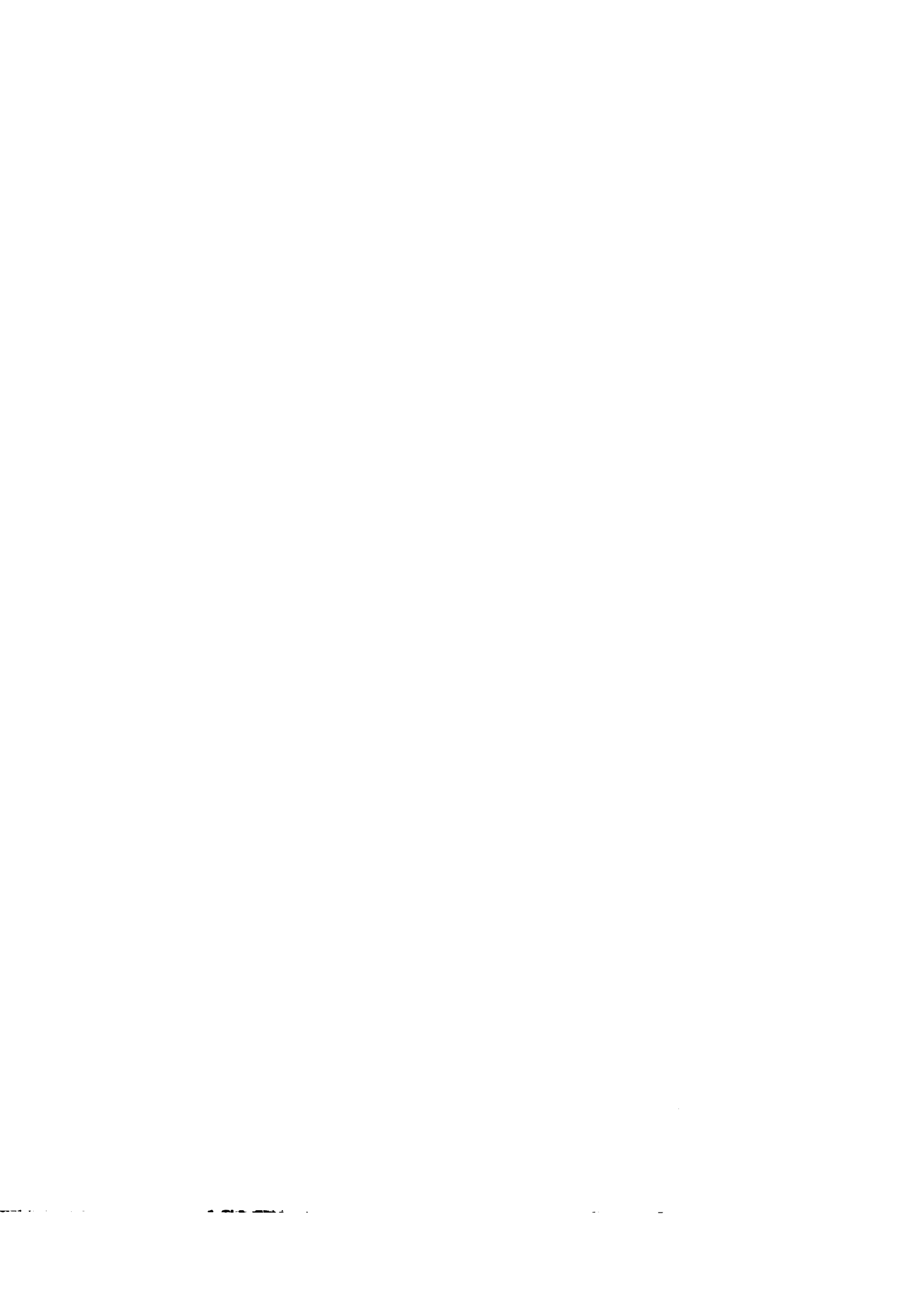
Structural and kinematic evolution of the Badwater Turtleback, Death Valley, California

Miller, Martin Gregg, Ph.D.

University of Washington, 1992

Structural and Kinematic Evolution of the Badwater Turtleback,
Death Valley, California

by

Martin Gregg Miller

A dissertation submitted in partial fulfillment
of the requirements for the degree of

Doctor of Philosophy

University of Washington

1992

Approved by _____
(Chairperson of Supervisory Committee)

Program Authorized
to Offer Degree _____ Department of Geological Sciences _____

Date _____ December 14, 1992 _____

In presenting this dissertation in partial fulfillment of the requirements for the Doctoral degree at the University of Washington, I agree that the Library shall make its copies freely available for inspection. I further agree that extensive copying of this dissertation is allowable only for scholarly purposes, consistent with "fair use" as prescribed in the U.S. Copyright Law. Requests for copying or reproduction of this dissertation may be referred to University Microfilms, 1490 Eisenhower Place, P.O. Box 975, Ann Arbor, MI 48106, to whom the author has granted "the right to reproduce and sell (a) copies of the manuscript in microform and/or (b) printed copies of the manuscript made from microform."

Signature _Matin Hiller_

Date _December 14, 1992_

University of Washington

Abstract

Structural and Kinematic Evolution of the Badwater Turtleback,
Death Valley, California

by Martin Gregg Miller

Chairperson of the Supervisory Committee: Professor Darrel S. Cowan
Department of Geological Sciences

The Badwater Turtleback is a small (~15 km^2) metamorphic core complex in Death Valley, California. It consists of an antiformal, mylonitic footwall and a brittlely faulted hangingwall separated by a moderate- to low-angle normal fault system. Much or all of its structural evolution can be confidently tied to late Tertiary extension. This evolution took place in two stages. The first stage involved the continuous, ductile to brittle evolution of the footwall as a ductile shear zone. Although this shear zone was linked with an extensional fault zone at the surface, it predated slip on the present-day Turtleback fault system. The second stage began with the formation of the present-day Turtleback fault system and probably continues today. During both stages, the fault system and footwall rotated eastwards and was structurally distinct from the Copper Canyon and Mormon Point turtlebacks farther south. Gravitational sliding reactivated some of the fault surfaces after rotation to low angles.

Each of the four principal rock types of the footwall --quartzofeldspathic gneiss, pegmatite, and dolomite and calcite marble-- displays a specific structural sequence indicative of top-to-the northwest transport that began with mylonitization and ended with brittle faulting. The rocks also exhibit cross-cutting relations which indicate that they ceased deforming ductilely in the sequence: pegmatite, dolomite marble, quartzofeldspathic gneiss, calcite marble. Initiation of earliest brittle faults occurred during ductile deformation of calcite marble in response to strain incompatibilites between the actively deforming calcite marble and the brittle footwall.

The overall N20°E-trending, antiformal geometry of the footwall suggests that the upper crustal fault which brought these rocks to the surface also had an antiformal geometry which "rolled back" in a direction opposite that of hangingwall transport. This geometry resembles that predicted by models for isostatic flexure during extensional unloading of the footwall. Because the Copper Canyon and Mormon Point turtlebacks show similar antiformal geometries, the three turtlebacks probably experienced similar histories as individual extensional systems.

Formation and evolution of the present-day Turtleback fault system must mark a second stage in the evolution of the Badwater Turtleback because the fault system cuts volcanic rocks which lie depositionally on the mylonitic footwall. The fault system consists of three distinct, originally planar fault surfaces which increase in dip, and decrease in age towards the west. This geometry implies that each fault initially formed at a higher angle, but rotated to its present lower angle with ongoing extension. The initially planar nature of the faults, plus their cross-cutting relations, are more consistent with domino-style rotation than rotation from isostatic flexure.

TABLE OF CONTENTS

LIST OF FIGURES

ACKNOWLEDGMENTS

INTRODUCTION TO THE BADWATER TURTLEBACK

Metamorphic core complexes of the western Cordillera display a wide range of Tertiary extensional structures which formed at various levels in the crust. These structures are generally well preserved because they formed within rising and cooling footwalls and have not been overprinted by later periods of deformation. Consequently, field-based research in metamorphic core complexes can yield insights into processes of crustal extension and fault- and shear-zone formation.

The Badwater Turtleback in Death Valley National Monument, southeastern California, displays three essential features of metamorphic core complexes. In ascending structural order, these features include (1) a mylonitic, antiformal metamorphic footwall, (2) a brittle, low-angle normal fault system, (3) a brittlely faulted hanging wall. The major conclusion from this study is that, as in other metamorphic core complexes, these three features formed during late Tertiary crustal extension and that the structural evolution of the footwall reflects its progressive unroofing along both a pre-existing, and the present-day, Turtleback normal-fault system.

The footwall, brittle fault system, and hanging wall of the Badwater Turtleback are unusually well exposed because of the extreme aridity and rugged topography of Death Valley. Because the footwall also contains a wide variety of rock types, it is mappable at detailed scales of greater than 1:6000. This combination of rock exposure and lithologic diversity makes the Badwater Turtleback an outstanding place to observe structural processes in an extensional environment.

Location and Access

The Badwater Turtleback makes up much of the western front of the northern Black Mountains on the east side of Death Valley (Figs. 1, 2). Its boundaries, as defined by the distribution of footwall mylonitic rocks, extend from Natural Bridge Canyon at its north end, southward to the canyon immediately below Dantes View. Two other turtlebacks, the Copper Canyon and Mormon Point turtlebacks, lie about 10 km and 18 km south respectively, of the Badwater Turtleback. These other turtlebacks also occupy part of the Black Mountains range front, and each consists of a metamorphic core separated from brittlely faulted rocks by a low-angle normal fault.

All locations on the Badwater Turtleback can be reached by day hikes. The numerous canyons along the range front which display exposures of the Turtleback fault and lower plate mylonites are easily reached by short hikes from the Badwater road. Passage up most of these canyons, however, becomes blocked by dryfalls near their bottoms. Approach to all other localities therefore requires moderate scrambling efforts on the steep mountain front. Access to locations at elevations of 3000' or greater is easiest from Dantes View which sits at an elevation of 5500' on the crest of the Black Mountains.

Previous Work

Historically, most early work on the three turtlebacks recognized, and tried to explain, the close geometrical and spatial relationship between the antiformal cores and brittle fault surfaces. Little of this work, however, addressed the extreme deformation within the cores because it was thought to reflect a much earlier period of deformation. This view changed during the early to mid 1980's. Geochronologic and structural work elsewhere in the Basin and Range, and a tectonic reconstruction for the Death
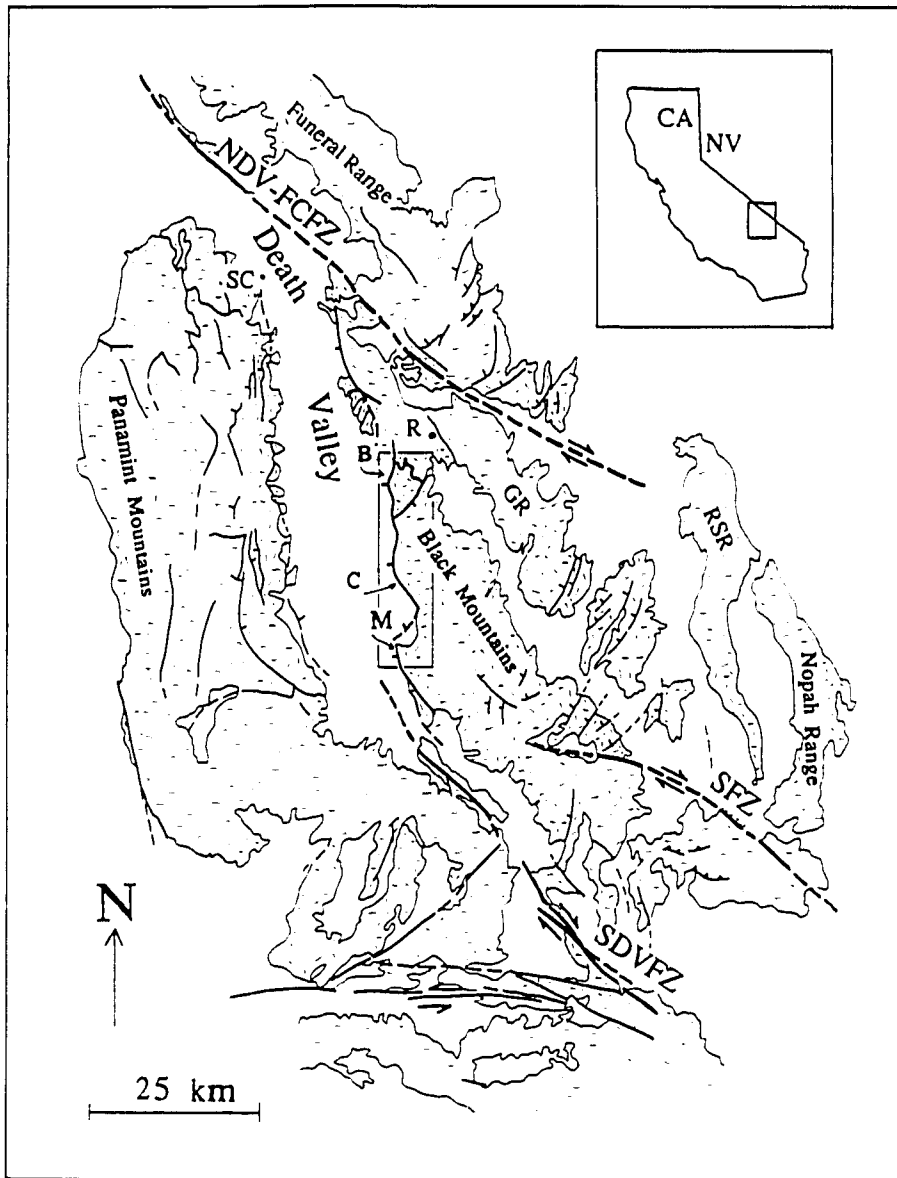
Figure 1: Fault map of the Death Valley region, modified after Wright, 1974. Inset shows location of figure 2. Abbreviations are as follows: NDV-FCFZ, Northern Death Valley-Furnace Creek fault zone; SFZ: Sheephead fault zone; SDVFZ, Southern Death Valley fault zone; GR, Greenwater Range; RSR, Resting Spring Range; SC, Salt Creek; R, Ryan; B, Badwater Turtleback; C, Copper Canyon Turtleback; M, Mormon Point Turtleback.
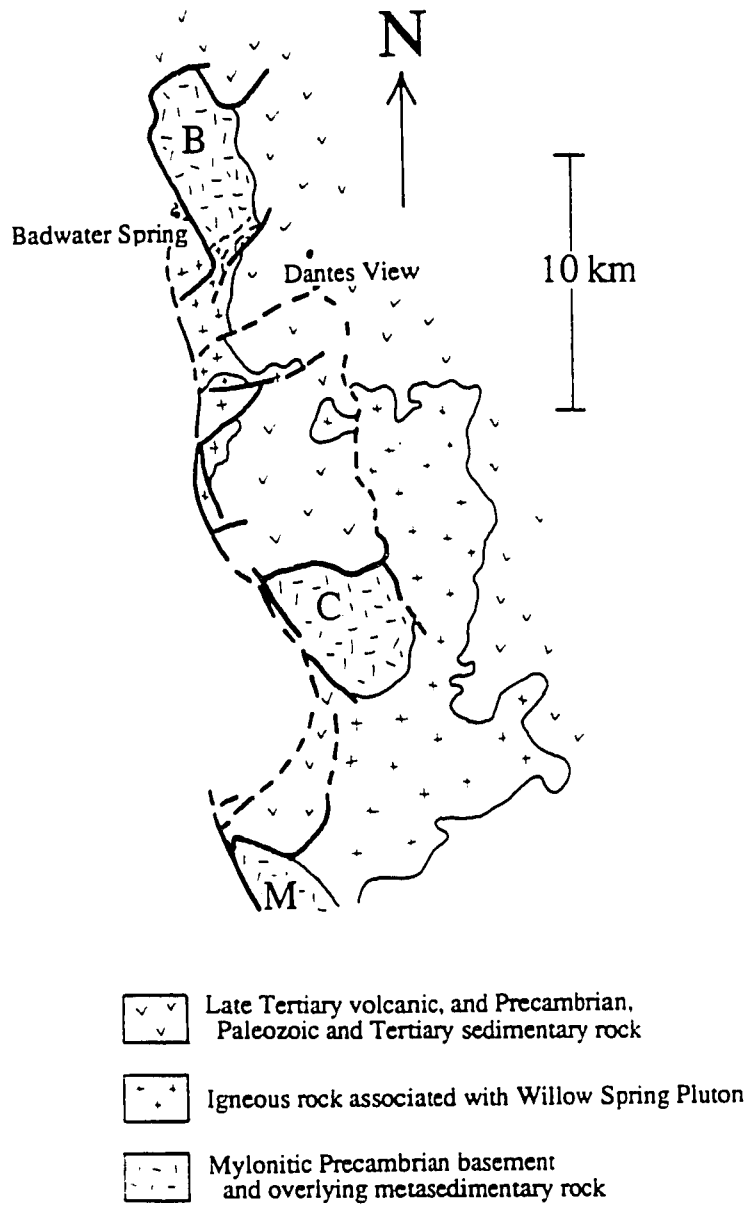
Figure 2: Generalized map of the Black Mountains. Distribution of rock types and faults taken from Drewes (1963) and personal mapping. Abbreviations are as follows: B, Badwater Turtleback; C, Copper Canyon Turtleback; M, Mormon Point Turtleback.

Valley region by Stewart (1983) both implied that footwall deformation on the Badwater Turtleback may be directly linked to the origin of the bounding fault system.

Curry (1938), the first ranger-naturalist of Death Valley National Monument, named the turtlebacks because their antiformal shapes resembled the backs of turtles. He mapped their locations and described the near-parallelism of the bounding faults to the antiformal cores. Curry (1954) suggested that the turtleback faults were thrust faults and that their relation to the core was a product of northeast-southwest folding which postdated slip on the fault.

Drewes (1963) mapped and described rocks in the Funeral Peak Quadrangle. This quadrangle includes the southern edge of the Badwater Turtleback and all of the Copper Canyon and Mormon Point turtlebacks. Based primarily on his work on the southern turtlebacks, Drewes (1959) proposed a gravitational origin for the three turtleback faults. By his model, the turtleback faults conformed to the antiformal cores because sliding occurred along the top of the previously folded surfaces.

Wright et al. (1974) were the first to recognize that the turtleback faults were products of Basin and Range extension but they too, mainained a separate origin for the metamorphic core. They noted that a carapace of carbonate rocks, between the fault surface and underlying basement, defined the actual turtleback antiforms. By their model, the carbonates received their forms during some earlier period of deformation; during the late Tertiary extension, they served as weak zones to guide the propagation of the brittle turtleback fault surfaces.

Elsewhere in the Basin and Range, geochronologic and structural work during the late 1970's and early 1980's led to a genetic model for metamorphic core complexes. Rehrig and Reynolds (1980), for example, found that footwall mylonitic fabrics in the Catalina Mountains of Arizona formed during the Tertiary at about the

same time as the bounding fault surface. Davis (1980) described a structural development which tied the mylonitic deformation to the brittle faulting. The resulting model therefore explained footwall mylonites as mid-crustal continuations of the brittle fault surfaces. Wernicke (1981) took this model a step further by suggesting that the brittle faults penetrated the entire crust at low angles. He noted that because the bounding fault surfaces typically dipped at angles of less than 30°, the presence of mylonitic rocks in their footwalls implied tens of kilometers of hangingwall transport on those extensional systems.

In the Death Valley region, Stewart (1983) sparked the ongoing debate regarding the magnitude and style of extension in the region by proposing 80 km of northwest transport of the Panamint Range from the top of the Black Mountains and adjacent to the Nopah Range (see figure 1). According to his reconstruction, much of this transport took place along the turtlebacks. His suggestion was the first to suggest large-magnitude extension in Death Valley, and by implication, to link deformation of the turtleback footwalls to the actual fault surfaces.

Other workers followed up on Stewart's 1983 proposal. Hodges et al. (1987) found kinematic evidence for a gradation from mylonitic to brittle deformation at Tucki Mountain, and Hamilton (1986) and Wernicke (1986) proposed various reconstructions which also required large-magnitude extension. The actual timing of mylonitic deformation anywhere in Death Valley, however, remained unknown until 1989 when Asmerom et. al, reported an 11.6 Ma U-Pb age for zircon in dioritic rocks which intruded during deformation in the Black Mountains. This age clinched the extensional nature of at least some of the mylonitic deformation in the footwalls of the Copper Canyon and Mormon Point turtlebacks and strongly suggested that similar fabrics in the Badwater Turtleback formed at approximately the same time. Miller

(1990) provided structural evidence that the mylonites in the Badwater Turtleback
formed during late Tertiary extension.

Tectonic Setting of the Black Mountains Block

The Black Mountains crustal block, as defined by Wright et al. (1987) consists
of the Black Mountains and Greenwater Range (Fig. 1). The boundaries of this block
are defined by three right-lateral fault zones: the Northern Death Valley-Furnace Creek
fault zone to the north, the southern Death Valley fault zone to the south, and the
Sheephead fault, which divides the block into northern and southern parts. For the
most part, the Black Mountains block consists of upper Tertiary plutonic and volcanic
rocks and associated sedimentary rocks. Upper Proterozoic and Paleozoic rocks,
which make up most of all the surrounding mountain ranges, crop out in only a few
localities in Gold Valley, in the Virgin Spring Chaos (Wright and Troxel, 1984) in
Jubilee Wash, and in scattered exposures along the front of the range. These
exposures are significant, however, because they contain many elements of the Upper
Proterozoic and Lower Paleozoic stratigraphy and are highly attenuated. Therefore,
these rocks attest to the large amount of tectonic denudation which must have occurred
in the Black Mountains since the onset of Tertiary extension. Middle Proterozoic
metamorphic rocks in the northern Black Mountains block are exposed in the cores of
the three turtlebacks and in the footwall of the Amargosa fault near Jubilee Pass.
South of the Sheephead fault, the southern Black Mountains consist of dominantly
Middle Proterozoic metamorphic and Late Proterozoic and Paleozoic sedimentary
rocks.

Much of the uncertainty regarding the age and significance of metamorphic
structures in the turtlebacks stems from an uncertain structural history. Besides late

Tertiary extensional deformation, the Black Mountains block probably experienced at least three earlier, poorly understood, periods of deformation. These periods occurred during the Middle Proterozoic, Late Proterozoic, and Mesozoic. The Black Mountains, however, contain few Pre-Tertiary rocks, all of which show either an extreme or unknown amount of late Tertiary deformation. Therefore, many of the details regarding pre-Tertiary deformation come from adjacent ranges.

Timing of Extension in Death Valley

Onset of late Tertiary extension in the Death Valley region began just prior to 13.9 Ma, the age of a tuff layer near the base of the Artist Drive Formation (Cemen et. al, 1982). This period of extension formed the Furnace Creek basin, coincided with voluminous magmatism in the Black Mountains, and predated opening of modern-day Death Valley. The Furnace Creek basin extended parallel to the Furnace Creek fault from south of Ryan in the Greenwater Range to Salt Creek, on the floor of modern Death Valley (Fig. 1). As the Furnace Creek basin contains a relatively continuous stratigraphic section deposited from about 14 Ma to about 4 Ma, it records the uplift history of the surrounding ranges (Cemen et al., 1985). The section consists of the Artist Drive Formation and the overlying Furnace Creek Formation. A prominent angular unconformity at 4 Ma in upper Furnace Creek Wash between the Furnace Creek Formation and overlying, undeformed basalt flows of the Funeral Formation marks the end of the Furnace Creek basin and a shift of extensional activity into modern-day Death Valley.

The timing of opening of modern-day Death Valley is poorly constrained. Range-bounding faults, however, cut the Furnace Creek Formation and locally appear responsible for deposition of Pliocene to Pleistocene alluvial fan deposits (Hunt and

Mabey, 1966). These sediments, which record extension within Death Valley are exposed locally along the edge of the valley and for the most part, have not been studied in great detail. Cichanski (1990), however, described three undated units in uplifted alluvial fan deposits along the front of the Badwater Turtleback. One of these units was deposited prior to exposure of the metamorphic core.

Because early extension in the Death Valley region formed the Furnace Creek basin and late extension formed the modern basin, it is tempting to treat extension in the Death Valley region as occurring in two temporally distinct phases. Such a distinction, however, may be misleading because there may be considerable overlap of extensional activity between the two areas. Cemen et. al (1985), for example, noted that activity in the northern part of the Furnace Creek Basin continued after it had stopped in the southern part. Furthermore, both Hunt and Mabey (1966) and Cemen et al. (1985) argued for some uplift of the Black Mountains concurrently with deposition of the Furnace Creek Formation. Ellis and Trexler (1991), treated 6-7 Ma deposition and later excisement of the Copper Canyon Formation, on the west side of the Black Mountains, as the product of an uninterrupted extensional process.

Extension prior to the late Tertiary may also have affected the Death Valley region. Cemen et al., (1985) described pre-25 Ma alluvial fan deposits near Bat Mountain in the southern Funeral Range. Some of these rocks overlie normal faults. Reynolds (1969) described the Oligocene Titus Canyon Formation and suggested that it represented a period of mountain building. On the basis of Ar work in the northern Funeral Range, Hodges and Walker (1990) found evidence for rapid uplift at the end of the Cretaceous. More recently, Applegate et al. (1992) suggested that some extensional shear zones in the northern Funeral Range formed prior to 70 Ma. They

reported U-Pb ages of 72 and 70 Ma on zircon from pegmatite dikes which intruded pre- or syn-kinematically and post-kinematically respectively with the shear zones.

Magnitude and Style of late Tertiary extension in the Death Valley region

Currently, there are two opposing viewpoints regarding the magnitude and style of extension in the Death Valley region. One viewpoint holds that the region experienced 400-500% extension prior to 6 or 7 Ma (examples include Stewart, 1983; Hamilton, 1986; Wernicke et. al, 1988). The other argues for large amounts of extension within the Black Mountains block, but only a moderate amount of extension in the surrounding ranges (examples include Wright et al., 1987; Wright and eight others, 1991). Much of the debate centers on three things: the near absence of Proterozoic and Paleozoic sedimentary rocks from the Black Mountains, the nature of the turtleback and Amargosa faults, and the nature of the large strike-slip faults which bound Death Valley to the northeast and southwest.

Proponents of large-scale (400-500%) regional extension argue that the sedimentary rocks were tectonically removed from the Black Mountains along a continuous detachment fault system prior to 6 or 7 Ma and transported northwest to the Panamint Mountains (Stewart, 1983; Hamilton, 1986; Wernicke et. al, 1988). These workers also hold that, during this time, strike-slip faulting was confined to the upper crust. Strike-slip faulting therefore played a passive role, primarily as a mechanism to accommodate differential extension. By their models, the Northern Death Valley-Furnace Creek fault zone provided the upturned northeastern edge of the detachment system; the fault zone terminated abruptly at the breakaway zone in the Amargosa Valley. At approximately 4 Ma, the detachment system was replaced by the modern, crustal penetrating strike-slip system.

Alternatively, Wright et al. (1987) and more recently Wright and eight others
(1991) attributed late Tertiary magmatism in the Black Mountains and Greenwater
Range to their position within regional-scale dilational jogs involving the Northern
Death Valley-Furnace Creek fault zone, the Sheephead fault zone, and the southern
Death Valley fault zone (Fig. 1). Their model therefore calls for large-magnitude
extension within the Black Mountains block only; the areas outside of the dilational
jogs experienced only moderate amounts of extension. Therefore, the Panamint Range
originated adjacent to the Black Mountains, rather than on top of them. By their
model, different fault-bounded parts of the Black Mountains evolved somewhat
independently of each other and much of the missing Proterozoic and Paleozoic
sedimentary rock was tectonically removed from the Black Mountains but not
transported a great distance away. Instead, it was buried beneath alluvium after being
tectonically removed. Furthermore, because strike-slip faults drive the extension
within the Black Mountains, these faults must penetrate deeply into the crust.

The turtleback faults and their footwalls are especially relevant to the problem
of style and magnitude of extension in the region because they separate rocks deformed
at mid-crustal conditions from those of the upper crust. Therefore, they are the main
faults which accommodated the extension in Death Valley. No stratigraphic markers
are available to help constrain the amount of slip on these faults, however, and so the
amount of extension in the region remains an open question. Most importantly, the
turtleback footwalls record the uplift history of the Black Mountains. Any constraints
that can be placed on the evolution of the turtlebacks places similar constraints on the
evolution of the Black Mountains.

Chapter One

ROCKS OF THE BADWATER TURTLEBACK

Introduction

Rocks of the Badwater turtleback can be split into three principal categories: those that lie in the footwall, those that lie in the hangingwall, and those that are found in both the hangingwall and footwall. In general, the hangingwall consists of late Tertiary volcanic rocks and Quaternary(?) sediments while the footwall consists of variably mylonitized, Precambrian quartzofeldspathic gneiss and marble, mylonitic pegmatite of probable Tertiary age, and late Tertiary dikes, plutonic, and volcanic rocks. Mafic dikes cut both the hangingwall and footwall (Fig. 1-1).

Hangingwall rocks

Volcanic Rocks

Volcanic rocks of the hangingwall consist of predominantly dacitic flows, lithic-rich tuffs and minor basalt. These rocks form the mountain front and ridge crest north and east of Natural Bridge Canyon (Fig. 1-1). They appear to be continuous with volcanic and sedimentary rocks of the Artist Drive Formation farther north, although no one has yet demonstrated actual continuity between the two areas. No ages presently exist for these volcanic rocks, but Cemen et al. (1985) found that the Artist Drive Formation was deposited from about 14 Ma to about 6 Ma.

Monolithologic brecciated volcanic rock crops out in the hangingwall along the front of the Badwater Turtleback between Natural Bridge and Nose Canyons. These breccias probably originated by gravitational sliding of the volcanic rocks along the Turtleback fault surfaces (Chapter 4).

13

Figure 1-1.   Generalized geologic map of the Badwater Turtleback area which shows the rocks and locations described in the text. Abbreviations are as follows: NBC, Natural Bridge Canyon; TC, Tank Canyon. Contour interval is 800 feet.

N

500 metres

NBC

Sea level

TC

Tav

pЄm

Tq

Tsv

4000

Badwater Spring

pЄm

Tw

Tq

Dantes View
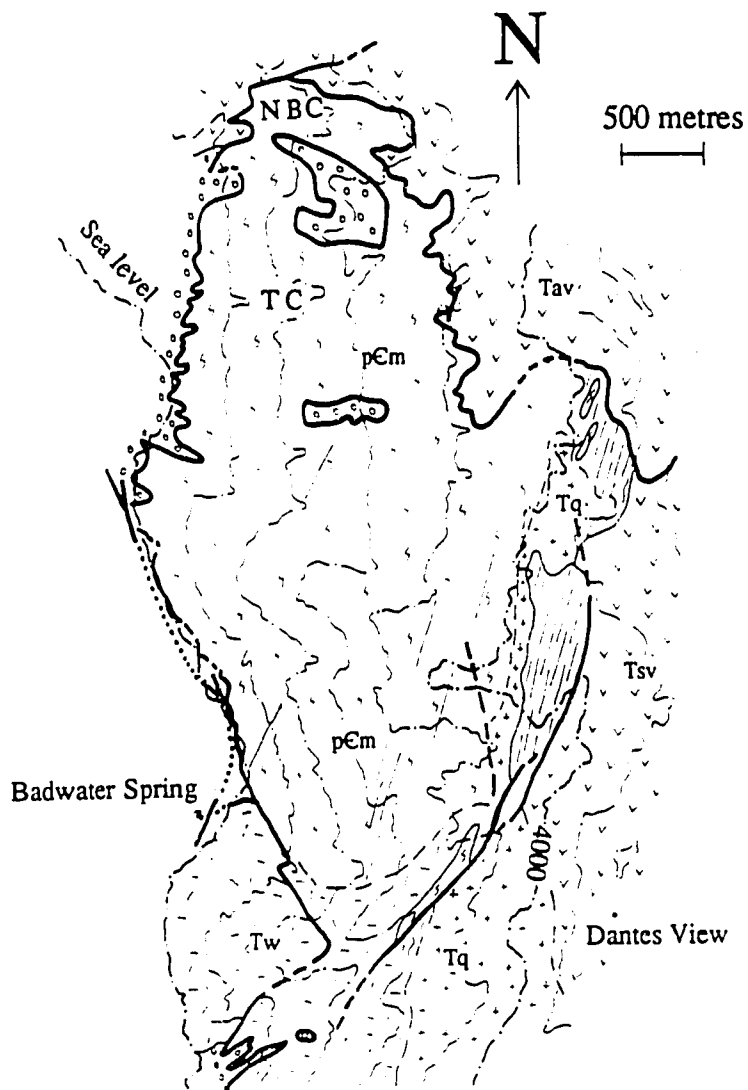
☐ Fanglomerate and monolithologic breccia

☐ Tertiary volcanic rocks: Tav, Artist Drive; Tsv: Shoshone Volcanics

☐ Quartz-latite dikes

☐ Tq: Quartz monzonite

☐ Tw: Dioritic-gabbroic rocks of Willow Spring pluton

☐ pЄm: Mylonitic rocks. Includes quartzofeldspathic gniess, carbonate and pegmatite of probable Tertiary age.

Quaternary(?) sediments

Fanglomerate of probable Quaternary age lies in the hangingwall of the Badwater Turtleback along the front of the Black Mountains between Natural Bridge and Nose Canyons (Fig. 1-1). These rocks were studied in some detail by Cichanski (1990) who found that they could be subdivided on the basis of their clast content. The lowest part of the succession contains only volcanic clasts while higher units contain an increasing abundance of metamorphic clasts. Cichanski (1990) attributed this change to progressive uplift of the Badwater Turtleback.

Footwall rocks

Mylonitic gneiss

Quartzofeldspathic mylonitic gneiss accounts for about 40% of the mylonitic footwall of the Badwater Turtleback north of Nose Canyon; it makes up more than 70% of the mylonitic component south of Nose Canyon. It consists of widely variable amounts of quartz, plagioclase and orthoclase feldspar, muscovite, and biotite with minor amounts of chlorite, epidote and garnet. High-aluminum minerals, such as kyanite or its polymorphs, are not found in these rocks. The gneiss consists dominantly of tabular bodies which locally exceed 1 km^2 in area. These bodies locally pinch out into carbonate marble, or join where marble pinches out into them. Smaller, apparently detached tabular bodies of gneiss also lie within marble units. Photographs of the gneiss appear as figures 5A, 5B and 10B in chapter three.

Based on field relationships, Miller (1991a) suggested the gneiss originated as a syn-extensional intrusion. Subsequent U-Pb work on two zircon fractions from the gneiss at the University of Washington, however, found a highly discordant age of 1.7 b.y. (Fig. 1-2). Therefore, the mylonitic gneiss is part of the basement complex
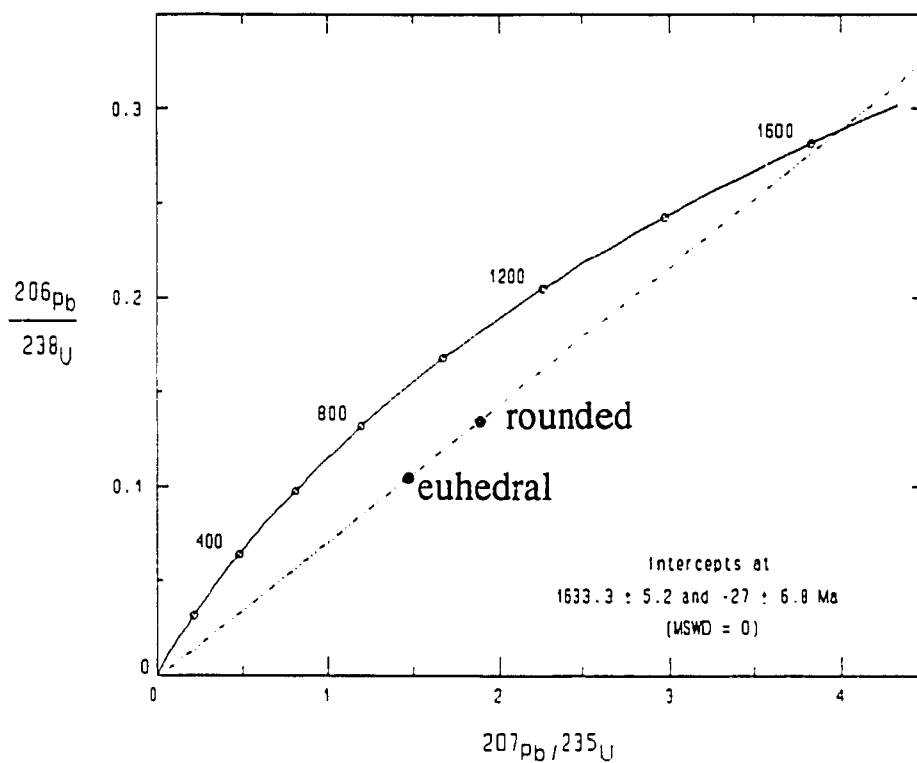
Figure 1-2. U-Pb isochron diagram for two fractions of zircons from quartzofeldspathic gneiss. Discordance is possibly a consequence of contamination by intruding pegmatite during the Tertiary.

described elsewhere in the Black Mountains (Wright and Troxel, 1974) and the complex interlayering must be a product of tectonism. The field relations described by Miller (1991a) as well as the highly discordant nature of the U-Pb age may instead be products of syn-tectonic intrusion of pegmatite (see section on pegmatite).

Mylonitic marble

Mylonitic marble occupies approximately 30% of the footwall of Badwater Turtleback north of Nose Canyon, but less than 10% to the south. The marble consists of both pure and impure calcite and dolomite marbles which, in some places, define individual mappable units with distinct contacts. In other places, the contact between the two rock types is gradational. Within these gradational zones, dolomite and calcite marbles are interlayered with each other at the cm to meter scale. There, the dolomite may show both pinch-and-swell and fracture boudinage. Both marbles display abrupt large thickness changes which locally cause them to pinch out between layers of the other marble, gneiss, or pegmatite bodies.

Both the dolomite and calcite marbles exhibit abundant evidence for high strain, described in detail in chapter three. Furthermore, the calcite marbles are typically associated with other rock types which tended to disintegrate during ductile deformation of the calcite. Consequently, the calcite marble contains abundant microscopic and macroscopic fragments of other rocks.

The calcite marble is typically fine-grained and shows a variable but strong foliation in outcrop. It locally contains cm-scale chert and quartzite layers which help define the foliation. While these rocks contain predominantly calcite, they also contain abundant white mica and locally, actinolite, diopside, quartz and plagioclase. Because of the highly strained nature of these rocks, quartz and plagioclase grains are almost

everywhere fragmented; actinolite and diopside are locally fragmented and are typically associated with bodies of pegmatite. The plagioclase grains may have been derived from inclusions of pegmatite.

At the outcrop scale, the dolomite displays a weak foliation which is typically overprinted by fractures. Microscopically, this foliation consists of anastomosing zones of extreme grain size reduction. As discussed in chapter three, these zones are likely products of dynamic recrystallization of the dolomite.

The protolith for these rocks remains an open question. Based on my own reconnaisance, these rocks most closely resemble the Crystal Spring Formation. Both contain calcite and dolomite marble, and both contain numerous chert laminations within the calcite marble. Furthermore, as discussed below, the marble on the Badwater Turtleback contains sills of ductilely deformed mafic rock which may be Precambrian diabase. This diabase cuts only the basement and the overlying Crystal Spring Formation. Alternately, Wright et al. (1974) suggested that all three turtlebacks were mantled by Noonday Dolomite, but the presence of thick zones of calcite marble seems to preclude this interpretation. Wernicke (B. Wernicke, 1991, personal communication), however, reported that at Tucki Mountain, at the north end of the Panamint Mountains, the Noonday Dolomite contains a large proportion of calcite marble.

Mylonitic pegmatite

The pegmatite makes up approximately 30% of the mylonitic footwall of the Badwater Turtleback north of Nose Canyon but probably less than 20% of it to the south. It consists dominantly of coarse grained albitic plagioclase with quartz, microcline, and muscovite. Modal abundances of these minerals range widely, from

nearly 100% quartz to nearly 100% plagioclase. The pegmatite forms boudins in the calcite and dolomite marbles, and boudinaged sills and dikes within the gneiss. It shows a complete range of fabric development from bodies with only local, weak foliation to bodies with penetrative foliation.

Field relations suggest that the pegmatite intruded during mylonitization of the gneiss and marble. While most of the pegmatite displays evidence for strong ductile deformation, some pegmatite clearly postdated it. Figure 1-3A shows a small pegmatite dike cutting boudinaged calc-silicate marble; figure 1-3B shows pegmatite with an inclusion of mylonitic gneiss. Furthermore, individual bodies of pegmatite locally cut across mylonitic foliation and lineations in adjacent rocks (Miller, 1990), but are themselves mylonitic. Farther south, near the Copper Canyon Turtleback, a pegmatite dike cuts 10.6 Ma rocks of the Willow Spring pluton. Its relation for the pegmatite of the Badwater Turtleback, however, is unknown.

A syntectonic origin for the pegmatite explains the highly discordant nature of the U-Pb age for the gneiss as a product of contamination by the pegmatite. It also explains the intimate association of pegmatite and gneiss in the field (Chapter 2, figures 2-2B, 2-5A and 2-10B). In general, the two rock types can be distinguished only where pegmatite bodies are greater than about 1 m in thickness. Where pegmatite bodies within the gneiss are thinner than 1 m, they typically pinch out into the gneiss as a series of increasingly small tabular sills and broken clasts. In fact, many thin leucocratic layers within the gneiss can be traced to progressively thicker ones which connect with cross-cutting dikes of pegmatite. Therefore, at the outcrop scale, it is sometimes impossible to distinguish between the gneiss and pegmatite.
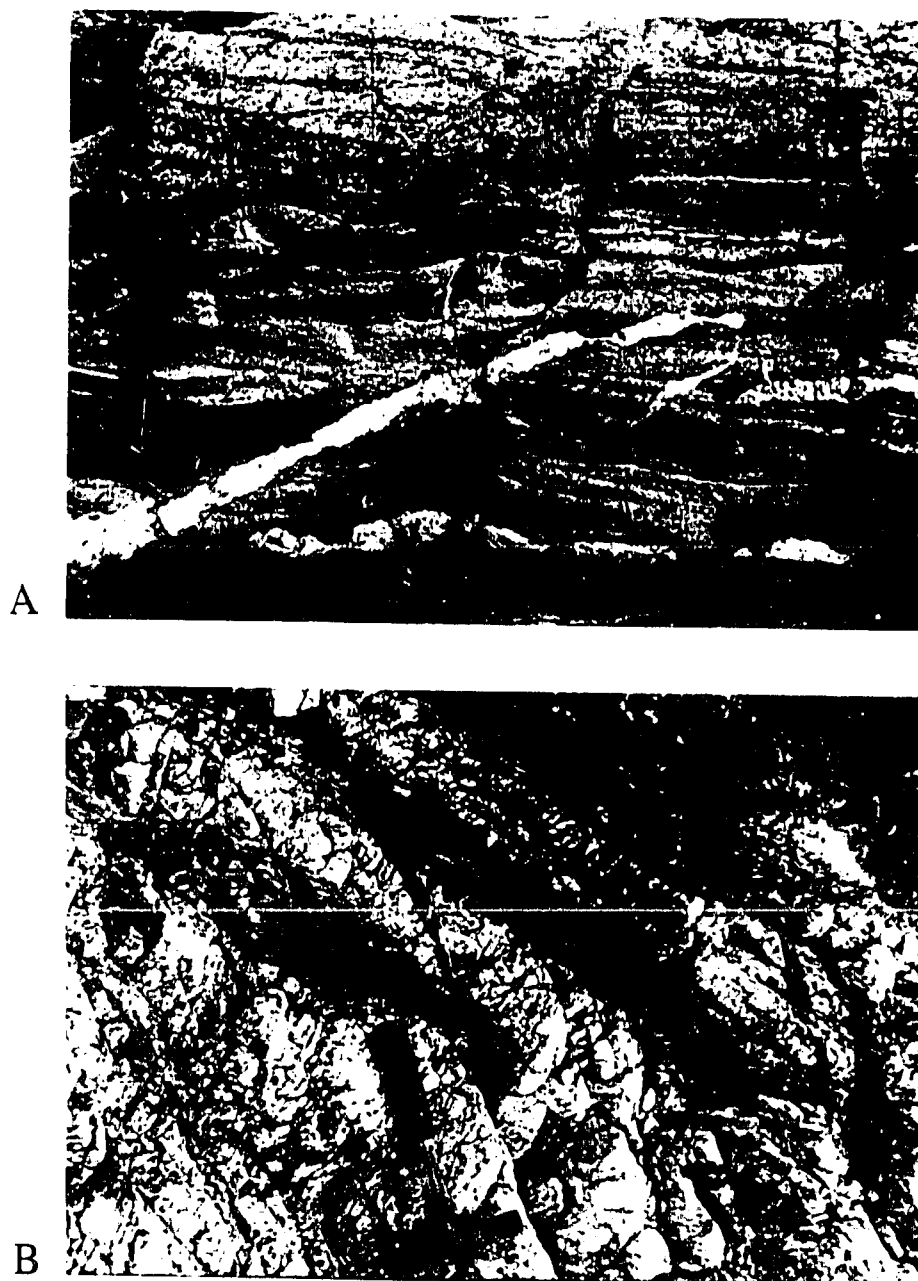
Figure 1-3. Photographs of pegmatite that illustrate how some of it postdates some mylonitic deformation. 1-3A, small pegmatite dike which cuts boudinaged calc-silicate rock; 1-3B, inclusion of mylonitic gneiss in pegmatite.

Pelitic rocks

Pelitic rocks occupy less than 1% of the footwall north of Nose Canyon and have not been found to the south. The largest and best exposed outcrops of these rocks lie in the bottom of Tank Canyon and contain predominantly kyanite, garnet, and quartz. These rocks also contain two varieties of zincian ilmenite (Whitney et al., in press). The presence of these ilmenites is significant because it suggests that the schist experienced significant hydrothermal alteration after formation of the metamorphic mineral assemblage and foliation. Also, the zincian ilmenite has been described from only two other localities worldwide.

Whitney et al. (in press) reported a pressure estimate of 7 ± 1 kbar for these rocks using the assemblage garnet-rutile-aluminosilicate-ilmenite-quartz (GRAIL). This mineral assemblage, however, must predate intrusion of pegmatite because foliation in these rocks is cut by pegmatite (Fig. 1-4). The dike in figure 1-4 is undeformed within the schist, but is strongly mylonitized where it cuts quartzofeldspathic gneiss. Given that the age of the pegmatite is synextensional at the latest, the mineral assemblage in these rocks, and therefore the pressure estimate, must reflect metamorphism prior to late Tertiary extension. Furthermore, the pegmatite may have provided the source of hydrothermal fluids which formed the zincian ilmenite.

Nonmylonitic plutonic rocks

Nonmylonitic plutonic rocks of the footwall of the Badwater Turtleback are found in two places: south of Badwater and above about 3000 feet in elevation (Fig. 1-1). South of Badwater, they consist of intermediate to mafic intrusive rocks which are continuous with the Willow Spring pluton of the Copper Canyon and Mormon Point turtlebacks. This pluton has a U-Pb age of 11.6 Ma according to Asmerom et. al,

Figure 1-4. Undeformed pegmatite dike cutting pelitic schist. This same dike becomes strongly deformed where it enters mylonitic gneiss.

(1990) and 10.6 Ma according to Dewitt (E. Dewitt, 1991, personal communication).
At high elevations, a sill-like body of quartz monzonite crops out. These rocks were
mapped and described by Drewes (1963).

Dikes

A set of nonmylonitic quartz latite dikes cuts mylonitic rocks and nonmylonitic
plutonic rocks of the footwall of the Badwater Turtleback (Fig. 1-1). The dikes trend
approximately N20°E. On the west side of the turtleback they form single, distinct
dikes, but on the east side, they form a prominent swarm of dikes. These dikes are
described in detail by Drewes (1963).

Volcanic rocks

As discussed in chapter 5, the Dantes View area lies in the footwall of the
present Badwater Turtleback fault system (Fig. 1-1). These rocks consist of
predominantly dacitic lava flows and welded tuffs which are generally grouped with
either the Shoshone Volcanics or Greenwater Volcanics (Wright et al., 1991). Fleck
(1971) determined a 6.3 Ma age for a welded tuff immediately north of Dantes View.
The contact of the volcanic rocks with the underlying plutonic and metamorphic rocks
is highly irregular and was mapped by Drewes (1963) as depositional. Holm et al.
(1992) and other workers who favor large-magnitude extension on a single detachment
surface, however, interpret the contact as a fault (see discussion in chapter five).

Mafic dikes of the footwall and hangingwall

A group of variably trending mafic dikes cuts both the footwall and
hangingwall of the Badwater Turtleback (Fig. 1-5A). These rocks are strongly altered

from their original compositions: they presently consist of euhedral magnetite grains, clots of chlorite aggregate, and fine grained relict plagioclase in a matrix of predominantly sericite and chlorite. The plagioclase is replaced by sericite, while the clots of chlorite probably replace olivine crystals.

The dikes are not nearly as prevalent or obvious in the hangingwall as they are in the footwall. In the hangingwall, they have been found at the north klippe only; in the footwall, they are found almost everywhere. In the footwall, these dikes generally dip steeply westward and eastward and cut mylonitic foliation (Fig. 1-5B); they also cut the latite dikes of the footwall. Holm et al. (1992) report a whole-rock Ar age of 6.2-6.5 Ma for these rocks.

Similar green-colored mafic rocks cut mylonitic foliation at low angles. While these rocks resemble the mafic dikes in appearance and overall degree of alteration, they are cut by the dikes and display a distinctly different REE pattern (Fig. 1-5C). These rocks are also much more limited in aerial extent than the dikes as they seem to be restricted to the area around Nose Canyon.

Other green-colored, mafic igneous rocks occur as sills which are locally foliated and concordant with mylonitic foliation in the footwall (Fig. 1-5D). These sills may reflect an earlier stage of intrusion of the same rock types, as they display similar, but slightly less enriched, REE patterns (Fig. 1-5C). In thin section, however, these rocks contain abundant amphibole crystals and lack the relict olivine crystals of the later, post-mylonitic dikes. While these rocks have not been dated, they may instead be deformed diabase dikes, which are reported elsewhere from both basement rocks and the overlying Crystal Spring Formation.
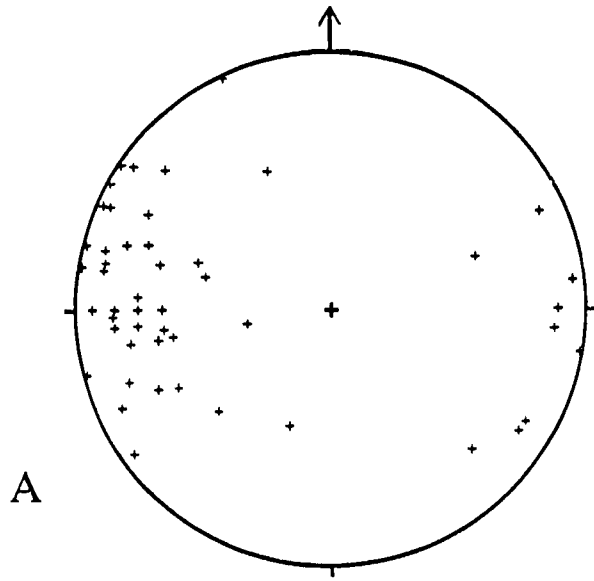
A
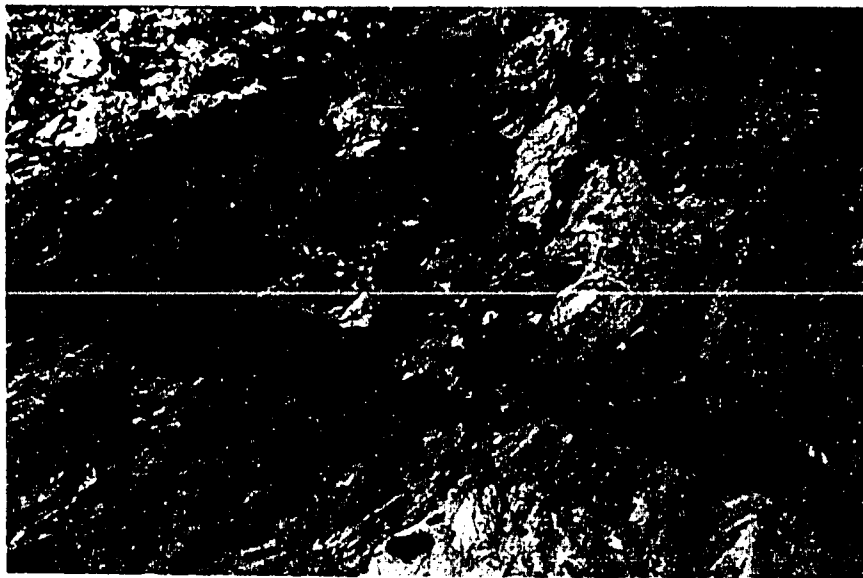
B

Figure 1-5. Mafic dikes. 1-5A, stereographic projection showing orientations of mafic dikes in the footwall. 1-5B, photograph of mafic dike cutting mylonitic foliation. 1-5C, REE patterns of mafic dikes from footwall and hangingwall, undeformed mafic sills, and deformed mafic sills. 1-5D, photograph of deformed mafic sills.

Badwater Turtleback–Mafic rocks

C

D
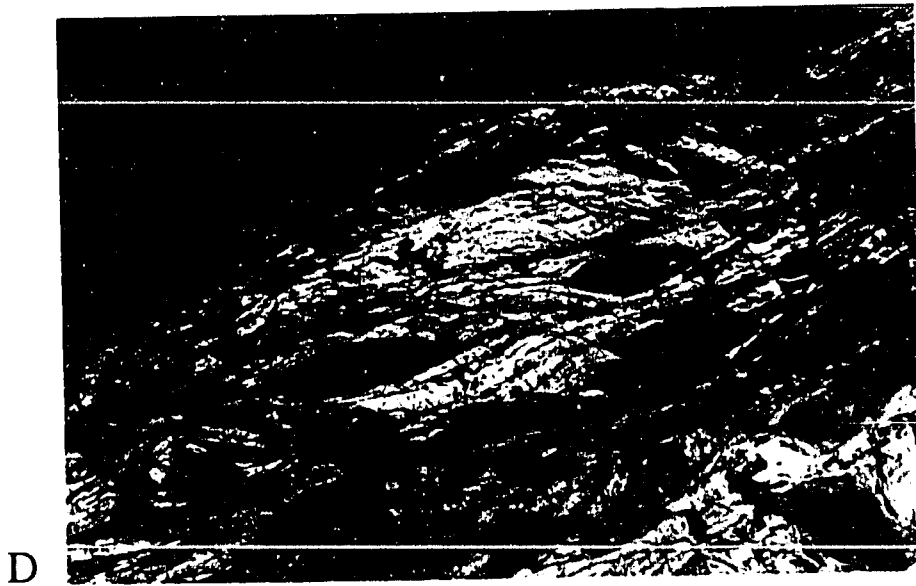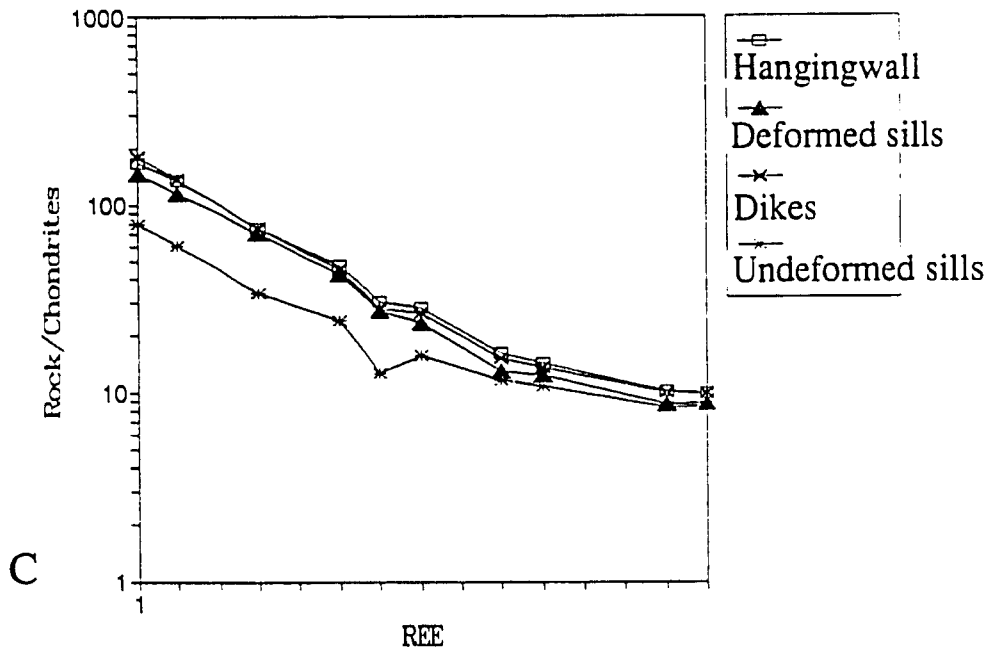
Summary

Cross-cutting relations and published and unpublished geochronology for rocks of the footwall and hangingwall of the Badwater Turtleback permit the construction of a generalized stratigraphy for the turtleback (Fig. 1-6). Mylonitic fabrics in the footwall are assumed to be products of Tertiary extension in Death Valley. The abundant structural and geochronologic evidence for this assumption is discussed in the introduction and chapter 2 of this report.

The oldest rocks in the footwall consist of Precambrian basement infolded with younger Precambrian carbonate rocks and minor associated pelitic rocks. Both the basement and carbonate contain deformed sills of amphibole-rich mafic rock. If these sills originated as Precambrian diabase dikes which were subsequently transposed into the mylonitic foliation, the carbonate rock can be confidently tied to the Crystal Spring Formation. If the sills are instead related to Tertiary magmatisim, then the carbonate rock may be either Crystal Spring Formation or Noonday Dolomite. The few small outcrops of pelitic rocks contain a metamorphic mineral assemblage which probably reflects metamorphism during the Mesozoic.

Pegmatite sills and dikes intruded the basement, carbonate, and pelitic rocks. They display a variably strong mylonitic foliation and are presently both concordant and discordant with mylonitic foliation in the basement and carbonate. Cross-cutting relations between the pegmatite and mylonitic fabrics as well as U-Pb geochronology on the gneiss, suggest that the pegmatite intruded concurrently with extensional deformation.

Undeformed rocks of the footwall include the northern limits of the Willow Spring pluton, the quartz monzonite of Drewes (1963), felsic and mafic dikes, and felsic volcanic rocks. The Willow Spring pluton intruded at about 11 Ma and

fanglomerate

volcanic breccia

mafic dikes

Artist Drive
volcanics
(14-6 Ma)

Badwater Turtleback fault

Shoshone volcanics (6.3 Ma)
erupted onto footwall

mafic dikes
latite dikes
quartz monzonite

Willow Spring pluton
(11.6 Ma)

pegmatite (Tertiary)

mafic sills

Crystal Spring Formation
--possibly Noonday Dolomite

quartzofeldspathic gneiss
(Precambrian basement)
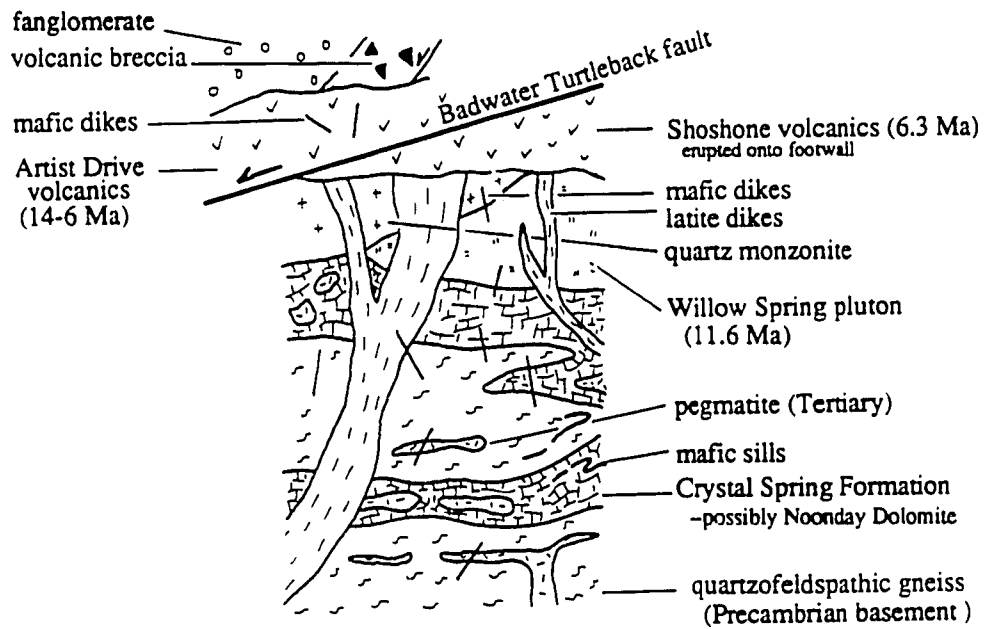
Figure 1-6. Summary diagram showing stratigraphic relations of rocks of the
Badwater Turtleback.

according to Drewes (1963), predates the quartz monzonite. Latite dikes intruded the mylonitic footwall as well as the undeformed plutonic rocks. The latite dikes, in turn, are cut by 6 Ma mafic dikes which are found in both the footwall and hangingwall. Volcanic rocks, which at Dantes View have an age of about 6.3 Ma, erupted onto the footwall. These rocks are here grouped with the Shoshone Volcanics although their 6.3 Ma age appears more suggestive of the Greenwater Volcanics (Wright et al., 1991). The age relationship between the mafic dikes and these volcanic rocks is not clear, but no mafic dikes have yet been observed in the volcanic rocks.

In the hangingwall, volcanic rocks, which are probably equivalent to the Artist Drive Formation, erupted sometime between about 14 and 6 Ma. They are intruded by mafic dikes and overlain by volcanic monolithologic breccias and Quaternary(?) fanglomerate.

Chapter Two

DUCTILE DEFORMATION OF THE FOOTWALL

Introduction

Since the general acceptance of the genetic relationship between ductile deformation in the footwalls of many metamorphic core complexes and the overlying low-angle brittle fault zones, the nature of footwall deformation in these complexes has become an increasingly important topic in structural geology. It is important for three reasons. First, if the evolution of the footwall led to the formation of the bounding fault zone, then study of the footwall should lend insight into the nature of the transition from ductile to brittle behavior. Any additional insight on the origins of the brittle fault surface may help place constraints on seismologic and regional tectonic models. Second, because these footwalls contain well-preserved ductile shear zones, their study can reveal information regarding shear zone formation and processes that take place within shear zones. Third, detailed descriptive information from footwalls of metamorphic core complexes can help constrain geodynamic models for crustal extension which call on the middle and upper crust to exhibit particular styles of behavior.

Mylonites are characteristic rocks in the footwalls of metamorphic core complexes. Mylonites show extreme grain size reduction by crystal-plastic mechanisms, typically contain an enhanced foliation and mineral lineation, and form within zones of high strain (Tullis et al., 1982). Because onset of crystal plasticity takes place at different temperatures for different minerals, polymineralic mylonites generally show a combination of microscopically ductile behavior and brittle fracture.

Many quartzofeldspathic mylonites, for example, contain dynamically recrystallized quartz and broken feldspar grains.

This rheological variability with respect to composition in single rock types applies to a variety of rock types. In general, those rocks which are supported by a framework of material that can deform crystal-plastically will deform ductilely while other rocks will fracture. The footwall of the Badwater Turtleback consists of four principal rock types: quartzo-feldspathic gneiss, pegmatite, calcite marble, and dolomite marble. The framework-supporting minerals of each rock are quartz, feldspar, calcite, and dolomite respectively. Each rock type exhibits a structural progression which begins with mylonitization and ends with the development of throughgoing brittle faults. Their strong lithologic contrasts, however, caused mylonitization to cease in the four rock types at different stages of deformation. It ceased first in pegmatite, second in dolomite marble, third in quartzofeldspathic gneiss, and fourth in calcite marble. This sequence is the reverse order of that found experimentally for onset of thermal weakening of the minerals which make up the framework-supporting matrix of each rock type (Turner and Weiss, 1963). In outcrop, this structural progression is revealed by primarily cross-cutting relations. Mylonitic foliation in calcite marble, for example, locally cuts across foliation in all other rock types.

This progressive change in behvioral styles provides a key to understanding the ductile deformation in the footwall. Specifically, the footwall shows a structural progression indicative of ongoing deformation at decreasing temperatures through time. Consequently, there must have been a kinematic link between mylonitization at depth and extensional faulting at the earth's surface. As discussed in chapter 5, this fault system must predate the present-day Turtleback fault system. The link between

faulting and mylonitization, however, suggests that the Badwater Turtleback fits both the descriptive and genetic model for metamorphic core complexes.

Viewed in the context of a rising and cooling footwall, other aspects of the ductile deformation become significant. The footwall, for example, displays antiformal geometries about northwest-trending and northeast-trending axes. Such geometries help constrain the kinematic history of the system and also bear on general models of rotation in extensional settings. Other features, such as local variations in shear directions and the roles played by calcite marble at later stages of deformation, have implications for rheological changes in the footwall, strain softening and localization mechanisms, and even the onset of brittle faulting.

This chapter describes the macroscopically ductile deformation in the footwall of the Badwater Turtleback. In particular, it details the structural evolution and cross-cutting relationships characteristic of each rock type and explains why these features indicate formation during uplift along an extensional fault system. After establishing the structural context, this chapter then addresses certain aspects of the deformation which can place specific constraints on the deformation as a whole.

Macroscopically ductile structural evolution of the footwall

Each of the four principal rock types of the footwall underwent mylonitization during early stages of deformation and brittle fracture and faulting at later stages. This transition from mylonite formation to brittle fracture involved the progressive development of structures which reflect increasingly localized deformation. While the complete structural progression has not yet been observed at one place, it consists of transposed mylonitic fabrics, followed by isoclinal folds, tight to open asymmetric

folds, outcrop-scale shear bands, boudinage and fracture. Kinematic indicators from all structures indicate overall top-to-the-northwest sense-of-shear.

Each rock type, however, behaved differently during deformation. The most notable differences concern the relative timing of cessation of mylonitization and degrees to which the rocks record the complete structural progression (Fig. 2-1). Calcite marble records the most complete progression, followed by quartzofeldspathic gneiss, dolomite marble, and pegmatite. In general, those rock types which continued to deform ductilely at later stages of deformation also show the most complete sequence of structural development. Furthermore, relatively thin bodies of dolomite marble and pegmatite tend to show a more evolved structural progression than thicker bodies.

Mylonitic fabrics

Pegmatite: The pegmatite crops out as differently shaped bodies within the other principal rock types. Within carbonate rocks, it forms pod-shaped outcrops which vary in size from less than 1 m to more than 10 m in length (Fig. 2-2A). Within the gneiss, it forms dikes and sills (Fig. 2-2B). The pegmatite shows a complete range of fabric development: some bodies display only local, weak foliation; others display penetrative foliation; still others display the entire range of fabric development. Stretching lineations in mylonitic pegmatite are defined by predominantly recrystallized quartz and minor feldspar, and broken and entrained feldspar grains. They plunge in a wide range of directions but concentrate in the northwest and southeast quadrants (Fig. 2-3). Mean orientation for these stretching lineations is 8, N53°W. Transport directions are ambiguous in many places. Where transport directions can unambiguously be inferred from grain shape fabrics in quartz, asymmetric

33

Figure 2-1. Preserved structural sequence for four principal rock types of the footwall.

	mylonitic foliation	transposition and isoclinal folding	asymmetric folds	shear bands	boudinage	fracture
Pegmatite	ubiquitous but of varying intensity	only in thin bodies	rare, only in thin bodies	-----	abundant	ubiquitous
Dolomite Marble	overprinted by fractures	only in thin bodies	rare	rare	abundant	ubiquitous
Quartzofeldspathic Gneiss	ubiquitous, very strong	ubiquitous	abundant	rare	rare, only where enclosed by calcite	ubiquitous
Calcite Marble	ubiquitous, very strong	ubiquitous	abundant	rare	-----	ubiquitous

OLDER ←――――――――――→ **YOUNGER**

Relative timing from cross-cutting relations
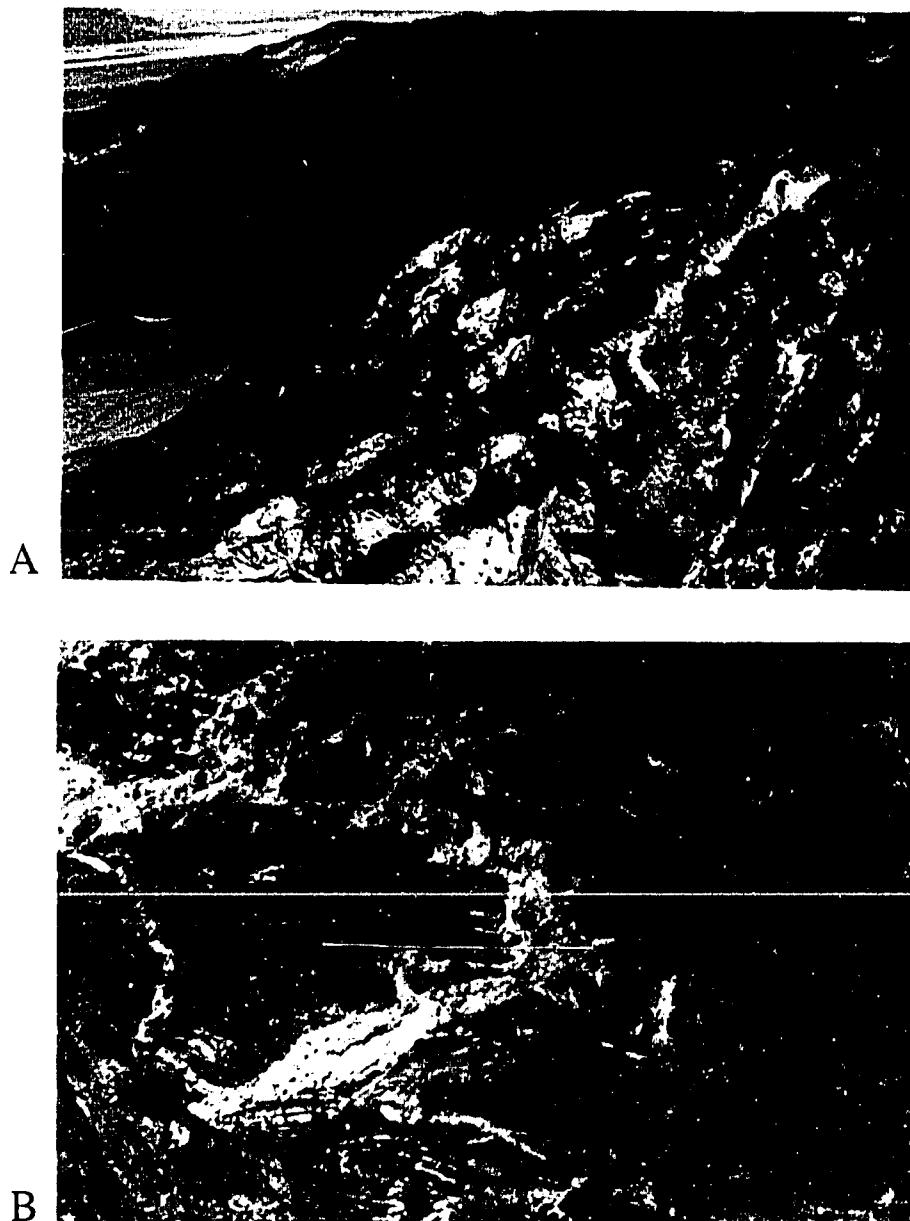
Figure 2-2. Photographs of pegmatite. 2-2A, bodies of pegmatite enclosed within darker, mylonitic carbonate. 2-2B, dikes and sills of pegmatite within quartzofeldspathic gneiss.

porphyroclasts, and rare C-S fabrics, however, they are overwhelmingly top-to-the-northwest.

Although modal abundances of minerals vary, the dominant feldspar typically defines the framework of the rock while quartz and muscovite occupy disconnected spaces between feldspar grains. In general, all the observed pegmatite contains dynamically recrystallized quartz while the more strongly deformed pegmatite also contains dynamically recrystallized feldspar. Other optical strain features in feldspar which are common to all the observed pegmatite consists of deformation twins (Vance, 1961), kinked and bent twins, undulatory extinction, and fractured grains. Quartz grains are not fractured at the microscopic scale.

Quartzofeldspathic gneiss: In outcrop, the gneiss displays a strong foliation which is defined primarily by alternating quartz- and feldspar-rich and mica-rich layers, flattened quartz grains, broken feldspars, and phyllosilicates. In homogeneous rock, this foliation is markedly planar and regularly spaced at the cm-scale. With increasing numbers of porphyroclasts, foliation becomes progressively disrupted. Prominent stretching lineations, defined by recrystallized quartz and broken feldspar grains, lie on most foliation surfaces. These lineations show a wide range of orientations but, like the pegmatite, plunge primarily to the northwest and southeast. Their mean orientation is 5, N55°W (Fig. 2-4). Locally, asymmetric porphyroclasts indicate top-to-the NW sense of shear (Fig. 2-5A). Stretching lineations become decreasingly prominent as the abundance of phyllosilicates rises relative to quartz.

Microscopically, the gneiss consists of alternating layers of predominantly ribbon quartz and quartz aggregate, phyllosilicates, and feldspars (fig. 2-5B). Locally, quartz displays C-S fabrics while some phyllosilicate "fish" are asymmetric with
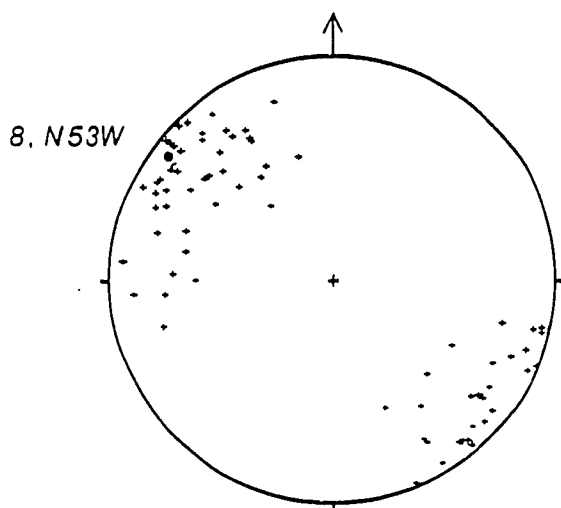
Figure 2-3. Stretching lineations in pegmatite. Solid circle shows mean lineation orientation.
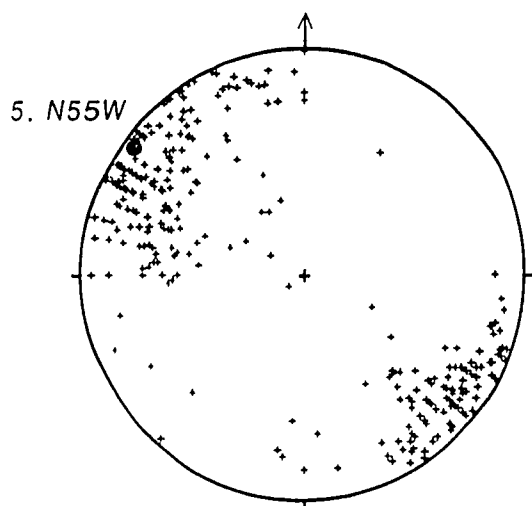
Figure 2-4. Stretching lineation in quartzofeldspathic gneiss. Solid circle shows mean lineation orientation.
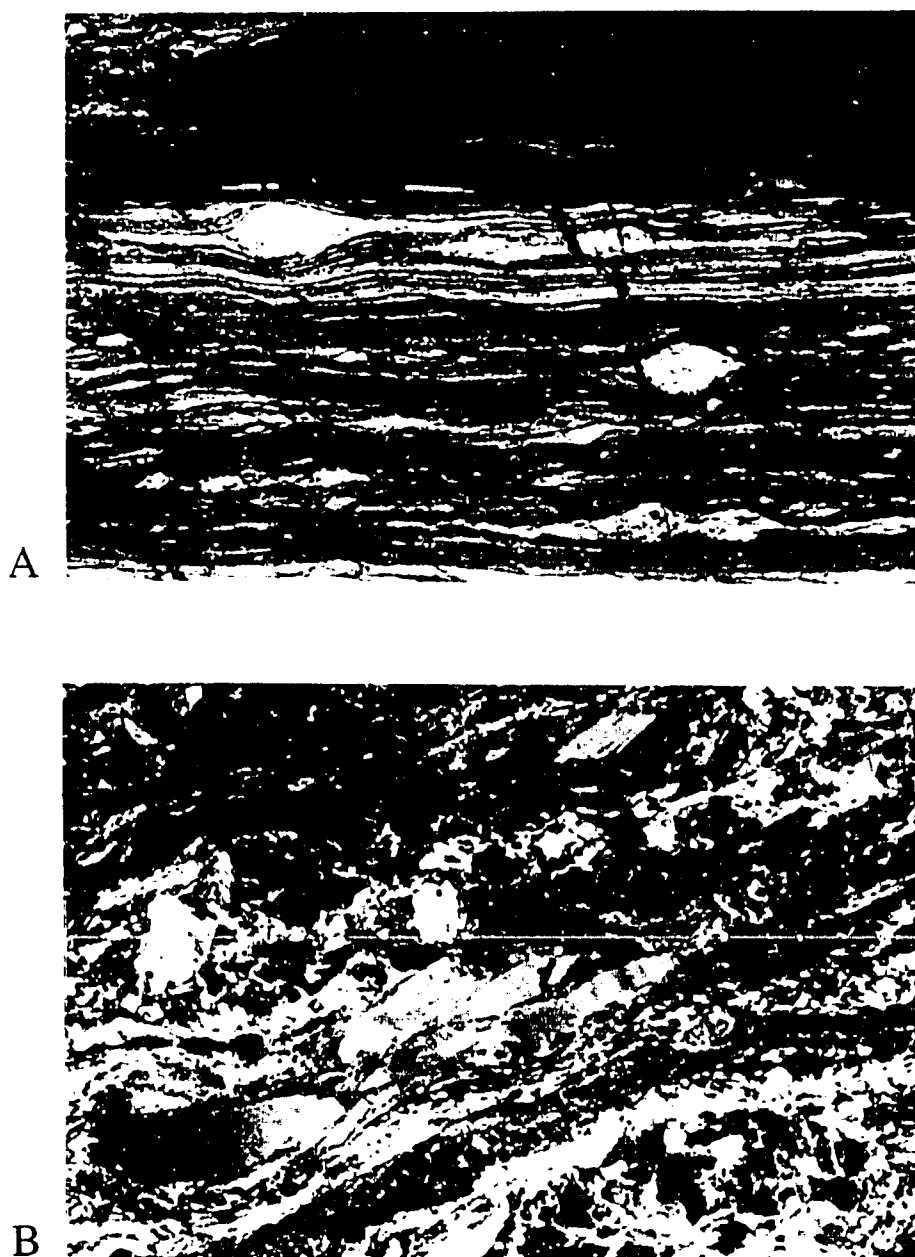
Figure 2-5. Photographs of quartzofeldspathic gneiss. 2-5A. outcrop photograph of asymmetric porphyroclast of pegmatite; plane of photo is parallel to stretching lineations. Sense-of-shear is top-to-the-northwest (right). 2-5B, photomicrograph of quartzofeldspathic gneiss showing alternating quartz and feldspar bands with phyllosilicate-rich bands.

respect to foliation. Both kinematic indicators suggest top-to-the-northwest transport. Grain sizes of quartz and phyllosilicate minerals range from less than 10 um in the more highly strained grains to greater than 2mm. Neither quartz ribbons nor quartz aggregates show fracturing at this scale; phyllosilicates locally show evidence of later strain in the form of top-to-the-northwest directed shear bands. Feldspar and epidote typically exist as broken porphyroclasts. Feldspar grains also show undulatory extinction, deformation twins, and recrystallization at grain margins.

Dolomite marble: At the outcrop scale, the dolomite displays a weak foliation which is typically overprinted by fractures (Fig. 2-6A). This foliation reflects development of mm to cm-scale zones of decreased grain size. Locally, the zones contain strongly foliated dolomite which, in some places, displays an asymmetry with respect to the more prominent, coarse foliation. All observed examples of this asymmetry lacked accompanying lineations in dolomite, but combined with lineations in adjacent gneiss or calcite marble, indicate approximately top-to-the-northwest transport (Fig. 2-6B). Lineations on dolomite marble were observed in only a few instances, and these were all weakly developed at best.

Microscopically, the coarse foliation in dolomite consists of anastomosing zones of high strain and extreme grain size reduction (Fig. 2-6C). Similar to the mylonitic gneiss and pegmatite, the grain size reduction in dolomite must be a product of dynamic recrystallization rather than cataclasis. Three lines of evidence suggest this mechanism: 1) isolated remnants of individual dolomite grains remain in optical continuity, 2) recrystallized grains tend to cluster about twin boundaries and may occur within grain interiors, 3) fractures exist as discrete features which clearly postdate the fabric.

Figure 2-6. Photographs of dolomite marble. 2-6A, outcrop-scale asymmetric fold which shows fracturing parallel to foliation. 2-6B, strongly foliated dolomite gives top-to-right (NW) sense-of-shear. 2-6C, anastomosing zones of extreme grain size reduction in polished slab of dolomite marble.

Calcite marble: In most places, the calcite marble is fine grained and shows a variable but strong foliation in outcrop (Fig. 2-7A). However, coarse grained, weakly foliated calcite marble crops out on the northern slope of Tank Canyon and in Open Canyon. Foliation in the calcite marble is defined primarily by recrystallized calcite grains, but it is locally defined by layers of calcite alternating with chert, dolomite, or aggregates of phyllosilicates in a planar preferred orientation. Lineations are best developed on quartz-rich surfaces, particularly the chert laminations. In quartz-poor, but dolomite- or talc-rich calcite marbles, lineations are locally defined by recrystallized calcite or entrained dolomite fragments. Their mean orientation is 11, N66°W (Fig. 2-7B). Lineations, however, typically are not easily discernable in pure calcite rocks, except those that show unusually strong foliation.

Variably wide, non-planar but tabular zones of especially fine-grained calcite marble occur within otherwise ordinary outcrops. These zones resemble melanges because they contain blocks of non-calcite wallrock set in a predominantly calcite matrix. The matrix displays both strong and weak foliations. These zones are described in detail near the end of this chapter.

In thin section, most pure calcite marble displays anastomosing to regular zones of fine grained calcite (10-100 um) alternating with zones of extremely fine-grained calcite (<10 um). Impure marbles display similar fabrics except that the impurities form broken and rotated porphyroclasts which locally disrupt the foliation. An exception is talc which typically forms pod-shaped aggregates that partially define the foliation.
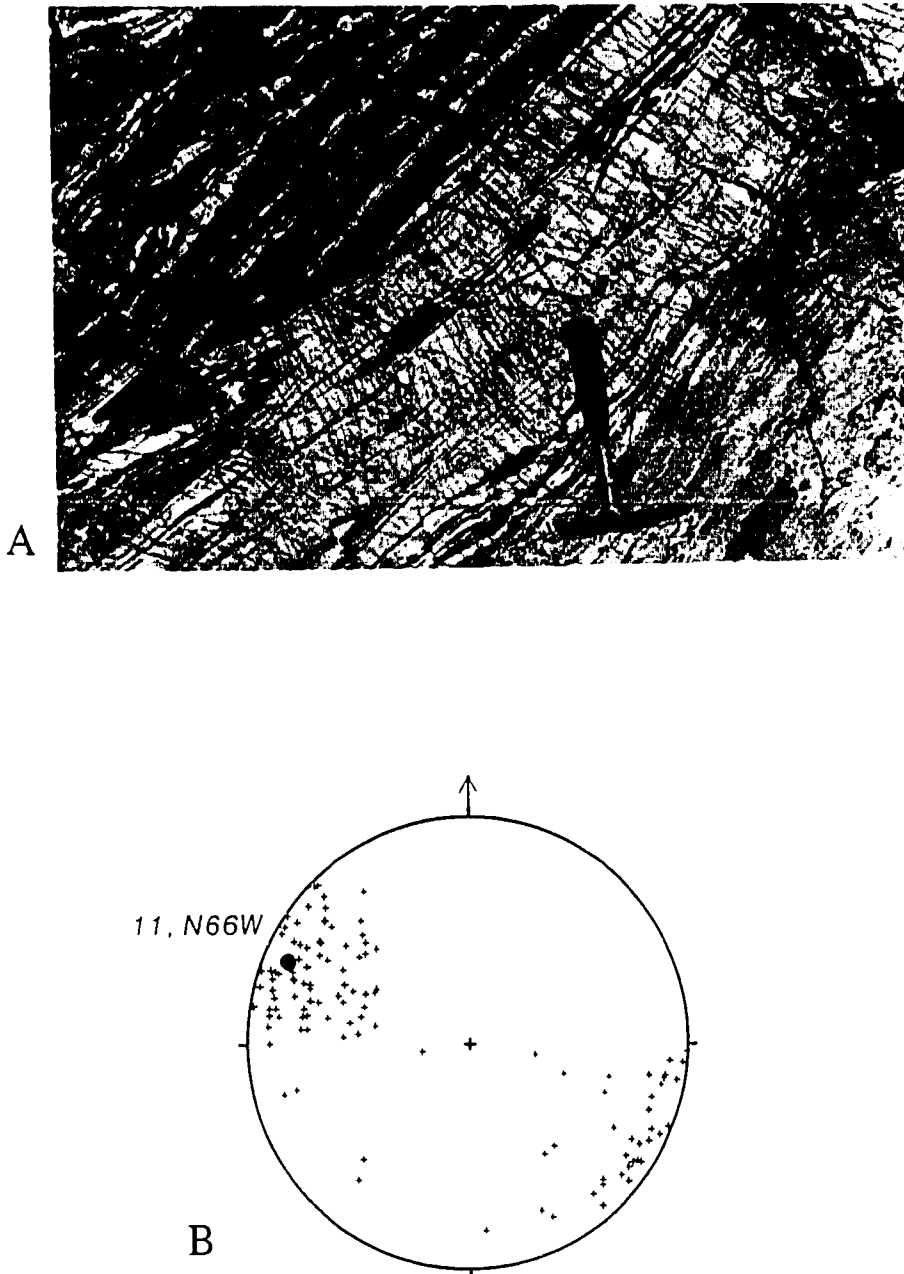
Figure 2-7. Calcite marble. 2-7A, photograph of calcite marble in outcrop. Surface of marble in this photograph is steeply inclined; west is to the left. 2-7B, stereographic projection of lineations in calcite marble. Solid circle shows mean orientation.

Transposition and Isoclinal Folding

Transposition and isoclinal folding affected all major rock types to some degree in the footwall of the Badwater turtleback. Evidence for transposition is relatively rare in the pegmatite and dolomite marble but nearly ubiquitous in the quartzofeldspathic gneiss and calcite marble. Likewise, preserved isoclinal folds are rare within pegmatite and dolomite marble but are locally abundant within gneiss and calcite marble. A few sheath folds with northwestward closure were observed in calcite marble. Isoclinal fold axes within all these rock types typically trend parallel to stretching lineations. Kinematic indicators on transposed foliation suggest predominantly top-to-NW transport.

Transposition and isoclinal folding did not affect the bodies of pegmatite with thicknesses greater than about 1 meter, but did affect thinner sill-like bodies of pegmatite enclosed within quartzofeldspathic gneiss. Dolomite marble is locally tightly infolded and transposed with quartzofeldspathic gneiss and calcite marble, but such exposures are rare, partly because the coarse foliation and pervasive fracturing in dolomite make it difficult to observe details of its fabric. More typically, the dolomite breaks into numerous porphyroclasts when intimately deformed with gneiss or calcite marble.

Asymmetric Folds

Throughout the footwall, asymmetric folds deform mylonitic foliation and lineation in all rock types, except thick bodies of pegmatite. The style and prevalence of folding, however, vary considerably depending on rock type. Rare asymmetric folds occur in dolomite and appear to be accommodated by fracture subparallel to the coarse foliation (see Fig. 2-6A).

Within quartzofeldspathic gneiss and calcite marble, asymmetric folds typically have wavelengths of <1 to 20 meters, plunge northwestward or gently southeastward, and display both southward and northward vergences (Fig. 2-8). Asymmetric folds within both the gneiss and calcite marble trend either oblique or approximately parallel to pre-existing lineations. Those folds which are oblique to the lineations display considerable scatter of lineation direction from limb to limb and clearly postdated the lineations. Those folds that trend roughly parallel to the lineations, however, produce little to no scatter and probably formed contemporaneously with the lineations.

A Hansen slip-line analysis of asymmetric folds greater than 1 meter in wavelength within either gneiss or calcite marble yields an overall transport direction of top-toward-N63°W (Fig. 2-9A), approximately the same as for folds in gneiss only (Fig. 2-9B) and calcite marble only (Fig. 2-9C). This transport direction was obtained by evaluating the mean of each population of folds and then selecting the line which approximately bisects those means and still retains the least overlap between the two populations. Considerable overlap, howver, exists between north and south-vergent folds, particularly in the calcite marble. As many of the folds in calcite marble are cored by pods of pegmatite which could disrupt an otherwise uniform flow field, this overlap is likely a product of inhomogeneities in the overall ductile flow.

Outcrop-Scale Shear Bands

Shear bands at the outcrop scale developed predominantly in calcite marble but only locally in the quartzofeldspathic gneiss and more rarely in strongly fractured dolomite marble. None have been observed in pegmatite. Most observed shear bands indicate top-to-the-northwest sense of shear but some indicate top-to-the-southeast sense of shear.

Figure 2-8. Photograph of asymmetric fold in carbonate, looking east.

□	N-vergent folds	ⓐ	N-vergent folds, mean
✦	S-vergent folds	ⓢ	S-vergent folds, mean
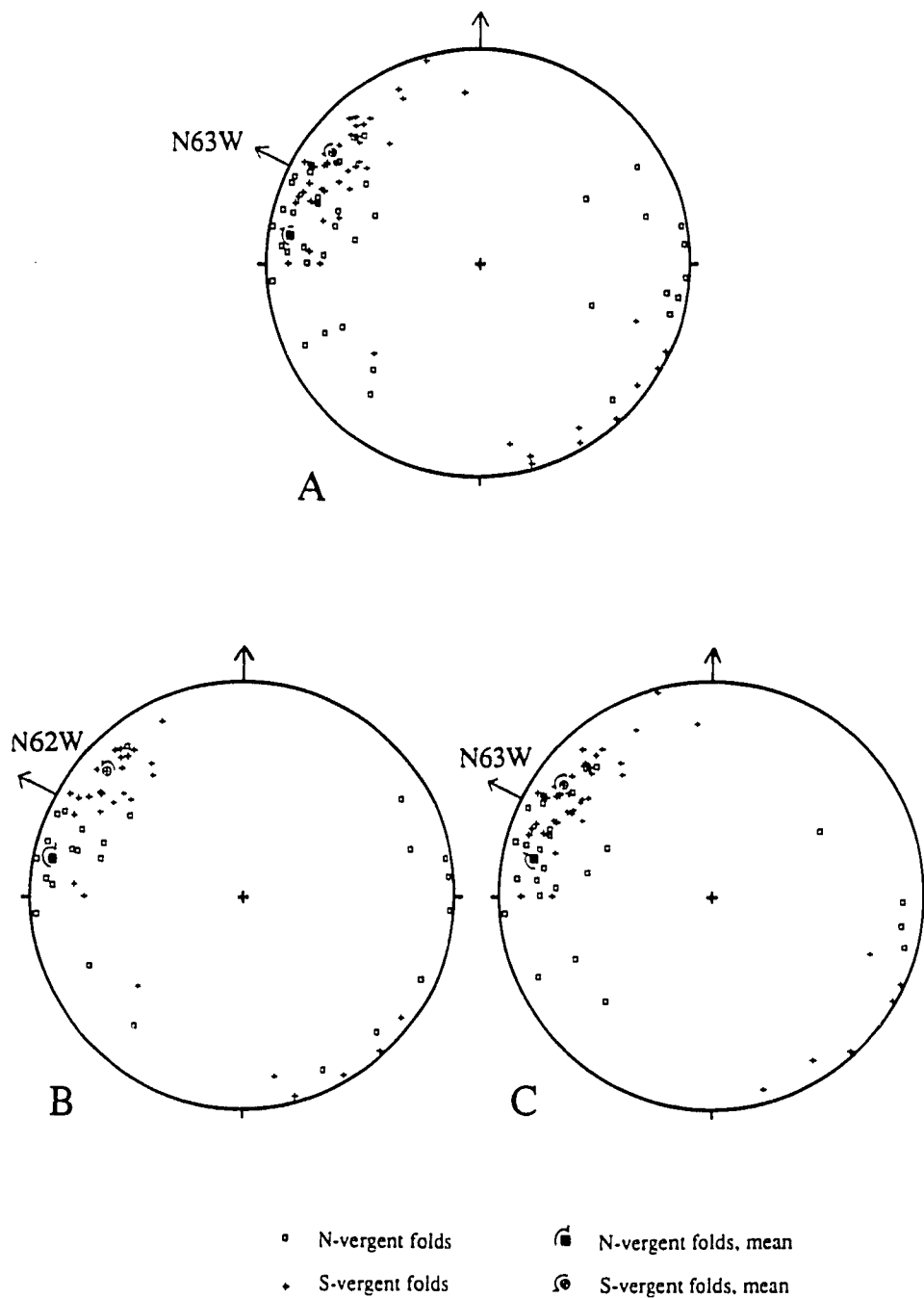
Figure 2-9. Hansen slip-line analyses of asymmetric folds in footwall mylonites. 2-9A, folds in either calcite marble or gneiss. 2-9B, folds in gneiss only. 2-9C, folds in calcite marble only.

Boudinage

Dolomite marble and pegmatite exhibit abundant boudinage at all scales. Calcite marble shows no boudinage at all, while the gneiss shows boudinage only where it is relatively thin and surrounded by calcite marble.

Pegmatite forms boudins and porphyroclasts within the other three principal rock types of the footwall (Fig. 2-2A). When enclosed in calcite or dolomite marble, the pegmatite typically forms pod-shaped outcrops which range in width from roughly 1m to greater than 10 m. I interpret these outcrops as large boudins. Many of the smaller outcrops exhibit clear boudin geometries in cross section which are linked by thin trails of pegmatite (Fig. 2-10A). Other larger pods are isolated but retain a boudin geometry, exhibit local pinch and swell relations with the enclosing carbonate, and display pervasive fracturing which does not affect the surrounding carbonate.

Within the gneiss, thick bodies of pegmatite form similar pod-shaped exposures as in the carbonate while the thin sill-like bodies form tabular boudins. These tabular boudins break up into isolated porphyroclasts at their margins. Necks of these boudins, as well as those within the carbonate, trend parallel and perpendicular to the local stretching lineation direction (Figs. 2-10A, B).

Dolomite marble forms boudins wherever it is surrounded by calcite marble. These boudins tend to be of two shapes: tabular and rounded. Tabular boudins tend to exist at the meter scale and are products of boudinage of compositional layering. Rounded dolomite boudins exist at both the centimeter and 10 meter scale. The small rounded boudins are locally abundant and probably reflect modification of broken tabular boudins. Those at the 10 meter scale are relatively rare and poorly defined. These boudins may have originated as thickened fold hinges which became detached
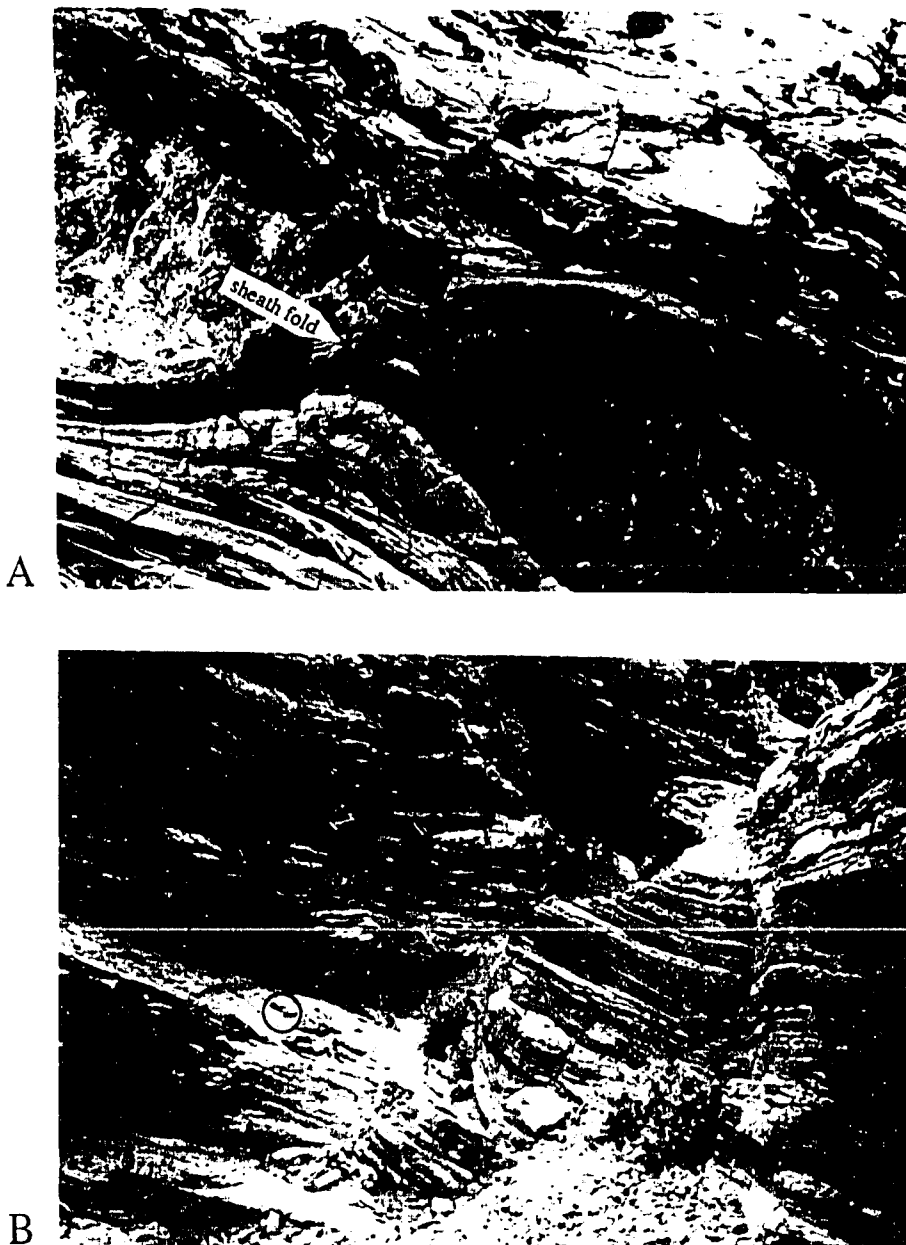
Figure 2-10. Photographs of boudinage of pegmatite in marble and gneiss. 2-10A, pegmatite boudin in marble. Note the sheath fold near the center of the photograph. It indicates that the boudin neck is parallel to the northwest transport direction. 2-10B, pegmatite boudins in gneiss. Rock hammer (circled) is parallel to lineation. Boudin necks in this photograph are parallel and perpendicular to the northwest-trending lineation.

from their limbs. Necks of boudins in dolomite marble also trend parallel and perpendicular to local stretching lineations.

Timing of Ductile Deformation

There are presently only two isotopic age determinations constraining the time of deformation on the Badwater Turtleback. Holm et al. (1992) obtained Ar-Ar ages of 24 and 13.4 Ma on muscovite and biotite respectively from a quartzofeldspathic gneiss. Because the Ar blocking temperature for muscovite is about 350°C and for biotite is about 300°C, these data indicate an approximate 11 million year time gap between when the footwall was hotter than 350°C and colder than 300°C. If these ages are correct, cooling of the footwall, and by inference, extension rates, must have been extremely slow between at least 24 Ma and 13.4 Ma.

An 11 Ma time gap is especially significant, however, given that the different rock types of the footwall show the same styles and directions of strain. Feldspar requires temperatures greater than 450°C to deform plastically (Tullis and Yund, 1985), dolomite requires temperatures greater than 400°C (Turner and Weiss, 1963), quartz requires temperatures greater than 300°C (Suppe, 1985), and calcite requires temperatures greater than about 250°C (Heard, 1960). Therefore, by the data of Holm et al. (1992), much of the ductile deformation in pegmatite and dolomite ceased by 24 Ma; ductile deformation in the gneiss probably continued until nearly 13 Ma while ductile deformation in calcite marble probably continued past 13 Ma. Given these ages, mylonitization of pegmatite and dolomite may reflect a distinctly different period of deformation than late Tertiary extension. Because the sense of shear recorded by the pegmatite and dolomite is approximately the same as the gneiss and calcite marble, however, the direction of hanging-wall transport during both events must have been

the same. A likely candidate for this deformation would be the poorly understood late

Cretaceous extension event recently suggested by Hodges and Walker (1990), and

Applegate et al. (1992).

Relative Timing of Footwall Structures

The preserved structural sequence shows the relative timing of footwall

structures only by rock type. Between different rock types, and even within single

ones, different structures show a great deal of temporal overlap. Within single rock

types, parallelism of isoclinal and some asymmetric fold axes with stretching lineations

suggest that transposition, isoclinal folding, and local asymmetric folding were

ongoing processes during mylonitization. Because processes that are listed early in the

sequence such as mylonitization or transposition tend to obliterate evidence of later

structures such as isoclinal or asymmetric folds, multiple structures within a given rock

type are preserved together only where the given structural processes ceased, rather

than began, in the order described.

Temporal overlap of different structures is even more pronounced between

different rock types. This overlap is particularly instructive where brittle structures in

one rock type formed concurrently with ductile structures in another. Such

relationships indicate that the transition from macroscopically ductile to brittle behavior

affected the different rocks at different stages of deformation. In fact, this concurrence

of different structural styles, plus cross-cutting relationships, suggests that pegmatite

stopped deforming ductilely first, followed by dolomite marble, quartzofeldspathic

gneiss, and finally calcite marble.

Figure 2-11 summarizes evidence that the four principal rock types stopped

deforming ductiley in the sequence pegmatite, dolomite marble, quartzofeldspathic
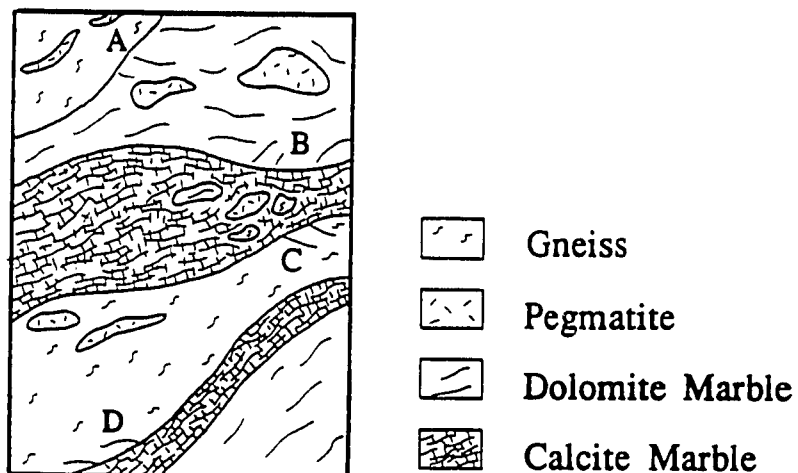
Figure 2-11. Idealized drawing showing cross-cutting relationships and boudinage of mylonitic rocks in the footwall of the Badwater Turtleback. Pegmatite boudins occur in all other rock types; gneiss truncates dolomite marble at A; calcite marble truncates dolomite marble at B, and gneiss at C, D. Note detached blocks of pegmatite, dolomite marble and gneiss within calcite marble.

gneiss, calcite marble. Pegmatite forms boudins in all other rock types in the footwall and must therefore have stopped deforming ductilely first. Dolomite marble, which followed pegmatite, forms boudins in calcite marble and is locally truncated by mylonitic foliation in quartzofeldspathic gneiss. In places with concordant foliation, the dolomite typically displays pervasive fracturing while adjacent gneiss or calcite marble show no loss of cohesion. Evidence that gneiss stopped deforming prior to the calcite marble appears as local truncations of foliation in gneiss against foliation in calcite marble. The calcite marble also contains melange-like zones which contain broken and rotated blocks of all other wall rocks, including the gneiss. These zones represent structures which are peculiar to the calcite marble and are discussed in detail in a later section.

Discussion of Preserved Structural Sequence

Most models for metamorphic core complexes describe the ductile deformation of the footwall as a product of mid-crustal deformation which is related to the brittle fault zone (Davis, 1980, 1983; Wernicke, 1981). Continued slip on the fault zone eventually transports the footwall into shallower parts of the crust where mylonites become overprinted by increasingly brittle structures. These models imply that the footwall undergoes a gradual change from ductile to brittle behavior. At the outcrop scale, however, this transition is difficult to see because it is typically obscured by later brittle faulting and fracturing. In fact, most structural interpretations of shear zones as evolving through the ductile to brittle transition rely primarily on the close spatial relationship of mylonitic rocks and brittle fault zones. These interpretations are necessarily ambiguous because similar associations form when brittle faulting postdates mylonitization. Because all mylonitic shear zones which are today exposed

at the earth's surface were uplifted through the brittle field, they all contain this ambiguity.

The preserved structural sequence in the footwall of the Badwater turtleback, however, does indicate a gradual change from predominantly ductile to brittle behavior. The sequence itself shows a consistent sense-of-shear and suggests that brittle behavior postdated ductile behavior. Most importantly, however, the structural progression displayed by the four rock types formed during different stages of footwall deformation. Calcite marble, for example, formed asymmetric folds while dolomite marble and pegmatite fractured; only at the latest stages of deformation did calcite marble actually fracture. Furthermore, the order in which these rocks stopped deforming ductilely was the reverse for onset of thermal weakening of their respective framework-supporting minerals (Turner and Weiss, 1963). Therefore, the footwall experienced a protracted period of mixed brittle and ductile behavior during which one rock type after another stopped deforming ductilely and began to fracture. Such a structural sequence, followed independently but in the observed order by four different rock types, could form only by continual strain in a gradually cooling environment. Chapter 4 describes how this ductile strain in the footwall led to brittle faulting.

Character of Ductile Flow

Ductile flow in the footwall of the Badwater turtleback occurred during mylonitization of the four principal rock types. The flow was largely heterogeneous with a component of shortening normal to the zone. With continued deformation, the flow probably became increasingly heterogeneous because more of the footwall behaved brittlely and interfered with the flow.

Heterogeneous flow is expressed nearly everywhere in the footwall, as widely dispersed foliation and lineation orientations (Figs. 2-3, 2-4, 2-7B, 2-12), and as asymmetric fold populations which differ in vergence directions but overlap in trend (Fig. 2-9). This heterogeneity was largely a product of rheologic variations in the footwall. As observed in the preserved structural sequence, compositional differences led to behavioral differences, and therefore heterogeneous flow, between different rock types. Within single rock types, ductile flow was similarly disrupted by the presence of different rheologies. Pegmatite boudins within calcite marble, for example, disrupted ductile flow of the calcite marble in their immediate vicinity.

Disruption of ductile flow probably increased as rheological contrasts increased. Pegmatite, the first of the four principal rock types to deform brittlely, appears to disrupt foliation in other rock types to a far greater degree than dolomite marble or quartzofeldspathic gneiss. Furthermore, it disrupts foliation in "weaker" rocks, such as calcite marble, more than it does in the "stronger" dolomite. This effect may be seen in the shapes and orientations of asymmetric folds. The Hansen slip-line analysis of folds in calcite-dominated carbonate shows nearly twice the overlap as the folds in quartzofeldspathic gneiss (Figs. 2-9B, C). As many of the folds in carbonate contain pegmatite in their cores, it is likely that the pegmatite disrupted ductile flow within them more than in the gneiss.

Uplift and consequent cooling of the footwall must have accentuated rheological differences within the footwall because it forced each rock type to change its behavioral mode from macroscopically ductile to brittle. As cooling continued, an increasingly greater proportion of the footwall made this transition while a smaller proportion continued to deform ductilely. Consequently, the ductilely deforming material was subjected to an increasing number of barriers and disruptions to flow.
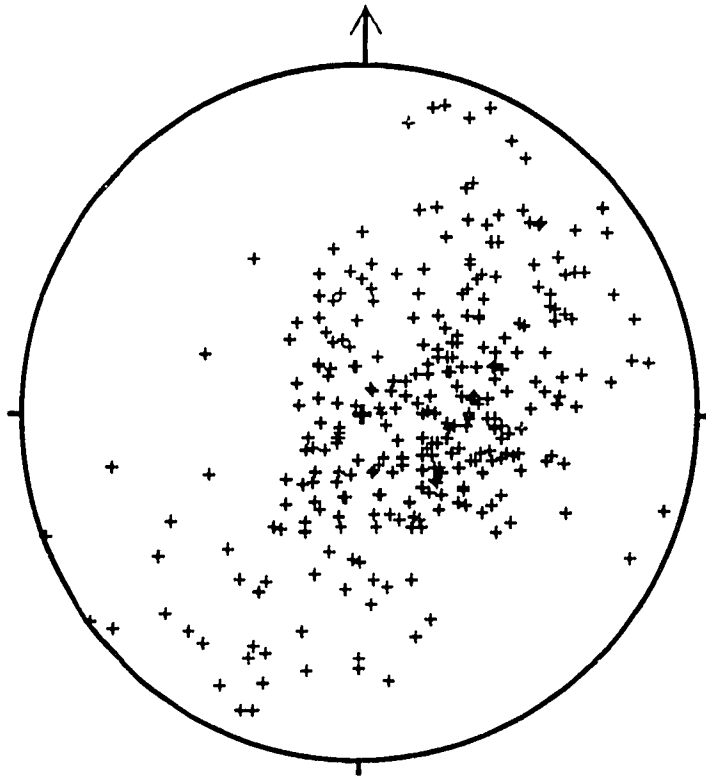
Figure 2-12. Stereographic projection of mylonitic foliations in the footwall of the Badwater Turtleback.

Therefore, as the footwall cooled and enhanced rheological differences, ductile flow probably became increasingly heterogeneous.

Shortening component normal to foliation

While ductile structures in the footwall display evidence for predominant top-to-the-northwest strain, they also suggest that strain was accompanied by a large component of shortening. Such ductile flow resembles the "general shear" of Simpson and DePaor (in press) because it cannot be accurately defined as either simple or pure shear. In outcrop, mylonitic rocks contain far more symmetric than asymmetric porphyroclasts. In thin section, these rocks locally display asymmetric mica fish, grain shapes, and C-S fabrics which allow determination of shear directions, but in most places, display only symmetrical relationships. The overall geometries of sill-like pegmatite boudins provide the most dramatic example of shortening normal to the foliation. These boudins pinch out within mylonitic foliation parallel and perpendicular to lineation (Fig. 2-10B) and therefore resemble the "chocolate-tablet" boudinage of Ramsay and Huber, 1983.

Melange zones within calcite marble mylonite

Introduction

Melanges are chaotic mixtures, consisting of blocks of different rock types set in a matrix of fine-grained, mechanically weaker, material. Melanges may form by either tectonic processes, which involve disruption of original stratigraphy, or sedimentary processes, such as submarine landsliding. Many workers suggest that melanges form prior to lithification because the extreme mobility exhibited by the matrix resembles soft-sediment deformation. This matrix is typically mudstone or

shale, which, prior to lithification, may be highly charged with water and subject to such disruption. Many tectonic and sedimentary melanges therefore originate in accretionary-prism environments which contain water-saturated sediments and are sites of both active faulting and submarine landsliding.

The footwall of the Badwater Turtleback fault contains melange zones in calcite marble mylonite which formed by tectonic disruption of greenschist- to amphibolite-grade metamorphic rocks. These melanges consist of macroscopic zones of variably disrupted foliation associated with inclusions of wallrock of various sizes, shapes, and orientations (Fig. 2-13). This section describes the geometries and internal structures of these zones and illustrates how deformation of rheologically variable rock sequences can lead to progressive disruption of the sequence. These zones are significant because this disruption occurred in metamorphic rock as opposed to non-lithified, water-rich sediment. Furthermore, because the matrix of these zones is predominantly calcite marble, they represent the last stages of ductile deformation in the footwall of the turtleback.

Wallrock

The term "wallrock" is here used to describe all rock in the footwall of the Badwater Turtleback which contains strongly mylonitic fabrics, and was therefore present during deformation of the melange, but is not physically included within the melange zones. The wallrock therefore consists of approximately equal proportions of pegmatite, quartzofeldspathic gneiss, and dolomite and calcite marble. It also contains <.1% quartzite. The gneiss and carbonate marble display variably thick but tabular geometries. The pegmatite, however, forms pod-shaped outcrops which vary in size
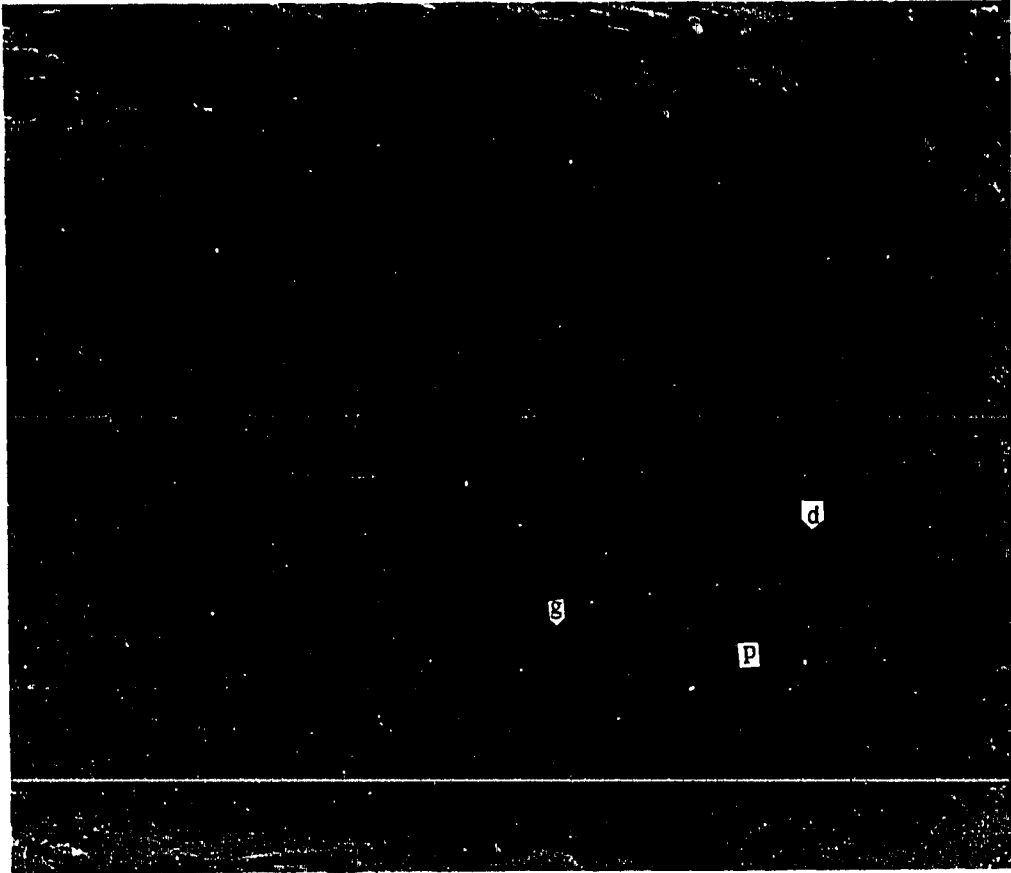
Figure 2-13. Photograph of part of a typical melange zone. Clasts in this photograph are predominantly pegmatite (p) but also gneiss (g) and dolomite (d) in a matrix of foliated calcite marble.

from less than 1 metre to greater than 10 metres in diameter. These pods probably formed during boudinage of the pegmatite at earlier stages of deformation.

Description of melange zones

Scale and Geometry: These melange zones are restricted to calcite-dominated carbonate marbles. They typically lie subparallel to foliation in the wallrock, are tabular but moderately non-planar, and exist at a wide range of scales. Small melange zones may be less than 50 cm thick and 100 cm long, while larger zones may exceed 5 m in thickness and crop out over an area larger than 1 km. Some individual zones exhibit abrupt thickness changes. In general, the smaller, narrower zones are discontinuous in outcrop while the larger zones are continuous.

Because of the outstanding rock exposure on the Badwater Turtleback, the contacts between melange and non-melange are readily visible. Within carbonate rocks, these contacts may be abrupt, where melange sits directly on well-foliated marble, or transitional, where the melange grades into non-chaotic rock over a distance of 10 cm or more. Locally, calcite marble from melange invades well-foliated marble (Fig. 2-14A). Contacts between melange and non-calcite rock are distinct because of the lithologic contrast, but also typically exhibit much invasiveness of calcite into the wall rock. This invasion occurs predominantly along extension fractures in pegmatite, extension fractures and fold limbs in dolomite marble, and along fold limbs in quartzofeldspathic gneiss (Figs. 2-14B, C).

Inclusions: All inclusions in the calcite marble melanges display mylonitic fabrics and have counterparts in adjacent wall rocks. In decreasing abundance, they consist of pegmatite, dolomite marble, and quartzofeldspathic gneiss, with rare quartzite.
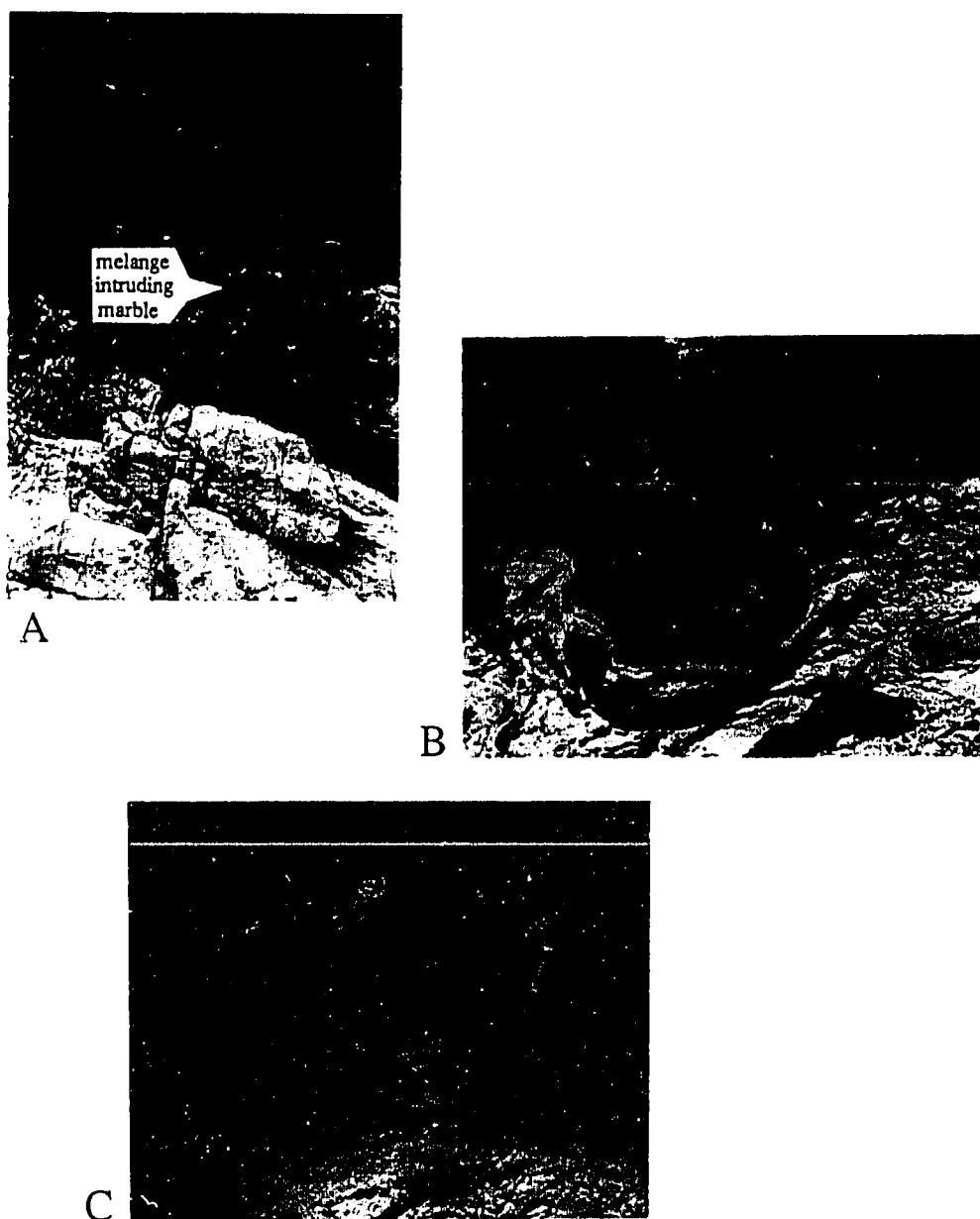
Figure 2-14. Photographs which illustrate invasion of calcite marble melange into wallrock. 2-14A, invasion of melange into non-melange calcite marble. 2-14B, invasion of melange into gneiss along fold limb. 2-14C, invasion of melange into pegmatite.

Inclusions range continuously in size from microscopic to greater than 2 meters in diameter. Many inclusions are asymmetric with respect to the zone in a sense that indicates overall top-to-the-northwest sense of shear. Aspect ratios of all inclusions range from 1:1 to greater than 20:1 but vary considerably according to rock type. Pegmatite clasts tend to be blocky and locally lozenge-shaped while quartzofeldspathic gneiss and rare quartzite inclusions tend to be elongate parallel to foliation in the inclusion. Gneiss and quartzite inclusions are also typically folded. Dolomite marble inclusions may be blocky or elongate. Inclusions of all rock types also show a complete range in angularity.

Extension fractures cut most inclusions but do not penetrate the surrounding calcite-rich matrix. These fractures also affect different rock types to different degrees; they affect pegmatite inclusions the most, followed by dolomite marble, followed by quartzofeldspathic gneiss and quartzite. Many smaller pegmatite and dolomite inclusions appear to have been derived from larger, extensively fractured inclusions because they fit back into the larger clast (Fig. 2-15).

Locally, inclusions appear to be derived directly from wallrock. Individual pegmatite and dolomite marble inclusions may fit back into the wallrock, while gneiss and quartzite can locally be traced into wallrock along severely attenuated fold limbs. This variation suggests different mechanisms of incorporation into the melange. Edges of pegmatite and dolomite bodies fractured and became incorporated while gneiss and quartzite became folded and transposed in with the melange.

Matrix and foliation in melange zones: The matrix consists of predominantly very fine-grained (10-100 um) calcite and various undetermined alteration products. EDS analysis of these products showed that they contain widely varying proportions

Figure 2-15. Photograph of broken pegmatite inclusion in melange zone.

of Mg, K, Al, Ca, and Fe, but their fine grain sizes precluded a rigorous examination. Relative proportions of calcite to alteration products also vary. In some places, the matrix consists of nearly pure calcite; elsewhere it consists of approximately equal proportions of calcite and alteration products. Scattered grains of quartz, plagioclase, white mica, actinolite, diopside, and talc "float" within the matrix. These crystals may exceed 1 mm in diameter.

In thin section, foliation is defined primarily by alternating bands of variably sized fine-grained matrix material. Calcite grains within these bands are dominantly equigranular but locally elongate in the plane of the foliation (Fig. 2-16). Foliation is also expressed in some places by white mica or talc with a planar-preferred orientation.

In outcrop, foliation in these melange zones ranges from penetrative and planar to dramatically non-planar to non-existent. The style of foliation closely corresponds to the abundance of fist-sized or larger inclusions within that part of the zone. As general rules: planar foliation is best preserved where there are the fewest inclusions; foliation wraps around inclusions; foliation becomes increasingly disrupted with increasing numbers of inclusions; strongly expressed planar foliation can grade into nonfoliated rock in places with numerous inclusions. Furthermore, stretching lineations are found on some foliation surfaces. Their azimuthal directions locally change markedly in close proximity to inclusions.

Discussion and suggested origin of melange zones

The photographs of the melange zones (Figs. 2-13 to 2-16) show that during deformation of the melange, different rock types behaved differently. Calcite marble, which forms most of the matrix material, was extremely mobile. Not only did it deform around the sides of inclusions and wallrock, but it invaded fractures within

Figure 2-16. Photomicrograph of calcite marble from melange zone.

those rocks. By contrast, pegmatite inclusions behaved rigidly; they are highly fractured and show little evidence for internal deformation within the melange zones. Between these two extremes, dolomite marble shows more evidence of ductility than pegmatite but it also deformed primarily by fracture; quartzofeldspathic gneiss and quartzite contain relatively few fractures but are instead locally infolded with the melange. These contrasting styles of behavior are further reflected in the shapes and relative abundances of inclusions. In general, those materials with low relative ductilities, such as pegmatite and dolomite marble, exhibit less internal deformation and more fracturing. Consequently, inclusions of these rocks are correspondingly more blocky and more abundant.

All involved rocks, however, contain strongly mylonitic fabrics, so even the "brittle" pegmatite deformed ductilely at one stage in its history. Because pegmatite and dolomite marble inclusions are typically fragmental and blocky, however, most ductile deformation of these rocks occurred prior to their incorporation into the melange zones. Ductile deformation of the gneiss and quartzite, by contrast, must have continued during and after incorporation into the zone.

Much of the rheological variation in the footwall probably reflects progressive uplift, denudation, and consequent cooling of the footwall during late Tertiary extension. Miller (1992) found that the transition from macroscopically ductile to brittle behavior took place for these different rocks at different stages of uplift within the same kinematic regime. This transition occurred first in pegmatite, second in dolomite marble, third in quartzofeldspathic gneiss, and finally in calcite marble. This sequence implies that the last stages of ductile deformation in the footwall occurred within the melange zones because they are supported by a calcite-rich matrix. This conclusion is further suggested by the observations that the melanges 1) contain

inclusions of the wallrock and 2) invade the wallrock. Miller (1992) also reported that these zones cut across mylonitic foliation in all other rock types. Therefore, it is likely that these melange zones reflect higher shear strains than in the rest of the mylonitic footwall of the turtleback.

The style of foliation within and outside of these melange zones reflects the character of ductile flow. Specifically, the plane of the foliation in these mylonite zones is assumed to be approximately the same as the flow plane while mineral lineations represent the azimuthal direction of flow. Therefore, planar-foliated wallrock with unidirectional mineral lineations reflects relatively uniform, two-dimensional flow while the zones of variable foliation and lineation directions reflect disrupted flow. As foliation and lineation directions within the melange zones are widely variable in the presence of either inclusions or protrusions of wallrock, the character of ductile flow must have been greatly disrupted in those places as well. Isolated melange zones between closely spaced pegmatite bodies abound in the footwall. Therefore, disruption of otherwise uniform flow must have served to break up relatively rigid wallrock and incorporate the pieces into the easily deformable calcite marble.

Figure 2-17 illustrates a model for the origin of these melanges. The key feature of this model is that with progressive uplift and cooling, rheological variations between different rock types became increasingly more pronounced. These variations served to increasingly disrupt the ductile flow. At early stages (A), pegmatite sills and dikes boudinaged within carbonate and locally within quartzofeldspathic gneiss. The presence of these rigid blocks in the more ductile calcite marble disrupted the ductile flow in that vicinity; where several pegmatite boudins were in close proximity, they interfered with each other to enhance this effect. Disturbance of an otherwise uniform,
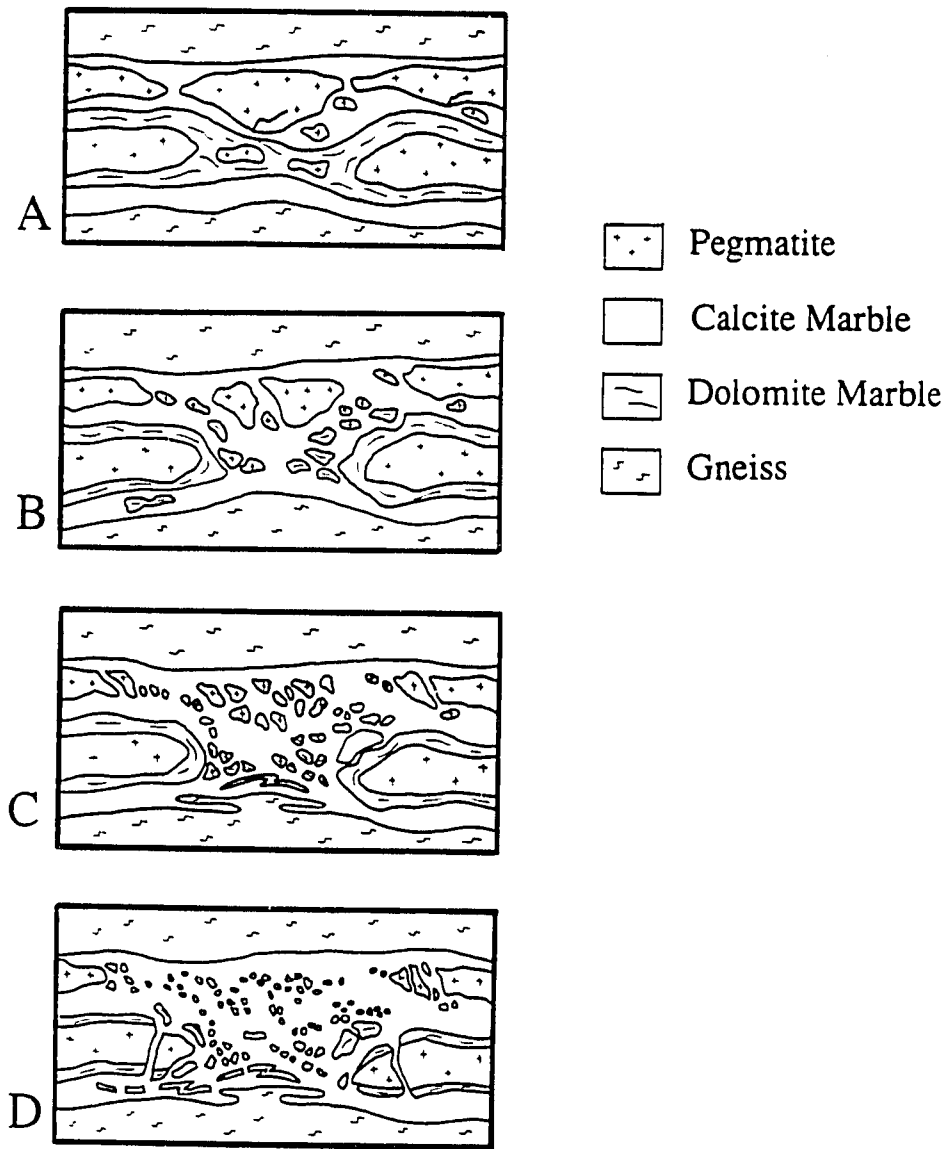
Figure 2-17. Model for origin of melanges. A, early stages: boudinage of pegmatite locally disrupts flow of carbonate. B, boudinage of dolomite and partial disintegration of pegmatite causes further disruption of flow. C, incorporation of folded gneiss into melange zone. Many boudins of dolomite and pegmatite at this stage are broken into relatively small fragments which disrupt the flow throughout the entire zone. D, further breakdown of clasts, without input of additional clasts, allows relatively uniform flow, and henze foliation, to be re-established.

two-dimensional flow path, allowed the extremely mobile calcite marble to intrude fractures within the pegmatite and assist in its disintegration and incorporation into the melange.

At later stages (B), boudinage and fracture of dolomite marble caused it to be incorporated into the zone. At still later stages (C), folds of quartzofeldspathic gneiss and melange became detached within the melange. During each stage, blocks of wallrock which protruded into the melange were continually incorporated into the zone, while inclusions were further broken down. Locally, where protruding wallrock had been abraded sufficiently so that it no longer disturbed the flow, it stopped contributing to the population of inclusions. In these places, inclusions gradually decreased in size to the point where they no longer disrupted the flow but were not replenished by new wallrock. This gradual breakdown of inclusions allowed relatively uniform, two-dimensional flow to re-establish itself and form planar foliation (D). This end product of melange development is a very fine-grained, strongly foliated rock with numerous inclusions which are typically smaller than 1 cm. A continuous layer of it lies 0-10 metres beneath the Badwater Turtleback fault (Fig. 18).

Conclusions

Melange zones on the Badwater Turtleback display a random assortment of variably sized and shaped inclusions set in a matrix of fine-grained calcite marble. The calcite marble was highly mobile during deformation. These melanges, however, formed by deformation of metamorphic rock instead of water saturated sediment. The involved rock was compositionally, and therefore rheologically variable which caused extreme variations in behavior: calcite marble was highly mobile while other rock types

Figure 3-18. Photograph of ledge of fine-grained, strongly foliated melange subjacent to Turtleback fault. This carbonate, labelled "c", crops out over much of the Turtleback surface.

deformed brittlely and disrupted the flow. Similar zones may form in other strongly
deformed zones which also contain a variety of rock types.

Summary and Conclusions

The footwall of the Badwater Turtleback consists of predominantly four rock
types: pegmatite, quartzofeldspathic gneiss, and dolomite and calcite marble. Each
rock type contains mylonitic fabrics which are overprinted by a succession of
increasingly "brittle" structures. Although mylonites and later structures in each rock
type indicate an approximately top-to-the-northwest sense-of-shear, the structures vary
in timing and detail according to lithology. Most importantly, cross-cutting relations
indicate that the transition from macroscopically ductile to brittle deformation took
place first in pegmatite, followed by dolomite marble, quartzofeldspathic gneiss, and
finally calcite marble. The consistent shear sense, sequence of structures, and
contemporaneity of brittle with macroscopically ductile deformation, together suggest
that the structural evolution of the footwall was a product of continuous deformation
within a shear zone which became increasingly cooler through time. Cross-cutting
relations between non-mylonitic dikes and brittle faults in the footwall discussed in
chapter 1, plus a 13.4 Ma biotite age from the gneiss reported by Holm et al. (1992),
indicate that much or all of this deformation took place during late Tertiary extension.

Widely variable orientations of mylonite fabrics within the footwall suggest that
ductile flow was largely heterogeneous, both between different rock types, and within
individual rock types. This heterogeneity was caused primarily by the presence of
relatively rigid parts or inclusions of wallrock that disrupted the flow of more easily
deformable rock. It was therefore a consequence of rheological variability which was
related to compositional differences in the footwall. Furthermore, because rheological

variability probably increased as the footwall cooled, the degree of flow heterogeneity probably increased as well.

The last stages of ductile deformation culminated with the formation of melange zones of variable width and continuity within the calcite marble. These zones, which exhibit many of the same features as sedimentary and tectonic melanges from accretionary prism settings, were products of disrupted ductile flow of the calcite marble. A four-stage model for their origin suggests that rigid wallrock which projected into zones of actively deforming calcite marble disrupted the flow of the marble and also became incorporated into the zone as inclusions. Presence of these inclusions further disrupted the flow. With continued deformation, however, the inclusions broke into progressively smaller particles while wallrock which once protruded into the shear zone became abraded. Consequently, the smaller inclusions disrupted the ductile flow less than the larger inclusions, and wallrock stopped disrupting and contributing inclusions to the flow. At this point, ductile flow became more uniform and re-established a moderately planar foliation.

Chapter Three

ORIGIN AND EVOLUTION OF BRITTLE FAULTS IN THE FOOTWALL OF THE BADWATER TURTLEBACK: A LINK BETWEEN DUCTILE AND BRITTLE BEHAVIOR

Introduction

The transition from brittle behavior in rocks at the earth's surface downward to macroscopically ductile behavior is the focus of much recent theoretical, experimental, and field-based research (e.g. Evans and others, 1990). This transition is important from a seismological viewpoint because onset of ductility in rocks is thought to play a role in limiting depths of brittle faulting and consequent earthquake generation (e.g. Sibson, 1977; Scholz, 1988). It is important from a structural and tectonic perspective because rheological changes in rocks greatly affect the formation of structural fabrics and geometries. Furthermore, an understanding of the rheology of a rock and the operative deformation mechanisms during deformation may lead to inferences regarding temperature conditions of deformation.

At the outcrop scale, interpretations of shear zones as evolving through the ductile to brittle transition rely primarily on the close spatial relationship of mylonitic rocks and brittle fault zones. These interpretations may be ambiguous because similar associations form when brittle faulting postdates mylonitization. Because all mylonitic shear zones which are today exposed at the earth's surface were uplifted through the brittle field, they all potentially contain this ambiguity. A clear-cut outcrop-scale example of the transition from ductile flow to brittle faulting must therefore establish that mylonitization and faulting were not only spatially and genetically related but also contemporaneous.

The Badwater Turtleback preserves evidence for a causal link between outcrop-scale ductile and brittle deformation. This link is apparent because the footwall of the northern half of the Badwater Turtleback (Fig. 3-1, 3-2A, B) is lithologically heterogeneous and therefore conducive to mapping at scales of 1:5000 and greater. There, the footwall consists primarily of four principal rock types: quartzofeldspathic gneiss, dolomite marble, calcite marble, and pegmatite. Each rock type contains strongly mylonitic fabrics. Cross-cutting relations indicate that at later stages of deformation, different rock types behaved differently. As the footwall rose and cooled, ductile deformation gave way to brittle fracture and faulting, first in the pegmatite, second in the dolomite, third in the quartzofeldspathic gniess, and finally in the calcite marble. Chapter 2 described the details of this sequence and suggested that it implied the footwall evolved continuously through the transition from macroscopically ductile to fully brittle behavior. This chapter confirms that conclusion because it links throughgoing brittle faults directly to the ductile deformation.

This chapter therefore describes brittle faults in the footwall of the Badwater Turtleback and shows how they 1) formed in the ductilely deforming footwall as a result of strain incompatibilities and 2) subsequently evolved in response to fully brittle conditions and progressively shallower dip angles. The brittle faults described here belong to two geometrically distinct sets: decollement-style faults which are subparallel to mylonitic foliation, and high-angle faults, which cut foliation at high angles. Miller, (1992) called the decollement-style faults "early stage faults" and suggested that they formed prior to the high-angle faults. This chapter reports new findings that indicate some members of both sets formed concurrently during earliest stages of brittle faulting. While these brittle faults probably account for only a minor proportion of the total strain in the footwall, they are important for two reasons: they mark the transition
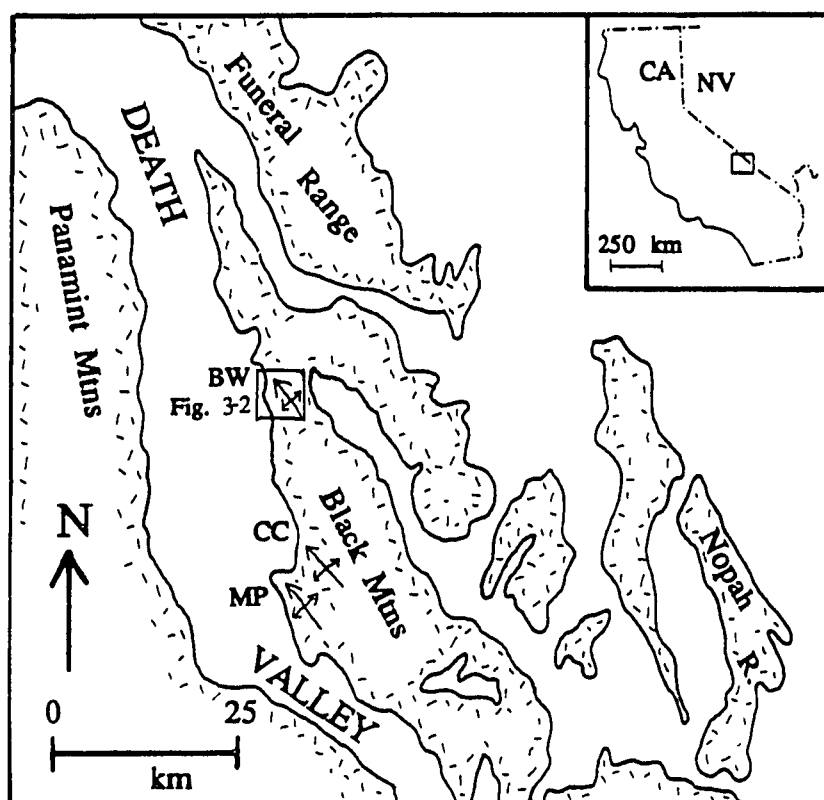
Figure. 3-1 Map of Death Valley region; pattern indicates margins of highlands. Anticlinal fold symbols mark the three turtlebacks: MP, Mormon Point Turtleback; CC, Copper Canyon Turtleback; BW, Badwater Turtleback.
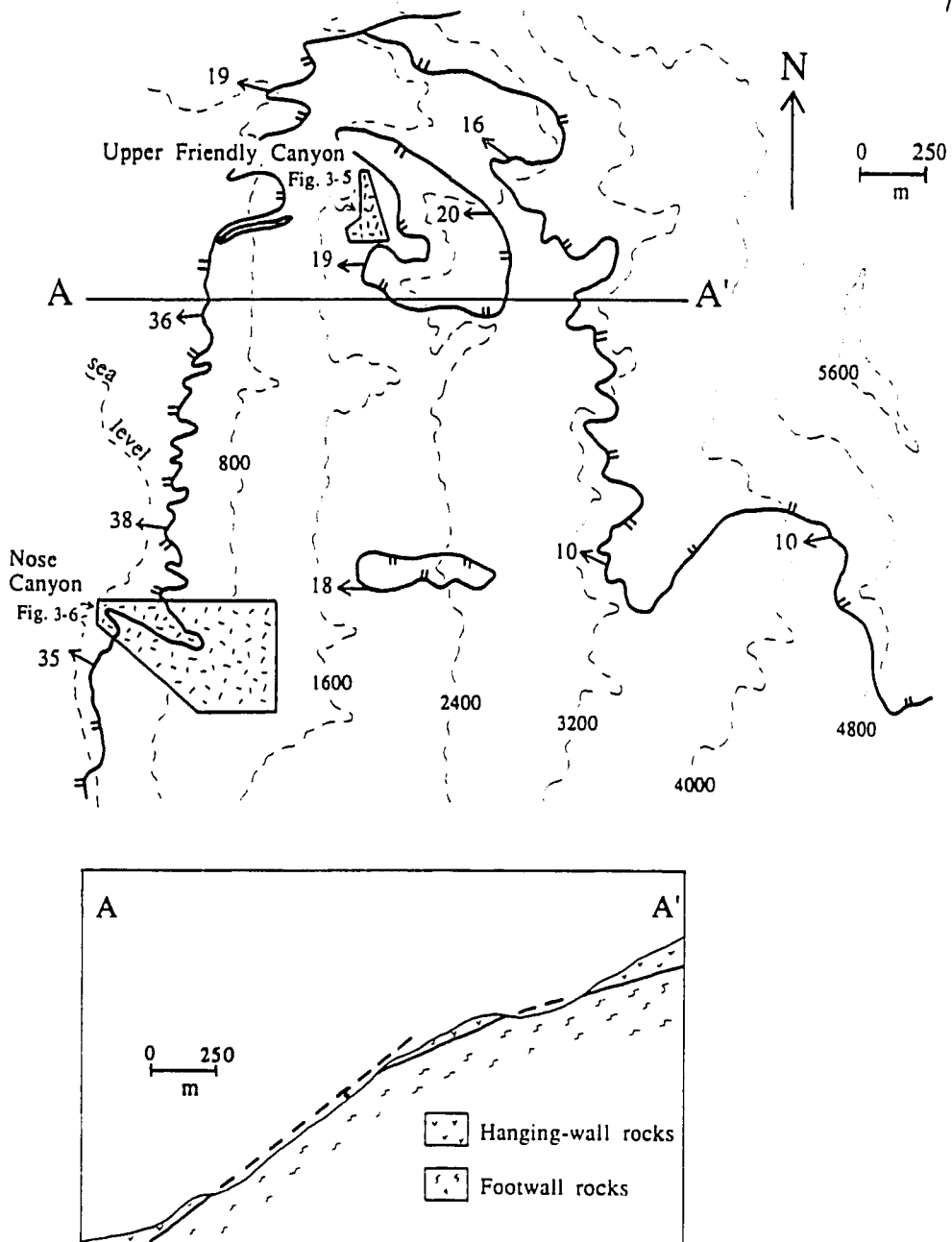
Figure. 3-2. Northern half of Badwater Turtleback. 3-2A. Map showing locations of Upper Friendly and Nose Canyons. Hachured lines mark hanging wall of fault. Dashed lines are 800 foot contours. 3-2B. Cross section from A to A', no vertical exaggeration. Cross-cutting relationship of turtleback fault surfaces from Miller, 1991.

from macroscopically ductile behavior in the footwall to brittle behavior, and they provide insight into possible mechanisms for fault growth and arrest.

Brittle faults of the footwall

Decollement-style faults

Decollement-style faults cut all mylonitic rock types on the Badwater Turtleback, but also typically involve either calcite or dolomite marble. These faults range from single, discrete fault surfaces to 1 meter-thick zones of cataclasis (Fig. 3-3A, B, C). The thicker zones locally exhibit asymmetric foliations which resemble the "P" foliation of Rutter and others (1986), as well as subsidiary shear fractures.

Most decollement-style faults are discontinuous and nonplanar in outcrop. They exhibit this geometry because they 1) locally disappear into subparallel, cleaved foliation, or 2) accommodated low enough strains so as to not develop through-going slip surfaces. In some places, well-defined faults disappear into contacts which are mylonitic but display no evidence for brittle deformation. These discontinuities strongly suggest that the faults accommodated only small amounts of strain.

Locations where calcite marble pinches out into other rock types provides evidence that early-stages of brittle faulting were partly concurrent with mylonitic deformation (Fig. 3-4). These places typically show evidence of faulting; some faults abruptly terminate within the marble while others follow the contact between the marble and the adjacent rock. Furthermore, kinematic data, although limited and somewhat ambiguous, suggest that these faults slipped in roughly the same direction as the mylonitic strain. Two areas on the Badwater Turtleback, described below, illustrate the geometries of the early stage faults as well as their relations to the

Figure 3-3. Photographs and sketches of early-stage fault in Nose Canyon. Heavy solid line in sketches marks main surface of early-stage fault, light solid lines mark minor faults: dashed lines show orientation of foliation. 3-3A. Occurrence of fault as narrow, discrete zone. Note coarse foliation and pegmatite boudins in overlying dolomite marble. West is to the right. Field of view is approximately 20 metres. 3-3B. Cataclastic zone within fault. West is to the right. Note fault that ends downward into the fault zone at the right-hand corner of the photograph. 3-3C. Small-scale duplex along fault zone. Note also the fault which ends downwards into the fault zone. West is to the right.

A

pegmatite

dolomite marble

gneiss

B

dolomite marble

gneiss

C

dolomite marble

gneiss
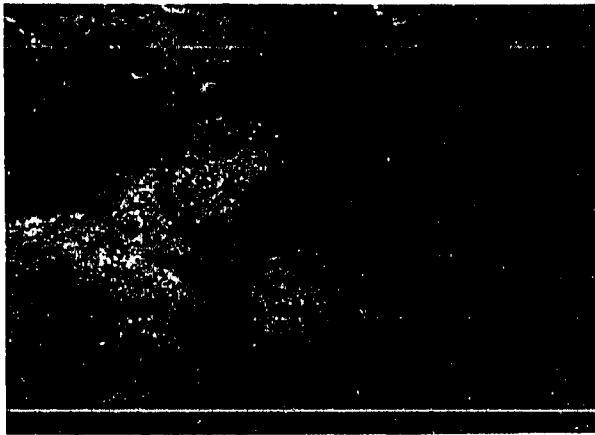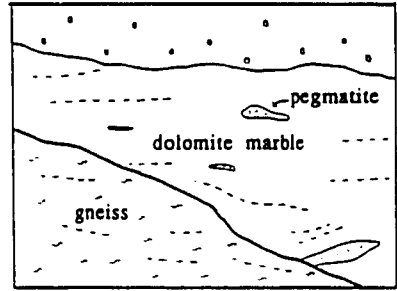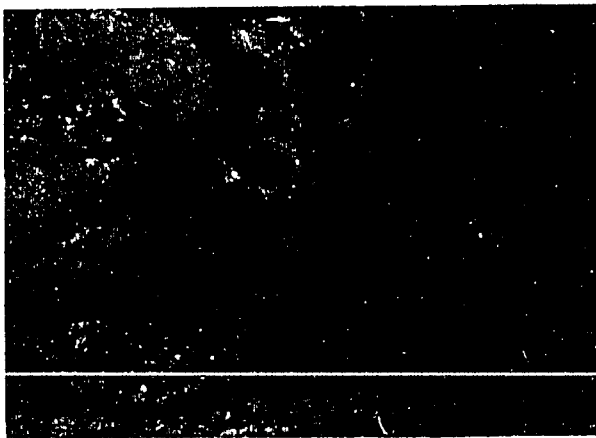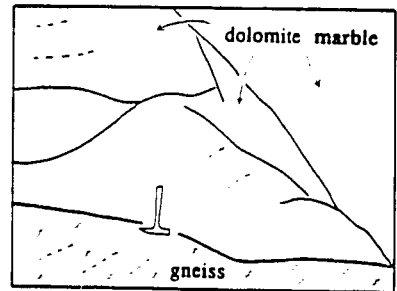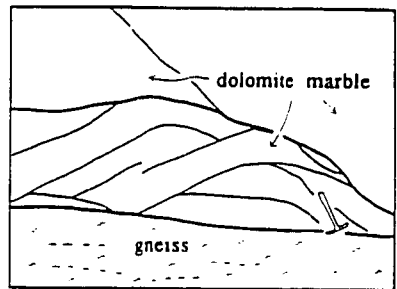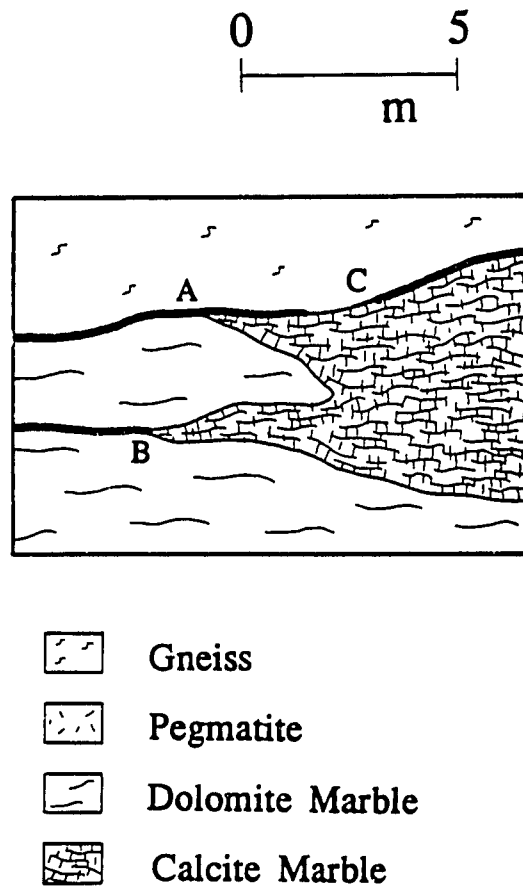
Figure 3-4. Idealized drawing which illustrates concurrent mylonitic deformation and brittle faulting. At A, brittle fault occurs along contact of pinched-out calcite marble and adjacent rocks. At B, brittle fault terminates at location of pinch-out of calcite marble. At C, brittle fault is discontinuous. Scale of figure is approximate.

mylonitic rocks particularly well. These areas, here informally named "Upper Friendly Canyon" and "Nose Canyon" (Nose Canyon after Curry, 1954) are shown on figure 3-2A. The early stage faults in Upper Friendly Canyon define a zone of discontinuous faults (Fig. 3-5). The fault in Nose Canyon is relatively continuous and occurs as a single fault surface over much of its length (Fig. 3-6).

Upper Friendly Canyon: Two zones of decollement-style faults crop out in Upper Friendly Canyon (Fig. 3-5). Both zones are cut by later, high-angle faults. These zones are markedly non-planar but are defined by numerous, nearly planar, individual fault segments. While the fault zones occur principally at the contact of mixed calcite and dolomite marble with gneiss and pegmatite, parts of numerous fault strands occur entirely within the marble.

The structurally higher fault zone is especially well exposed. It lies about 30 meters below the turtleback fault; carbonate makes up its hanging wall and gneiss makes up its footwall. A close look at the map and cross section of figures 3-5A, and 3-5B shows that this decollement-style fault zone is associated with calcite marble that pinches out southward between dolomite and gneiss. This attenuation in the calcite marble appears related to large-scale boudinage of dolomite marble which pinches out northward into the calcite marble. Figure 3-5C shows an interpretation of this structure with the later-stage brittle faults and pegmatite removed.

On the north sides of the figures 3-5A, 3-5B, and 3-5C, the carbonate consists of calcite marble with thin, discontinuous layers of dolomite near its base. On the south sides, the carbonate consists of dolomite marble with a thin, discontinuous layer of calcite marble along its base. In the middle of the map and cross-section, dolomite and calcite marble are interlayered and cut by numerous decollement-style faults.

Figure 3-5. Map, cross-section, and schematic interpretation of Upper Friendly Canyon. 3-5A, map of Upper Friendly Canyon. 3-5B, cross-section from A to A'. 3-5C, schematic interpretation of Upper Friendly Canyon. Dashed-dotted line shows 1800 and 2000 foot contours. Open circles near center of map show location of colluvium. Although cross-section is oblique to transport direction, it shows a southward pinch-out of calcite marble between dolomite and gneiss. The two locations marked "B" indicate places where individual brittle faults terminate at small pinch-outs of calcite marble.

A'

A

B

2000'

1800'

30

20

40

15

61

22

37

40

25

314

39

B

N

metres

0   100
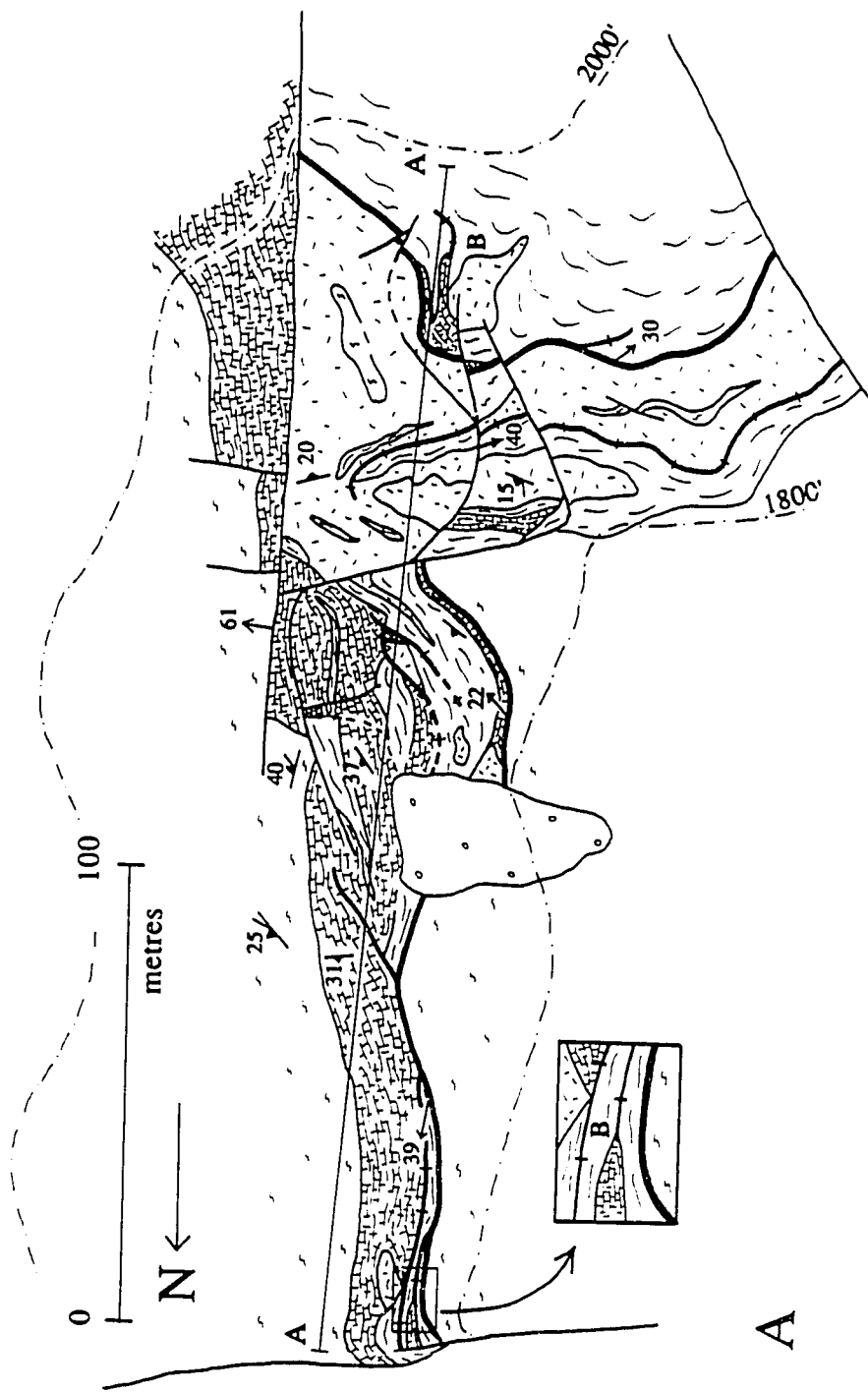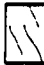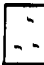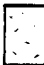
Figure 3-5 (continued).
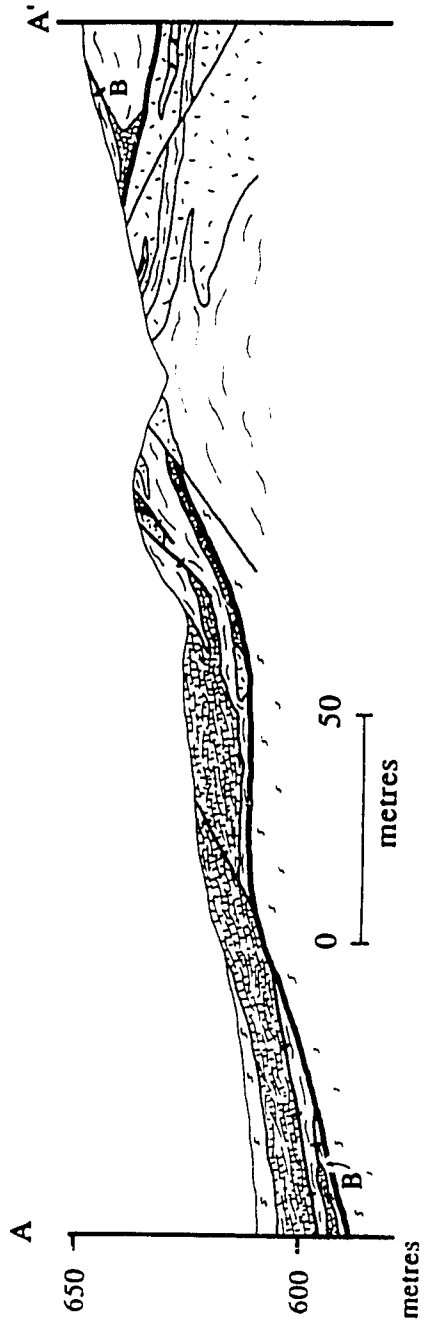
Dolomite Marble

Calcite Marble

Gneiss

Pegmatite

Main surface of early-stage fault

Minor early-stage faults

Later - stage faults

650

600

metres

A

A'

B

B

50

0

metres

B

C

~ 200 m
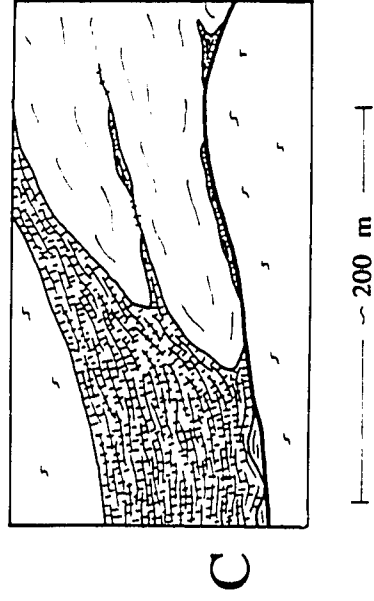
There, the dolomite pinches out into the calcite marble. The main fault follows the gneiss-carbonate contact along discontinuous layers of highly strained calcite marble below the dolomite boudin. Because the fault cuts calcite marble rather than terminates within it, the fault resembles fault "A" of figure 4. Some individual fault strands, marked "B" on figure 5, do terminate within layers of calcite marble. These faults resemble fault "B" of figure 4.

Limited kinematic evidence suggests that hanging-wall transport on this fault zone was approximately parallel to the transport recorded in the mylonitic rocks. Although striated fault surfaces are rare, small-scale faults with visible separations and asymmetric foliations exist locally within the fault zone. Both sets of features suggest normal, top-to-northwest, transport.

Nose Canyon: The fault in Nose Canyon separates gneiss in its footwall from predominantly dolomite marble in its hanging wall (Fig. 6A). Although this fault is continuous over much of its length, it is non-planar because it follows a deformed lithologic contact. Like the fault zones in Upper Friendly Canyon, this fault is also cut by later high-angle faults.

The fault in Nose Canyon also resembles the zone in Upper Friendly Canyon in that it is associated with a pinched-out layer of calcite marble. This marble appears near the eastern edge of figure 6A. The marble pinches out into gneiss at locations "A" and "B" on figures 6A and 6B. To the southwest, at "C" (figs 6A, 6C), the calcite marble must pinch out within gneiss or between dolomite marble and gneiss because it does not occur on the opposite side of the canyon.

The fault in Nose Canyon differs from the zone in Upper Friendly Canyon, however, in that the fault is traceable only where it cuts dolomite and gneiss; it

Figure 3-6. Geologic relations in Nose Canyon. 3-6A, simplified map of Nose Canyon. 3-6B, cross section from A to A'. 3-6C, cross-section from B to B'. 3-3A, B, C do not show outcrops of pegmatite and areas mapped as calcite marble also contain a minor proportion of dolomite marble. 3-6D, orientations of striations on variably oriented surfaces of early-stage brittle fault in Nose Canyon. Note that most striations occur in the northwest or southeast quadrants.

N

0   100
metres

Dolomite Marble

Calcite Marble

Gneiss

Rock not discussed in text.
Dominantly carbonate in canyon bottom.

Badwater Turtleback fault

Early-stage fault

Canyon or wash bottom;
arrow points downhill; lines mark cliffs.

A

A'

B'

B

B

C

22

24

5

35

70

16

36

34

22

4

27

25

12

16

35

16

83
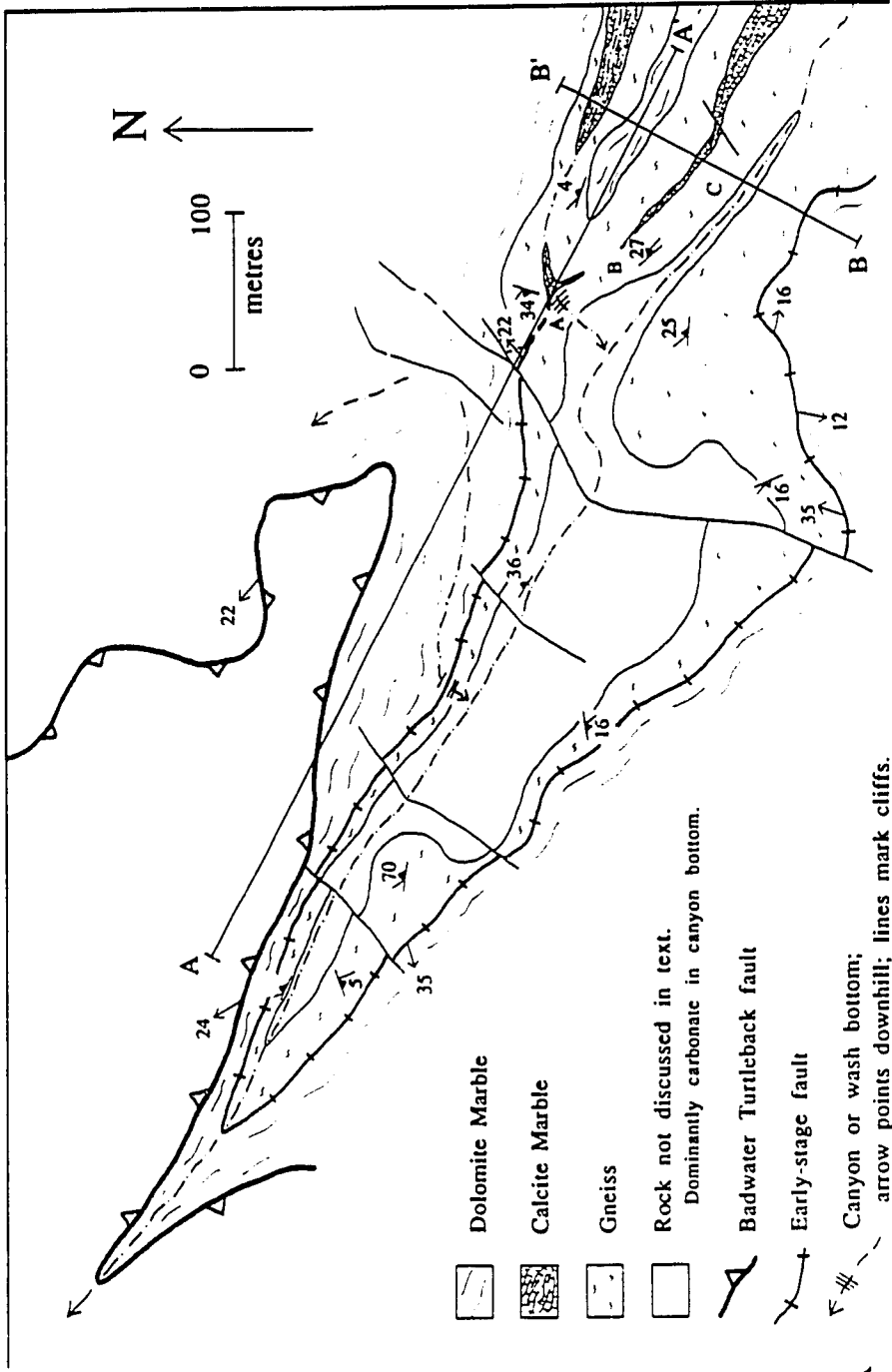
Figure 3-6 (continued).
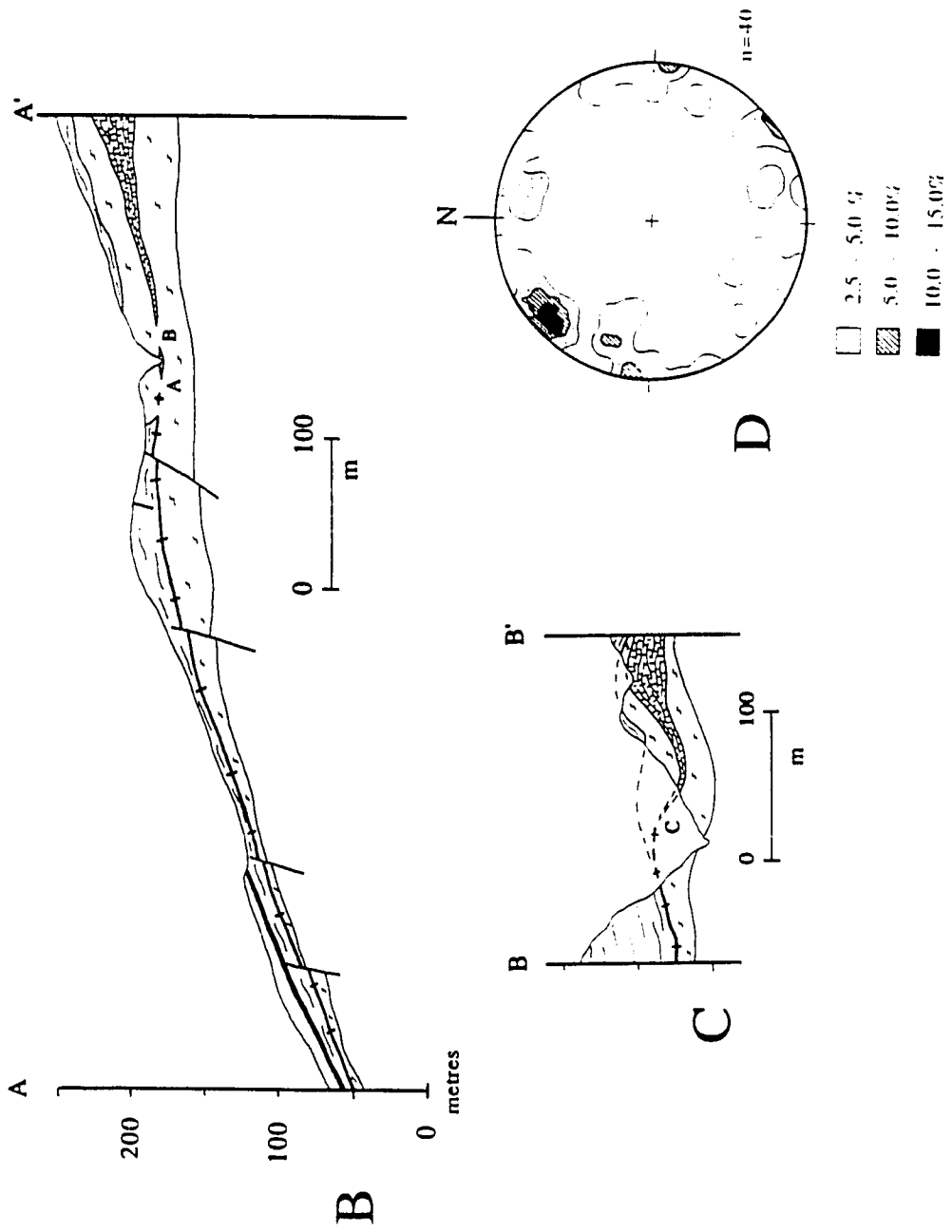
typically does not occur at the calcite marble-gneiss contact. The fault therefore resembles fault "B" of figure 4. The calcite marble at the contact exhibits features characteristic of especially high strains. These features include grain sizes that are less than 10 um in diameter, locally enhanced foliation, and variably-sized and rotated inclusions (<1 cm to >50 cm in diameter) of gneiss, pegmatite, and dolomite marble.

The dolomite and calcite marbles in Nose Canyon display far less interlayering than they do in Upper Friendly Canyon. Farther north, however, beyond figure 3-6A, calcite and dolomite marble are interlayered at a scale of about 1 meter. There, faulting along the gneiss-marble contact is more similar to that in Upper Friendly Canyon in that it typically is discontinuous and may also occur in zones. Faulting is more prevalent where dolomite is the dominant rock type at the contact.

Kinematic data from the fault in Nose Canyon suggest that its movement direction was similar to the sense of shear recorded in the mylonitic rocks. Striations on variably oriented fault surfaces concentrate in the northwest and southeast quadrants (Fig. 3-6D). Directional indicators within the fault zone, consistently suggest northwestward transport of the hangingwall. These indicators include many smaller faults with normal, top-to-northwest, separations that root into the main fault surface as well as northwest-verging imbricated blocks and small-scale duplexes (Fig. 3-3B, C). Stretching lineations, combined with predominantly S-C fabrics and asymmetric porphyroclasts within mylonitic gneiss, and rare lineations and asymmetric fabrics in the dolomite all indicate top-to-northwest transport.

High-angle faults

High-angle faults are the most abundant and obvious fault type in the footwall. They typically strike roughly north-northeast, dip moderately westwards, and show

normal separations. These faults range from less than 1 m to greater than 500 meters in length, and penetrate to the deepest levels of the exposed footwall. They exist as single, discrete fault surfaces, or variably wide (0-2 m) zones of anastomosing slip surfaces. Individual surfaces are locally unmineralized, but typically host Fe-oxides.

These high-angle faults are typically planar, but locally show both convex-upwards and downwards geometries. In map view, individual faults are strongly segmented, with numerous right- and left-stepping en echelon segments (Fig. 3-7). Individual segments locally die out within strongly foliated quartzofeldspathic gneiss or marble. The two large faults in Tank Canyon, for example (Fig. 3-7), cannot be traced south of the canyon.

The high-angle faults display evidence for a protracted history of slip. Some of the smaller high-angle faults terminate abruptly at calcite shear zones by ending downwards at high angles to the zone (Fig. 3-8). This situation implies that these faults slipped concurrently with ductile strain in the calcite marble. Most high-angle faults, however, cut all rocks in the footwall, including calcite marble and non-mylonitic dikes and sills; some high-angle faults even cut the Turtleback fault (see chapter 5). Therefore, high-angle faulting affected the footwall during late stages of ductile strain, and during the most recent episodes of brittle faulting.

Slip on these faults was probably right-lateral normal. As a group, high-angle faults contain abundant evidence for normal as well as strike-slip motion; evidence regarding the direction of the strike-slip component is more rare, but the overall right-lateral geologic setting of Death Valley and some local features suggest it is right-lateral. Striations do not exist on most fault surfaces, but those that were found pitch from 0 to 90° (Fig. 3-9). Almost every observed high-angle fault showed normal separations, but as the thicknesses of particular units do not match on either side of
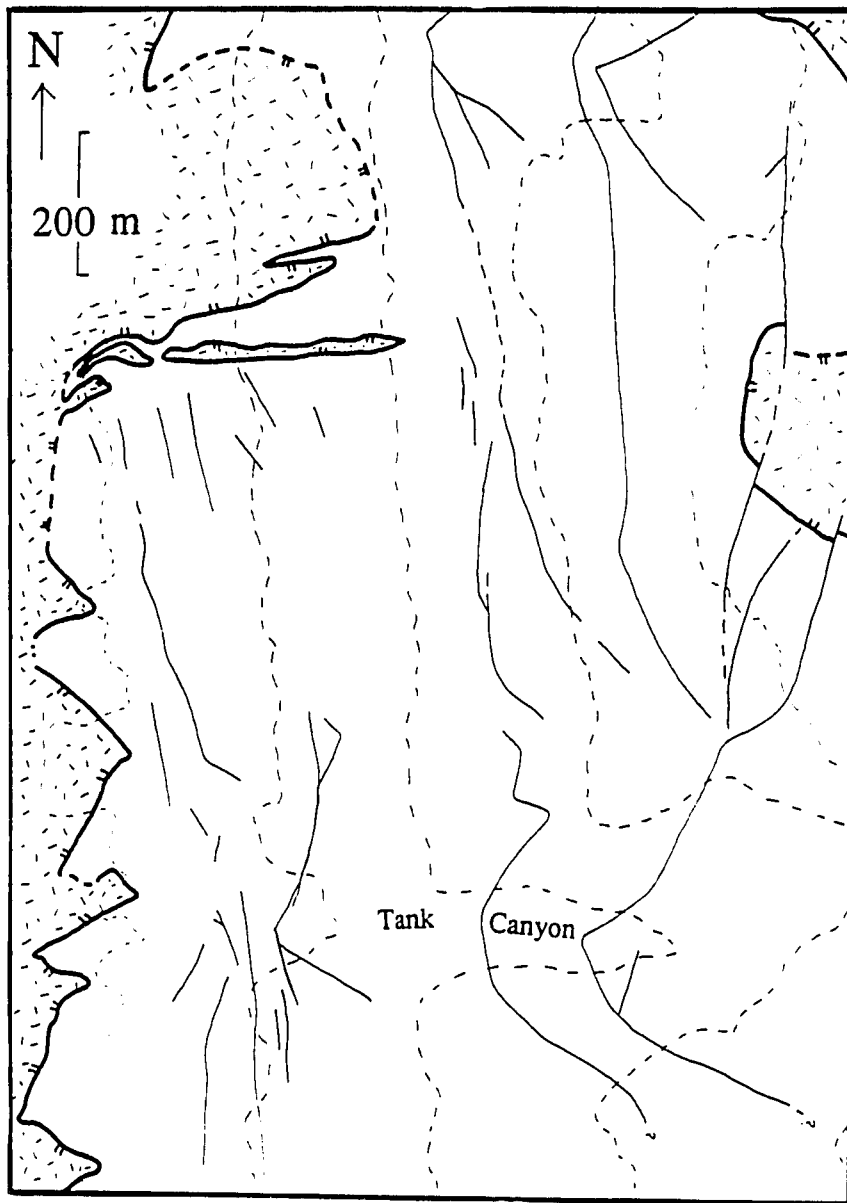
Figure 3-7. Map showing high-angle faults in the footwall of part of the Badwater Turtleback. heavy line with barbs denotes turtleback fault; dashed lines show 400' contours. Question marks indicate locations where the two large faults in Tank Canyon can no longer be traced.
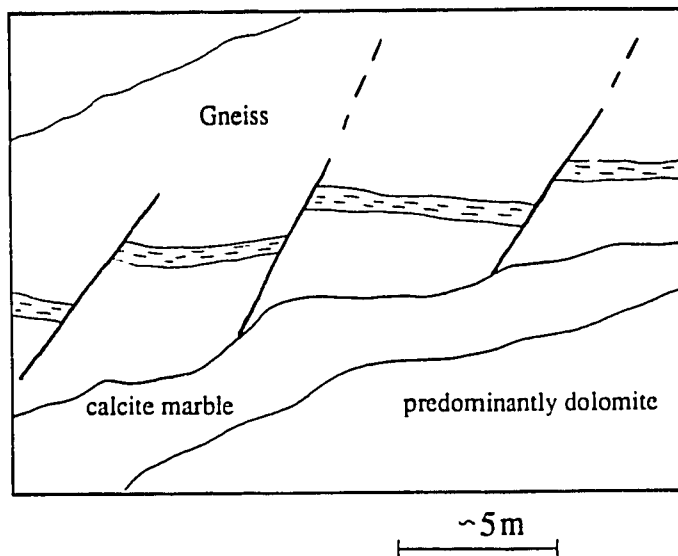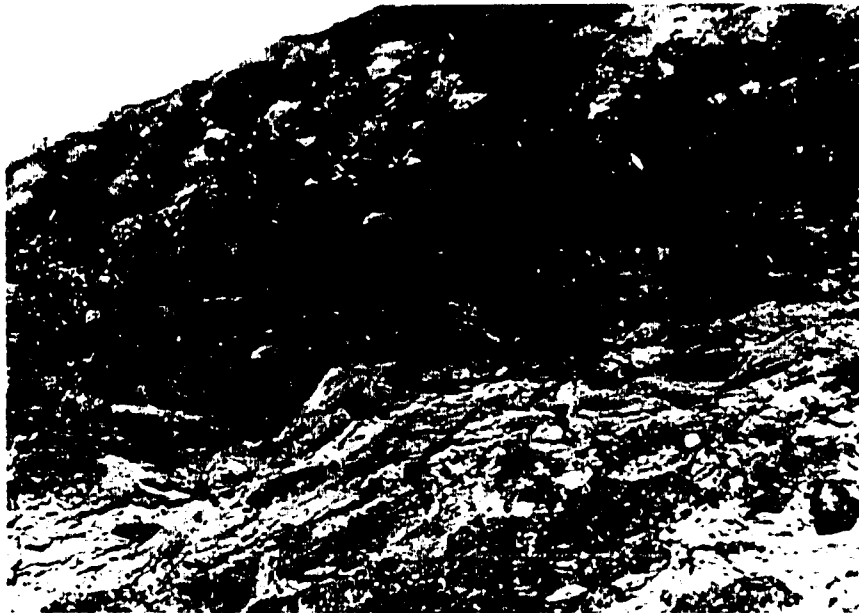
Figure 3-8. Photograph and accompanying sketch of high-angle faults in gneiss which end downwards into calcite marble shear zone (tan). Note brittle faulting in shear zone, parallel to foliation.
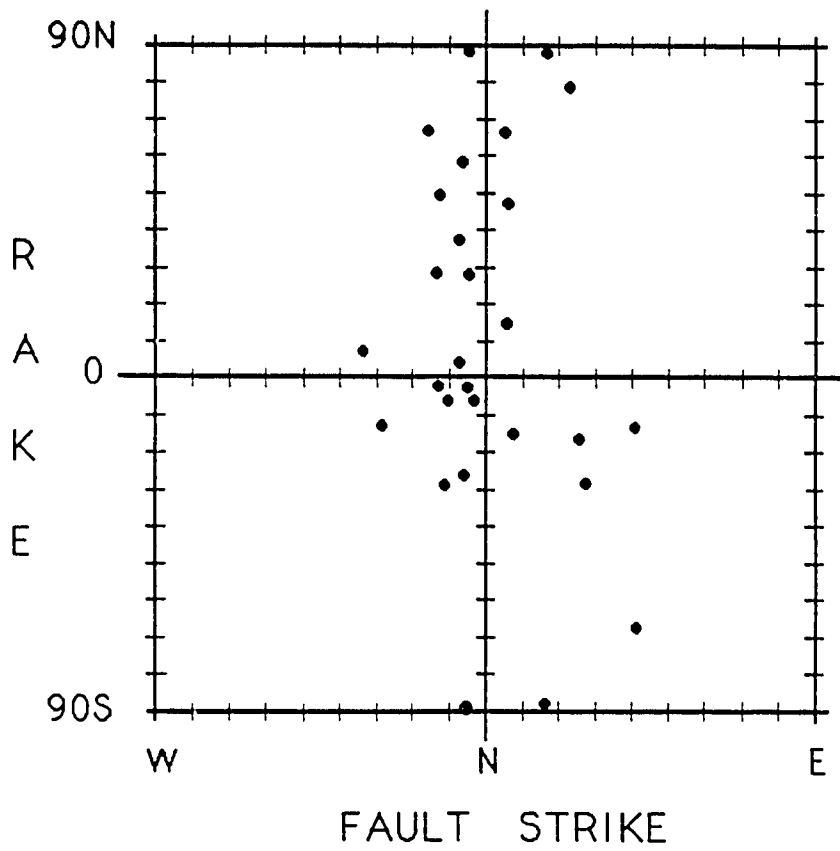
Figure 3-9. Graph of striation rake vs. strike of some high-angle faults. It illustrates the strike-slip component of many high-angle faults.

many of these faults, they must have also had a strike-slip component to their motion. For example, quartzofeldspathic gneiss in the footwall of fault "A" on figure 3-5A is much thicker than it is in the hangingwall. Figures 3-10A and 3-10B gives a similar example of thickness variations across a high-angle fault, but also suggest that the fault had a right-lateral component of slip. There, the gneiss in the footwall is much thinner than in the hanging wall on the north side of the canyon. As the gneiss in the footwall thickens to the south, however, slip on the fault can be approximately restored by right-lateral motion.

Spatial and Cross-cutting Relations between High-angle faults, Decollement-style faults, and Calcite Marble Shear zones

Figure 3-11 and Miller (1992) summarize the complex relationship between calcite marble shear zones and these two sets of faults. Many decollement-style faults reoccupy calcite marble shear zones, labelled "cm" in figure 3-11. High-angle faults, however, relate to the decollement-style faults and calcite shear zones in either of four ways. Each relationship is labelled "A", "B", "C", or "D" on figure 3-11. Faults labelled "A" in figure 3-11 end abruptly at calcite shear zones in the manner of figure 8, while those faults labelled "B" cut the shear zone and join the brittle decollement. Faults such as "C" cut and offset both the shear zone and decollement, but merge with the decollement in their hangingwalls. Most of the high-angle faults, including all large high-angle faults, however, cut both the calcite marble shear zones and the decollement-style faults. These faults are labelled "D" in figure 3-11.

Faults A, B, and C display domino-style rotation as they end downwards into either a ductile or brittle decollement respectively. Fault A, however, terminates at the calcite marble, whereas faults B and C maintain their integrity as discrete fault surfaces within the decollement-style fault zone (Fig. 3-11, inset). These faults actually cut part
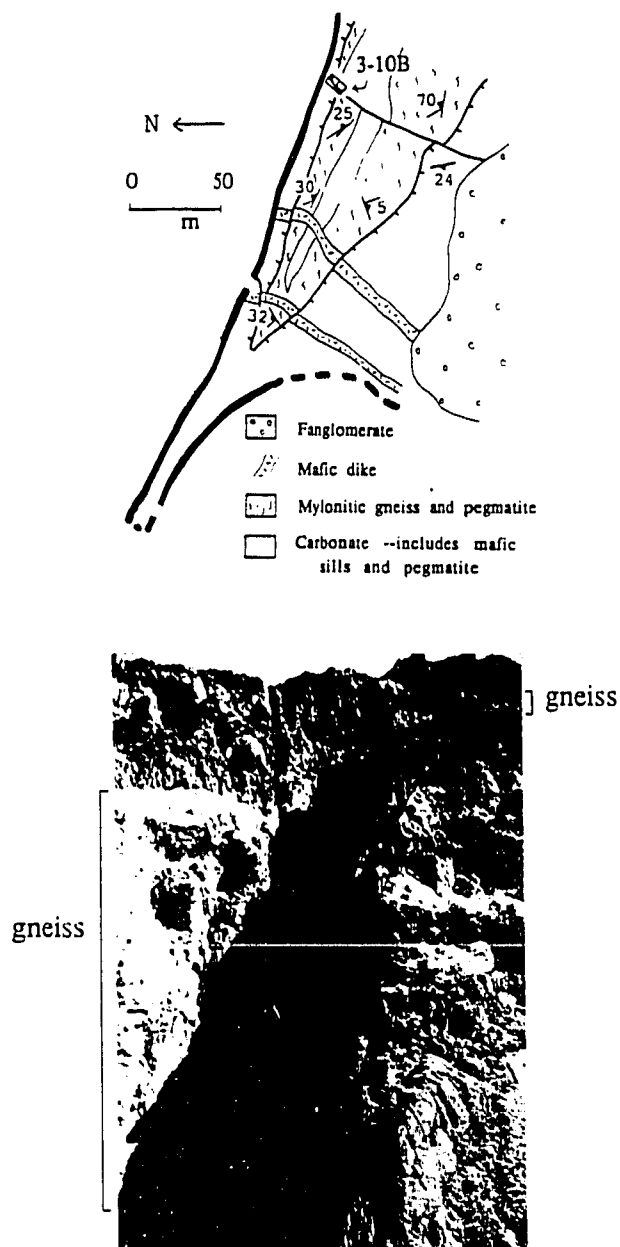
Figure 3-10. Map and photograph of high-angle fault relations in Nose Canyon. 3-10A, map of lower Nose Canyon. Gneiss thickens southward. Note that, on the north side of the canyon, the thickness of gneiss in the footwall is much less than in the hangingwall of the fault; to the south, the gneiss in the footwall becomes thicker. 3-10B, photograph of high-angle fault on north side of Nose Canyon.
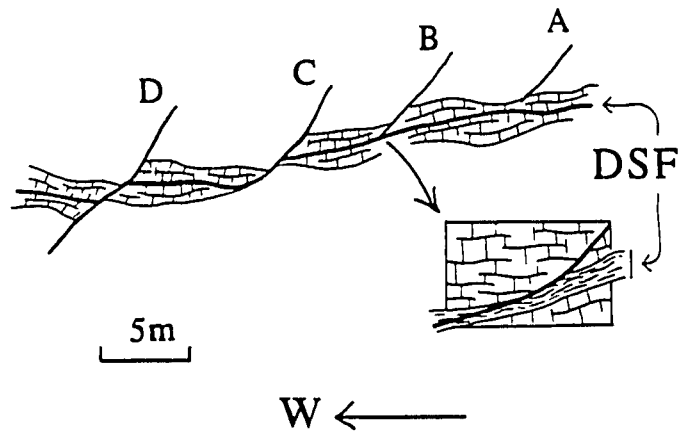
Figure 3-11. Schematic diagram which illustrates various relations between high-angle faults and decollement-style faults (DSF). Scale is approximate.

of the decollement zone; fault B cuts a relatively small part of the zone while fault C cuts the entire zone in its footwall. Slip on these faults, which must postdate at least some of the slip on the decollement, is therefore transferred into further slip on that part of the decollement which is in the hangwall of faults B and C.

Suggested origins of brittle faults within the ductile to brittle transition

Decollement-Style faults

Decollement-style faults in the footwall of the Badwater Turtleback exhibit a strong dependence on rock type. They lie subparallel to mylonitic foliation and nearly everywhere cut two different rock types, one of which is typically a carbonate. Furthermore, these fault zones may be markedly non-planar where they follow non-planar lithologic contacts.

Given that the four principal rock types of the mylonitic footwall evolved through the ductile to brittle transition at different stages of denudation, the locations of faults at lithologic boundaries suggests that differences in rock rheology probably controlled the faulting. Further evidence for a rheologic control lies in the relation of the faulting to the ductile deformation: faulting and mylonitization were partly concurrent, and they record approximately the same sense of shear. Such a rheologic control is significant because it may be used to predict where faulting may initiate in a deforming, layered medium.

A rheologic control also suggests two mechanisms by which ductile deformation may actually cause brittle faulting. First, (Fig. 3-12), ductile deformation involving mylonitization of rheologically stratified rocks causes extreme thickness variations of all rock types. As the footwall rises and cools, ductile deformation becomes restricted to progressively weaker rock types. Eventually ductile strain
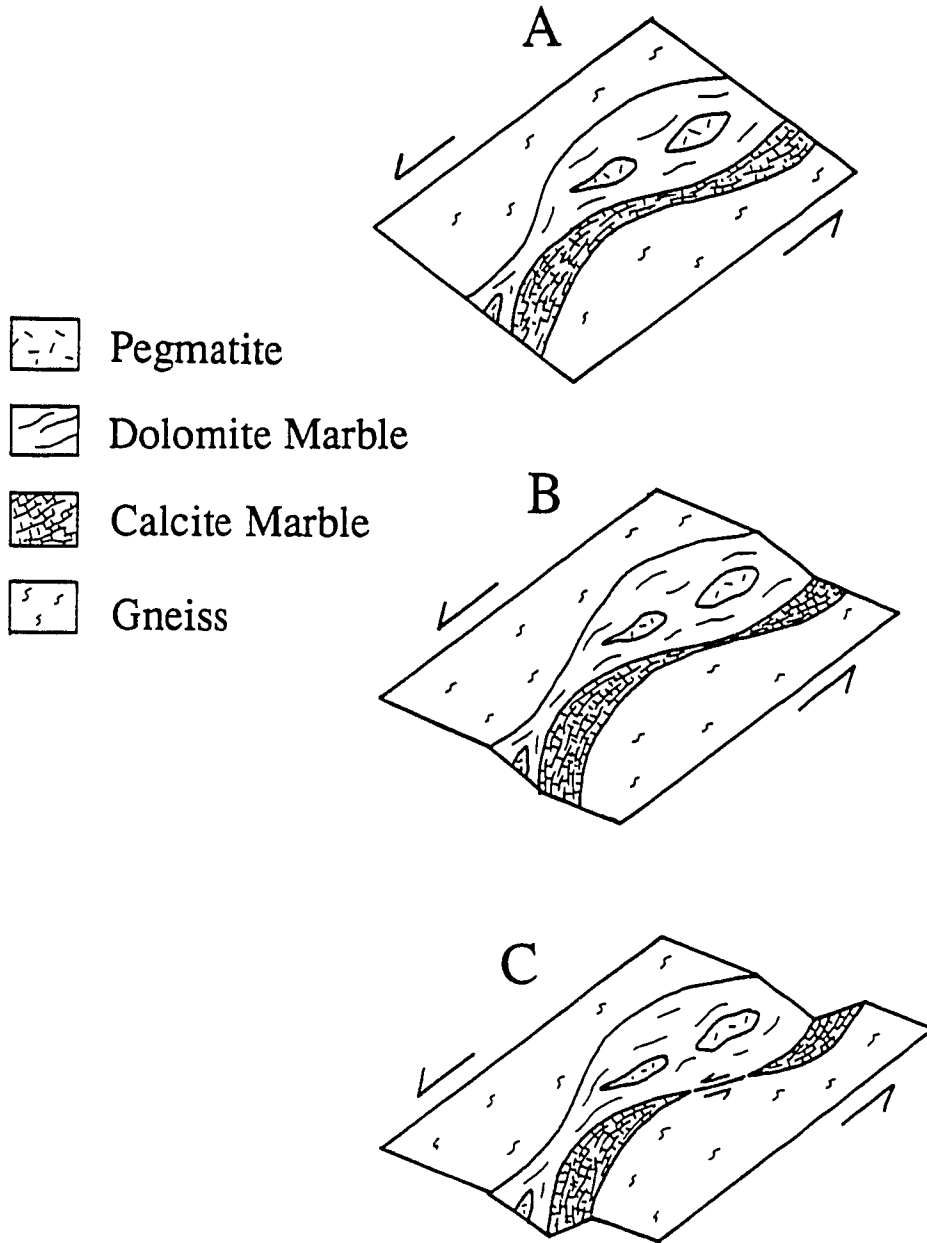
Figure 3-12. Model for initiation of brittle faults. At A, strain is distributed throughout the footwall because all rock types except pegmatite are deforming by predominantly crystal-plastic mechanisms (ductilely). Pegmatite occurs as boudins. B. Dolomite marble stops deforming ductilely; therefore further strain is partitioned into gneiss and calcite marble. C. Only calcite marble deforms ductilely. Where it pinches out, brittle faults form within adjacent rock.

occurs only within one rock type and all other rocks must deform by brittle mechanisms. Where the ductilely deforming rock type pinches out between brittle rocks, the resulting strain incompatibility causes fracturing and faulting in the surrounding rock. Such faulting will necessarily occur subparallel to lithologic contacts; if these contacts are nonplanar, the faulting will initially be discontinuous and nonplanar. At later stages, the fault may break through the rock which had been deforming ductilely and become more planar and continuous.

By the second mechanism, ductile deformation of rheologically stratified rocks causes preferential fracturing at rheologic boundaries. This fracturing is simply the product of local strain incompatibilities which form where two greatly different materials are forced to deform adjacent to each other. Goods and Brown (1979) found that cavities form along edges of inclusions in otherwise ductilely flowing matrix material. These cavities facilitate fracturing of the material with further deformation. This second mechanism may explain many of the smaller decollement-style faults which lie at lithologic contacts but cannot be tied to pinched-out calcite marble.

High-Angle faults

Unlike decollement-style faults, high-angle faults typically cut all rock types and do not show an immediate lithologic control. These faults are more difficult to evaluate because their long slip histories precludes a definite understanding of the controls on their initial geometries and kinematics. Small high-angle faults that cut only pegmatite or dolomite and are surrounded by unfaulted calcite marble, however, indicate that, during mixed brittle and ductile deformation some high-angle faulting was controlled by rock type: faults cut those rocks which could not deform ductilely.

Similarly, the high-angle faults labelled "A" in figure 3-11 are restricted to quartzofeldspathic gneiss and end downwards at calcite marble.

A possible explanation for these early-stage high-angle faults is that they initially formed as shear or extension fractures to accommodate local extensional strains within brittle hangingwalls of calcite shear zones. Therefore, these faults, like the decollement-style faults, formed in response to ongoing ductile strain in the calcite marble. This mechanism applies only to those high-angle faults which formed during mixed brittle and ductile deformation. Many of the high-angle faults of the footwall probably formed at later stages when the footwall was fully brittle.

Evolution of brittle faults

Although decollement-style faults and many of the high-angle faults originated during mixed ductile and brittle deformation, many of the faults now cut calcite marble shear zones and so must have continued to slip after the footwall became fully brittle. The evolution of these faults was affected by two major changes in the footwall: the transition to fully brittle deformation and the continual eastward rotation of the footwall. Miller (1991b and next chapter) suggested that the Badwater Turtleback fault system and its footwall rotated more than 35° eastward during late Tertiary extension.

Figure 3-13 illustrates the evolution of these faults in four stages. At the earliest stage (Fig. 3-13A), calcite marble deformed ductilely while the rest of the footwall deformed brittlely. During this time, decollement style faults formed at lithologic contacts within ductilely deforming rocks and at places where calcite marble pinched out into brittle rocks; high-angle faults formed within brittle rocks and terminated at the calcite shear zones. As the footwall continued cooling and calcite marble started to fracture (Fig. 3-13B), decollement-style faults grew along the calcite
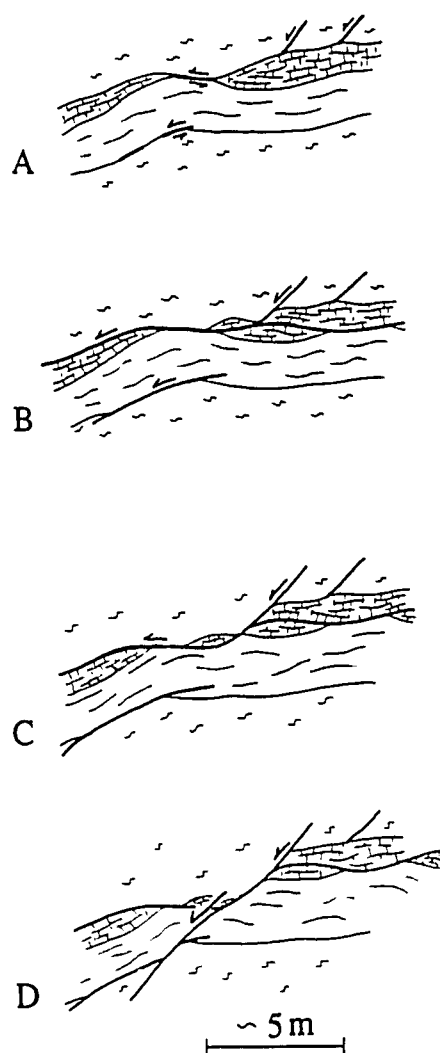
Figure 3-13. Evolution of brittle faults. In each diagram, active faults are shown with arrows; inactive faults have no arrows. 3-13A, onset of brittle faulting; decollement-style faults form at pinch-outs of calcite marble and along rheologic boundaries; high-angle faults form in brittle upper plate of calcite shear zone. 3-13B, onset of fully brittle conditions. Decollement-style faults grow while some high-angle faults break through calcite marble and join the decollement. High-angle faults slip to accommodate extension in upper plate of decollement. 3-13C, decollement-style fault slips only in response to slip on high-angle fault. High-angle fault cuts off decollement-style fault in its footwall. 3-13D, high-angle fault breaks through and offsets decollement.

shear zones while high-angle faults broke through the calcite and joined them. At this stage, the decollement-style faults acted as true decollement because they detached an upper from a lower plate. The high-angle faults, however, eventually became the principal slip surfaces; slip on them was transferred onto the decollement in front of the high-angle fault. Continued slip on these high-angle faults gradually offset the decollement (Fig. 3-13C). Eventually, high-angle faults broke through the decollement as a distinct fault surfaces (Fig. 3-13D). Other high-angle faults, unrelated to this mechanism, probably formed at any time after the earliest stages of mixed ductile and brittle behavior.

Continual eastward rotation of the footwall explains the cessation of slip on the decollement-style faults and the increasing dominance of the high-angle faults. Eastward rotation would cause both sets of faults to rotate to lower angles. The decollement-style faults, which were already at fairly low angles, would be unfavorably oriented for continued slip, while the high-angle faults would still be suitably oriented. Eventually, the high-angle faults found it easier to break completely through the decollement rather than continue to root into it.

Discussion

The early-stage faults and footwall rocks of the Badwater Turtleback provide a large-scale analog to the mixed-mode behavior of Scholz (1988). Scholz (1988) defined a region of concurrent grain-scale brittle and crystal-plastic behavior in the earth's crust. The depth and width of this region necessarily vary with rock type, but for quartzofeldspathic rocks, it occurs between about 300°C and 450°C, the onset of plasticity in quartz and feldspar respectively. On the Badwater Turtleback, different rock types, rather than different mineral grains within a single rock type, behaved

differently during uplift. Consequently, just as intergranular faults and fractures may affect feldspars within quartzo-feldspathic mylonites, larger-scale faults can accommodate differences in behavior between different rock types.

This study proposes three mechanisms by which brittle faults may initiate below the base of the fully brittle crust provided that deformation involves a variety of rock types. Such lithologic variation is typical of most metasedimentary sequences although probably atypical of most plutonic complexes. The depth at which such faults initiate is not limited by the onset of ductility within the bulk rock mass. In that circumstance, strain will concentrate within the weaker layers and cause faulting where those layers pinch out between stronger rocks. Instead, the depth of faulting is controlled by the onset of ductility in all involved rock types. In the case of decollement-style faults which form at places where calcite marble pinched out into brittle rocks, the depth of faulting is also controlled by the thickness variations of all involved rocks. Greater thickness variations may drive faulting to greater depths because it will likely cause more pronounced and more frequent strain imcompatabilities within the rock mass.

The evolution of these faults lends support to the suggestion by Miller (1991b and next chapter) that the footwall rotated significantly towards the east. While both sets of these faults initially formed at the same time, the high-angle faults continued to slip well after the decollement-style faults had ceased moving. The evolution of these two sets therefore shows how ultimately, in this extensional setting, high-angle faults were favored over lower angle ones. Furthermore, the evolution of these faults suggests that a reversal in the relative importance of the two fault sets occurred sometime after the footwall was fully brittle. At early stages, the high-angle faults slipped to accommodate strain on the decollement, but at later stages, the decollement

slipped only to accommodate motion on the high-angle faults. Continual eastward rotation provides a mechanism whereby the initially dominant, decollement-style faults rotated to unfavorable orientations and were replaced by an initially, minor, but more favorably oriented set of faults.

Conclusions

Two distinct sets of brittle faults, "decollement-style faults" that are subparallel to foliation, and "high-angle faults" that are at high angles to foliation, cut the footwall of the Badwater Turtleback. Members of both sets formed during ductile deformation of the footwall as a result of strain incompatibilities between brittlely and ductilely deforming rock. Decollement-style faults formed in two settings: 1) where actively deforming calcite marble pinched out between other rock types, or, 2) where ductile deformation of two different but adjacent rheologies caused vacancies to form at their contact. High-angle faults formed in brittle hanging walls of calcite marble shear zones to accommodate local extension of the hanging walls. The origins of these early-stage brittle faults therefore provide a direct link between ductile deformation, characteristic of the middle crust, with brittle deformation, characteristic of the upper crust. Their origins also imply that in similar settings involving a variety of rock types, brittle faulting may initiate within the zone of mixed ductile and brittle deformation.

The evolution of these faults was marked by a reversal of the relative importance of each fault type. Slip on high-angle faults was initially in response to slip on decollement-style faults; at later stages of deformation, decollement-style faults slipped in response to motion on high-angle faults. This reversal, plus the progression from low-angle to high-angle faulting through time, suggests that the footwall rotated eastwards during extension.

Chapter Four

HIGH-ANGLE ORIGIN AND GRAVITATIONAL REACTIVATION OF THE BADWATER TURTLEBACK FAULT, DEATH VALLEY, CALIFORNIA

Introduction

Low-angle normal faults, sometimes called "detachment" faults, play an important but enigmatic role in extensional tectonics. While they are closely tied to the development of many highly extended areas, their present low dip angles pose severe mechanical problems for normal slip. In fact, few if any, large low-angle normal faults are currently seismically active (Jackson and White, 1989; c.f. Johnson and Loy, 1992 for a possible example). Many workers have suggested that, in the Basin and Range province, low-angle normal faults formed at low angles and served as sites for tens of kilometres of horizontal transport (e.g., Wernicke, 1981; Lister and Davis, 1989). Other workers who have suggested that detachment faults originate at higher angles invoke various mechanisms to rotate the initially high-angle faults to low angles (e.g., Miller et al., 1983; Davis, 1983; Buck, 1988).

From a regional standpoint, the initial dip of a fault surface bears on estimates of magnitudes of uplift and strain. For a given amount of slip, more extensional strain can be accommodated on lower-angle faults. Furthermore, for a given extensional strain, high-angle faults require greater relative uplift of footwall rocks than do low-angle faults. Therefore, although there are several objections to large-scale, horizontal transport on detachment faults, they provide an appealing mechanism to permit the estimated high extensional strains of some regions.

Proponents of a high-angle origin for detachment faults argue that high extensional strains may result if slip takes place on several generations of normal faults (Miller et al., 1983; Buck, 1988; Smith, 1992). With increasing strain, the initially high-angle fault gradually rotates to a lower angle, eventually becoming unfavorably oriented for continued slip. At that point, a new high-angle fault must form to accommodate further strain. This fault then gradually rotates until it becomes overprinted by an even later high-angle fault.

The roles that many of these faults play in extending the crust is further complicated by the growing awareness of low-angle landslide surfaces in the Basin and Range (Yarnold and Lombard, 1989; Moores, 1966; Topping, 1990). In fact, some apparently rooted, low-angle normal fault surfaces may actually be partially buried landslide surfaces (Boyer and Allison, 1987; Boyer and Hossack, 1992). In the Death Valley region, Drewes (1959) suggested a gravitational origin for all three turtlebacks. These observations therefore raise uncertainties regarding the suggested tectonic origins of many low-angle "rooted" normal faults. In turn, these uncertainies allow for radically different interpretations, and therefore structural and tectonic implications, of individual low-angle normal fault surfaces.

The Badwater Turtleback in Death Valley, California, provides an outstanding example of a large moderately low-angle normal fault system (Fig. 4-1). Like the faults at the Copper Canyon and Mormon Point Turtlebacks farther south, the Badwater Turtleback fault separates an upper plate of brittlely faulted Tertiary and Quaternary volcanic and sedimentary rocks from a strongly mylonitic, mostly Precambrian, lower plate. The fault therefore separates mid-crustal from upper-crustal rocks and must have played a critical role in extending the Death Valley region. According to argon geochronology by Holm et al. (1992), much of the ductile
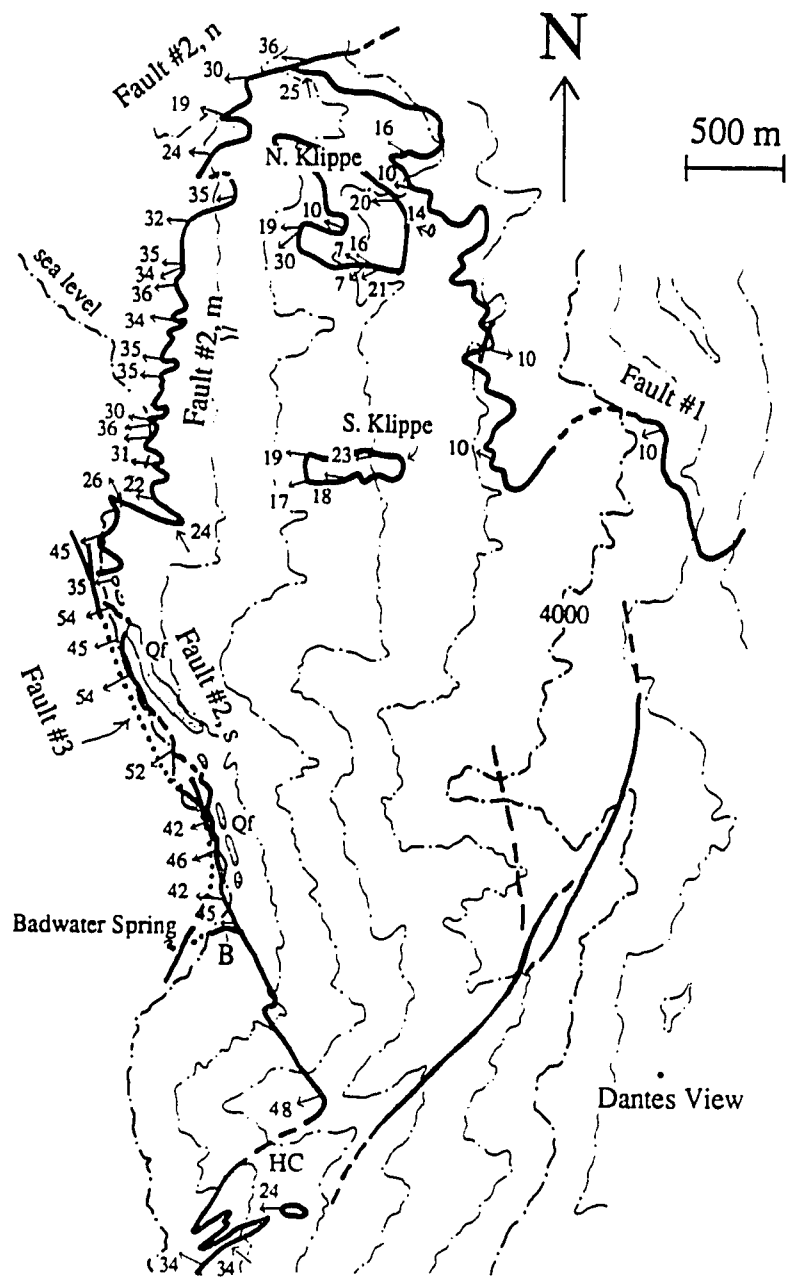
Figure 4-1. Map of Badwater Turtleback fault system. Individual faults are labelled as faults #1, 2, and 3. Different segments of fault #2 are labelled as "Fault #2, n" (northern segment), "Fault #2, m" (middle segment), "Fault #2, s" (southern segment). Qf stands for Quaternary fanglomerate; HC stands for Hades Canyon.

deformation in the footwall of the Badwater turtleback occurred at about 13 Ma; this chapter provides evidence that the present surfaces of the turtleback fault system slipped after 6.3 Ma. The Badwater Turtleback fault system is exposed continuously for more than 5 km horizontally and 1 km vertically along the western front of the Black Mountains (Fig. 4-1). Its geometry, kinematics, and associated fault rocks, described here, suggest that it consists of at least three generations of nearly planar faults that formed at initially high angles and then evolved from seismotectonic origins present-day gravitational features.

Geometry of the Badwater Turtleback fault system

The Badwater Turtleback fault system is approximately parallel to the exposed Turtleback surface and has been described as a continuous, convex-upward fault (Curry, 1954; Wright et al., 1974). In fact, it consists of three distinct west-dipping faults which decrease in age and increase in dip westward. For the purpose of identification, the faults are labeled from oldest to youngest as faults #1, #2, and #3 (Fig. 4-1) These faults are referred to as the "low-angle segment, frontal segment, and active segment" respectively by Miller (1991b). Faults #1 and #2 crop out as either distinct, planar, single slip surfaces, or zones of broken and altered rock cut by several slip surfaces. In the latter case, individual slip surfaces may be continuous or discontinuous. Because of the outstanding exposure on the Turtleback, the age relationships and geometries of faults #1 and #2 are clear. Fault #3, however, which is probably still active, is expressed solely as fault scarps in Quaternary alluvium and a prominent fault-line scarp at the front of the range. Other relationships, however, indicate that it post-dates the other faults.

Fault #1

Fault #1 lies in the footwall of Fault #2. From its truncation by fault #2, fault #1 may be traced over the crest of the Black Mountains to where it disappears under alluvium to the northeast (Fig. 4-1). Consequently, this fault projects over the top of the Black Mountains to the south. The volcanic rocks in the vicinity of Dantes View are therefore in its footwall.

The exposure of the fault #1 below two klippen of upper plate rocks sheds light on its original geometry (Fig. 4-1). At the north klippe, as well as to the north and east, the fault as a whole is markedly non-planar but is also cut by many later faults. Stretches of fault #1 between the cross-cutting faults are typically planar. At the south klippe, which is unbroken by cross-cutting faults, the low-angle segment is planar with a westward dip of approximately 17° (Figs. 4-1, 4-2A). Therefore, this part of the low-angle segment is probably an undeformed remnant of an originally planar surface.

An offset continuation of fault #1 may be exposed near Badwater Spring in the hanging wall of fault #2. This fault, labeled B in figure 4-1, resembles fault #1 in that it bounds the top of mylonitic rocks and is disrupted by later faulting. Its hanging wall consists of both fanglomerate and underlying diorite. This correlation requires that fault #1 originally extended at least 2.5 km south of its present exposure.

Fault #2

Fault #2 (Fig. 4-1) cuts both Tertiary volcanic rocks and Quaternary(?) fanglomerates in its hangingwall. It truncates smaller faults in both its hangingwall and footwall and displays a variably wide (1 to 5 metres) zone of intense cataclasis. A broad N50°W trending undulation in the fault surface, at the mouth of Nose Canyon,

and a short right-step in the fault at Friendly Canyon, divides fault #2 into three segments, here called the northern, middle, and southern segments (Fig. 4-1).

The northern segment of fault #2 visibly cuts fault #1 on the north side of Natural Bridge Canyon (Figs. 4-1, 4-2B). There, the fault enters volcanic rocks in the hangingwall of fault #1 and continues for an unknown distance northward. This segment is moderately listric as it decreases in dip from 36° westward at the place where it cuts fault #1 to only 19° westward in the bottom of Natural Bridge Canyon. South of Natural Bridge Canyon, at approximately the same structural level, the fault dips 24° westward.

The right-handed stepover from the northern to middle segment is not exposed. It is expressed, however, near the southern wall of Friendly Canyon. There, the middle segment is visible above the southward projection of the northern segment (Fig. 4-2C). The middle segment separates hangingwall fanglomerate and brecciated volcanic rock, described by Cichanski (1990), from mylonitic rock of the footwall. This segment, which is beautifully exposed over its entire length, is distinctly planar with a consistent westward dip of about 35° (Figs. 4-1, 4-2D).

The southern segment is approximately planar, but is steeper than either the middle or northern segments (Fig. 4-2E). Near Badwater Spring, mylonitic rocks occur in its hanging wall, below a fault which may be equivalent to fault #1 (fault B in Fig. 4-1). Because mylonitic rocks are restricted to the lower plate of the Turtleback system, their presence in the hanging wall of the fault #2 further indicates that it cuts and offsets fault #1.

South of Badwater Spring, the southern segment of fault #2 cuts into the rangefront before rejoining it at Hades Canyon. There, it separates a footwall of mylonitic gneiss and intermediate to mafic plutonic rock of the Willow Spring pluton

from a hanging wall of the Willow Spring pluton (Fig. 4-1). A klippe of brecciated rock lies just south of Hades Canyon, approximately 500 metres above the valley floor (Fig. 4-2F). This klippe is adjacent to the continuous trace of the southern segment and may therefore be an erosional remnant of that fault. Because its angle of dip is appreciably less than the rest of the southern segment, however, it may instead be a remnant of fault #1.

Fault #3

Fault #3 appears as a series of fault scarps that cut Quaternary alluvium near Badwater Spring and along the front of the Black Mountains (Fig. 4-1). Its presence may also be inferred from uplifted fanglomerate, volcanic rocks, and rocks of the Willow Spring pluton in the hanging wall of all three segments of fault #2. Some of the fanglomerate depositionally overlies the fault #2 (Fig. 4-1). Therefore, slip on fault #3 must postdate fault #2

Near-vertical fault scarps and a steep fault-line scarp suggest that fault #3 probably dips at least 60° westward. This steep dip requires that the fault intersects the more gently dipping fault #2. Furthermore, fault #3 probably cuts fault #2 because (1) it postdates fault #2 and (2) geophysical evidence presented by Keener et al. (1990) suggests that the active fault in an equivalent structural position near Mormon Point cuts the Mormon Point Turtleback fault.

Boundaries of the Badwater Turtleback

The boundaries of the Badwater Turtleback have never been clearly defined. Curry (1954) described it as the convex-upwards part of the rangefront between Natural Bridge and Nose Canyons, but Drewes (1963) showed that metamorphic

A

Figure 4-2. Photographs of Badwater Turtleback fault system. Dashed line marks fault. 4-2A: Fault #1 at south klippe, looking west. 4-2B: truncation of fault #1 by fault #2; dashed lines mark faults. 4-2C: South wall of Friendly Canyon. Middle segment of fault #2 is above this wall while the northern segment underlies volcanic rock in foreground. 4-2D: Middle segment of fault #2, looking north from side of Nose Canyon. 4-2E: View northward along southern segment of fault #2 from north side of Hades Canyon; dashed line indicates fault. 4-2F: Klippe on low-angle surface of Turtleback fault near Hades Canyon.

108

Figure 4-2 (continued).

B

Figure 4-2 (continued).

E

F
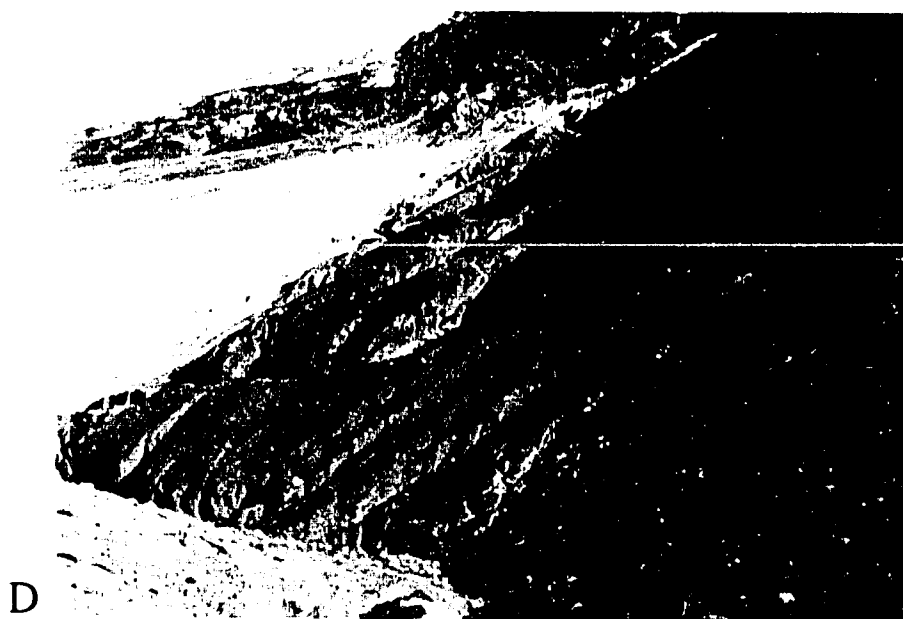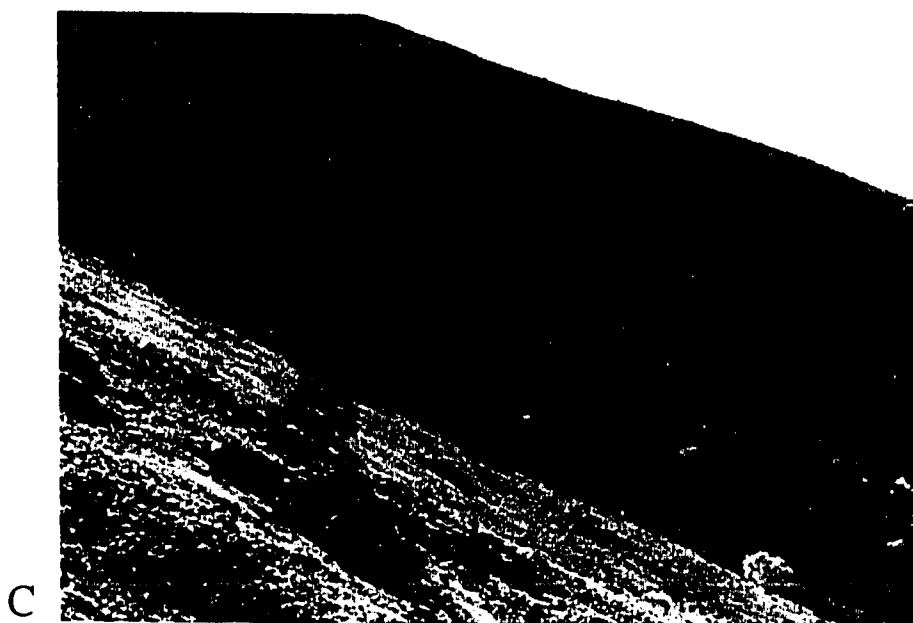
Figure 4-2 (continued).

rocks extended south beyond Badwater almost as far as a north-northeast-trending high-angle fault in the canyon bottom below Dantes View (Fig. 4-1). In order to support models for large-scale extension in the Death Valley region, some recent workers interpret all boundaries of the Badwater turtleback as faults (for example, Hamilton, 1988; Holm et al., 1992).

While the northern and western boundaries of the Badwater Turtleback consist of faults #1 and #2 respectively, the eastern and southern boundaries are not faults. These findings are significant because they provide a maximum age for uplift on fault #1 and indicate that the footwall of the Badwater Turtleback is continuous with the rest of the Black Mountains. The eastern edge of the turtleback consists of a felsic intrusive complex (Curry, 1954; Drewes, 1963) which intrudes metamorphic rocks of the footwall; volcanic rocks, which are continuous with 6.3 Ma volcanic rocks at Dantes View, lie depositionally on these intrusions (Fig. 4-1). Therefore, fault #1 must have slipped after 6.3 Ma.

The southern edge of the turtleback, on the other hand, is poorly defined, in part because the fault mapped by Drewes (1963) in Hades Canyon lies in only the upper part of the canyon. Rather than follow the entire canyon, this fault bends southward at point "A" on fig. 4-1. Therefore, the southernmost mylonitic rocks, which lie at the bottom of Hades Canyon, are continuous with intermediate to mafic intrusive rocks of the Willow Spring pluton. These rocks, in turn, are continuous with the Copper Canyon and Mormon Point Turtlebacks farther south. Pavlis (1991) showed that the Willow Spring pluton lies in the hanging walls of these other two turtlebacks.

Discussion: Implications of the Turtleback fault geometry

Figure 4-3 illustrates the overall cross-sectional geometry of the Badwater Turtleback. The westward progression into successively younger, higher-angle faults, combined with moderate to steeply dipping rocks in the hangingwall of fault #1, suggests that the two older faults originated at higher angles but rotated with increasing extensional strain. This interpretation resembles models by Miller et al. (1983), Davis (1983), and Buck (1988), who suggested a similar origin for other low-angle normal faults. In Death Valley, Hamilton (1988) also suggested that the Turtleback faults and other low-angle normal faults in the region originated at high-angles.

Miller et al. (1983) and Davis (1983) described domino-style rotation along a series of concurrently active normal faults. In the Death Valley region, several other large normal fault systems were probably concurrently active with the Badwater Turtleback fault system. These faults include the Tucki Mountain fault system at the north end of the Panamint Mountains (Wernicke et al., 1986), the Boundary Canyon fault in the Funeral Range (B. Troxel, 1990, personal commur \, and the Copper Canyon and Mormon Point turtleback faults in the southern Black Mountains. The observed geometry of the Badwater Turtleback fault differs from the concepts presented by Buck (1988) and Hamilton (1988), however, in that fault #2 *cuts* and *offsets* fault #1. Buck (1988), Hamilton (1988) and a recent cross-section of the Death Valley region (Asmerom et al., 1990), showed later, high-angle faults as upper-plate splays off a master detachment fault. Because both faults #1 and #2 separate mid-crustal mylonitic rocks from upper-crustal, volcanic rocks, they are fundamental parts of the Turtleback fault rather than upper-plate splays of an unseen detachment fault.
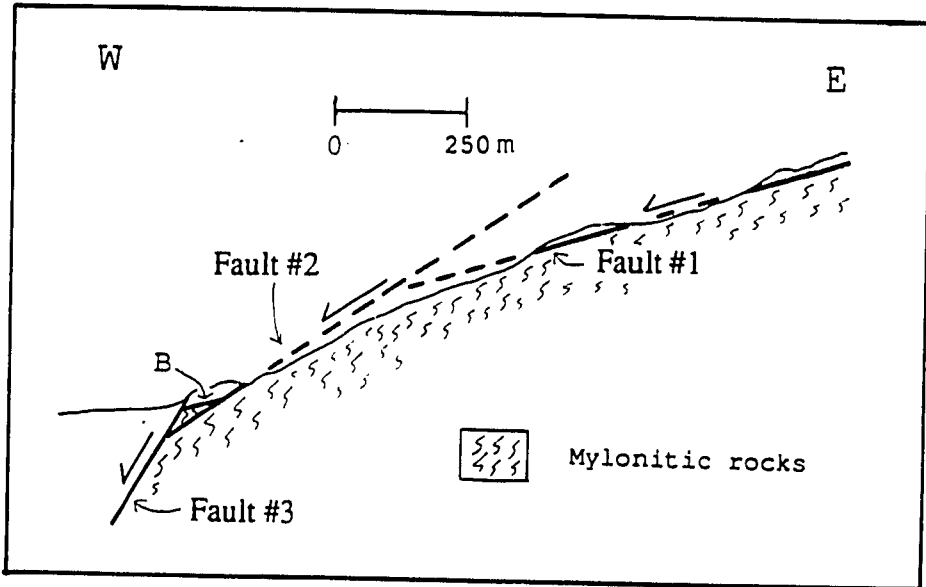
Figure 4-3. Composite cross-section of Badwater Turtleback.

The difference in dip between the low-angle segment at the undeformed south klippe and the active segment probably approximates the amount of rotation of the Badwater Turtleback. Because the active segment is not exposed, however, the difference in dip between the south klippe (17° W) and the maximum dip on the frontal segment (54° W) gives a minimum approximation of 37°.

A Hansen slip-line analysis of folded mylonitic rocks from the footwalls of faults #1 and #2, shows that upper-plate transport was approximately 14° to N65°W (Fig. 4-4A). Assuming that the Turtleback rotated a minimum of 37° eastward, the analysis restores to an initial average transport direction of 43°, N56°W (Fig. 4-4B). Similarly, if the Turtleback rotated 37° to the S60°E, which is more in line with the overall northwestward transport direction, the analysis restores to 50°, N72°W (Fig. 4-4C). Although these reconstructions are necessarily approximate, they indicate that transport of upper-plate rocks occurred on a moderately to steeply dipping shear zone. The late-stage mylonitic zone dipped at 43° or more while the later brittle fault dipped between 35° and 60°.

A moderate- to high-angle origin for the faults and mylonitic rocks of the Badwater Turtleback may eventually help constrain estimates for extension prior to, and after about 6 Ma in the Death Valley region. Current models for Death Valley fall into two major categories: those that favor the low to moderate amounts of extension of 30% to 50% or slightly more (Wright and Troxel 1973; Wright et al., 1981), and those that favor 400% to 500% extension (Stewart, 1983; Wernicke et al., 1988). These latter models call for approximately 80 km of pre-6 Ma horizontal transport of the Panamint Mountains off the top of the Black Mountains from a location adjacent to the Nopah Range. The probable surfaces of transport are the turtlebacks, because they are the interface between mid-crustal mylonitic and upper crustal rocks.

A. Present

43, N56W

B. Restored by westward rotation

50, N72W

C. Restored by rotation towards N60°W

□ N-vergent folds   ◪ N-vergent folds, mean

+ S-vergent folds   ◈ S-vergent folds, mean

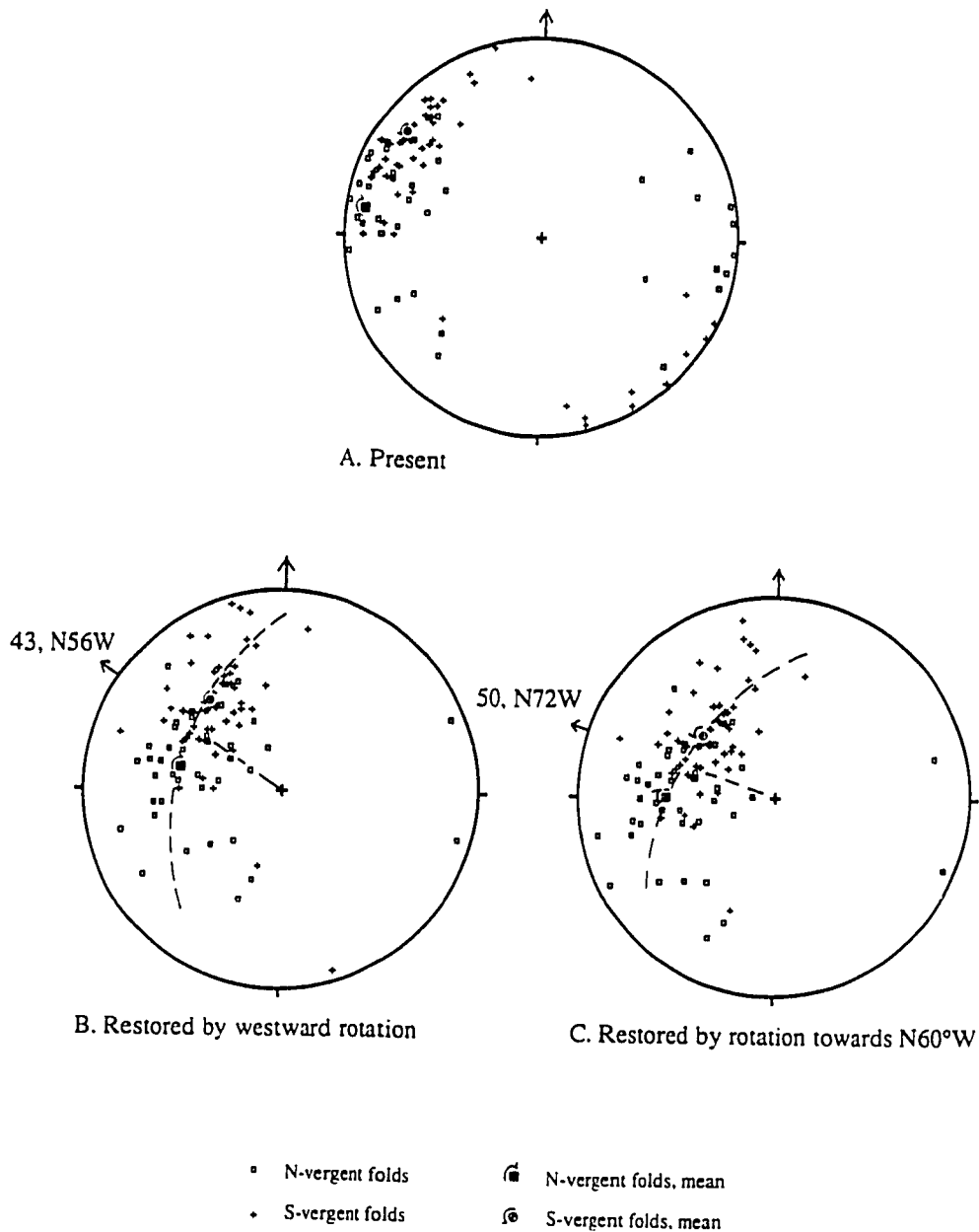**Figure 4-4.** Present and restored orientations of asymmetric folds in lower plate of Badwater Turtleback. Because there is some overlap of north- and south-vergent folds, mean for each group was used to determine approximate slip line. 4-4A, present orientations of folds. 4-4B, orientations of folds after restoration by 37° westward rotation. 4-4C, orientations of folds after restoration by 37° rotation towards N60°W.

The geometry of the Badwater Turtleback fault favors low to moderate amounts of extension on both the post-6 Ma Badwater Turtleback fault system and on the pre-6 Ma mylonitic shear zone. Because these fault surfaces slipped at moderate to high angles, and ductile strain in the mylonitic rocks occurred at a dip of about 40 degrees westward, the amount of uplift during pure normal slip should approximate the amount of extension. Holm and Wernicke (1990) estimated 10 to 30 km of uplift for the Black Mountains, which on a surface that dips consistently at 45° and has a rigid footwall, would allow only 10 to 30 km of horizontal, extensional transport. If transport occurred at these high angles during oblique slip such as that observed at Mormon Point (T. Pavlis, 1990, personal commun.), the corresponding extension would be even less. Finally, the correlation of fault B near Badwater with the low-angle segment limits transport on the brittle frontal segment to only a few kilometres.

The eastern and southern boundaries of the Badwater turtleback are also consistent with low to moderate amounts of extension on the post-6 Ma fault system. The volcanic rocks on the footwall of the turtleback at its eastern boundary indicate that mylonitic rocks must have already been near the earth's surface by 6.3 Ma. At the southern boundary of the turtleback, fault #2 rejoins the rangefront and its mylonitic footwall grades into rocks which are continuous with the hangingwall of the Copper Canyon turtleback. These relations indicate that the Badwater and Copper Canyon turtlebacks are separate features and not a single crustal-scale detachment as advocated by Hamilton (1988) and Holm et al. (1992).
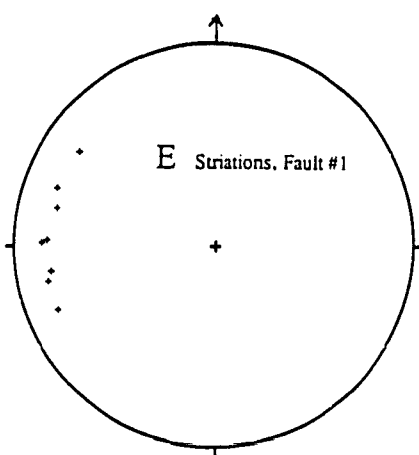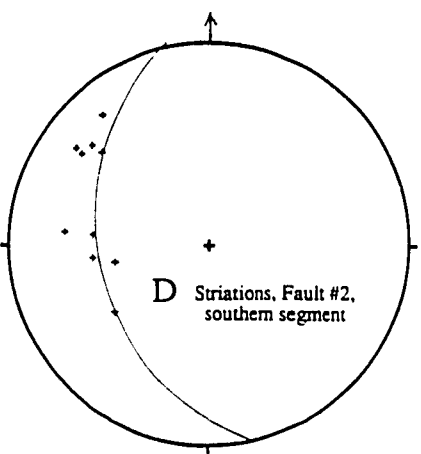
Movement directions of Turtleback fault system

Of the three faults of the Badwater Turtleback fault system, the middle segment of fault #2 contains the most abundant kinematic information. Striated fault surfaces

plunge nearly due west, parallel to the dip on the fault (Fig. 4-5A), while subjacent mesoscopic faults typically dip westward and show normal separations (Fig. 4-5B). Together, these data indicate top-to-the-west transport. A Hansen slip-line analysis of brittle fault-related mesoscopic folds in the fault zone, however, indicates a transport direction of approximately N66°W (Fig. 4-5C). This value corresponds to the line that, on a stereographic projection, most closely bisects and separates populations of "s" and "z" folds.

The different directions of transport indicated by these two methods is likely a product of different periods of slip on the fault. While striations tend to be easily obliterated by later motion on a given fault surface, the mesoscopic folds lie within a relatively wide part of the fault zone and would tend to be much less affected by later slip on the fault. Furthermore, striations from the middle segment of fault #2 lie on the underside of the relatively soft, clay rich, hangingwall. Therefore, they may reflect later motion on the turtleback fault than the more "durable" folds. An early slip history of oblique, top-to-the-northwest, followed by normal, top-to-the-west motion can explain both sets of data.

The southern segment of fault #2 displays two sets of striations (Fig. 4-5D). One set of these striations plunges to the northwest, oblique to the strike of the fault. Given the extensional setting, these striations indicate right-lateral normal slip, consistent with the transport direction obtained from the mesoscopic folds of figure 4-5C. The other set plunges approximately west-southwest, nearly parallel to local dip directions. In one locality, the dip-parallel striations overprint the northwest-plunging, oblique striations. These data therefore imply a two-stage slip history, of right-lateral normal followed by normal slip, similar to the middle segment.

Figure 4-5. Orientations of some structural features associated with Turtleback fault. 4-5A: Striations on middle segment of fault #2; approximate average orientation of the fault is shown as great circle. Note that striations are approximately parallel to dip. 4-5B: Poles to anastomosing fault surfaces immediately below Badwater Turtleback fault, Nose Canyon (Fault #2, middle segment). 4-5C: Hansen analysis of S and Z folds immediately below Badwater Turtleback fault (Fault #2, middle segment); derived transport direction is top-to-N66°W. 4-5D: Striations along southern segment of Fault #2; approximate average orientation of fault shown as great circle. Note that striations fall into an oblique, and dip-parallel group. 4-5E: Striations on fault #1.

A   Striations, Fault #2, middle segment

B   Poles to faults subjacent to Fault #2

C   Folds subjacent to Fault #2
    ▫ z folds
    + s folds

D   Striations, Fault #2, southern segment

E   Striations, Fault #1
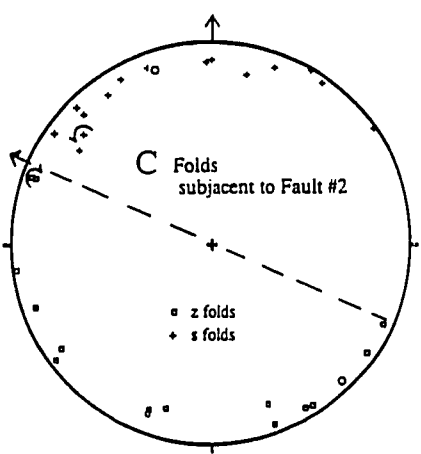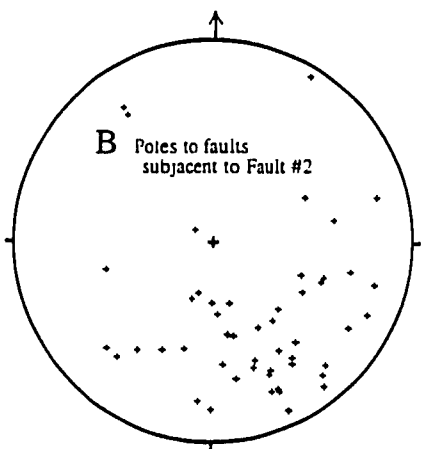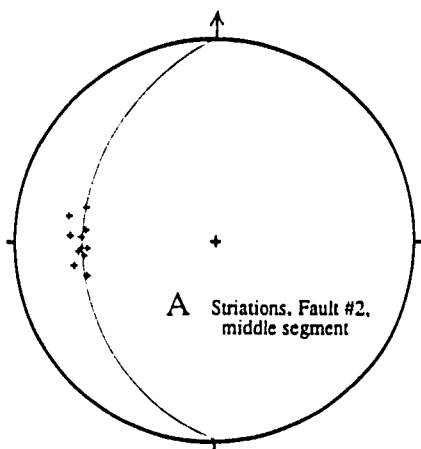
Fault #1 locally displays striations which plunge variably towards the northwest (Fig. 4-5E). This fault, however, has been broken by numerous smaller faults. Therefore, many of these orientations may reflect only local slip directions which are not reliable indicators of transport for the hanging wall as a whole.

Fault rocks of the turtleback fault system

Clay-rich gouge, foliated and nonfoliated cataclasite, monolithologic breccias, and zones of anastomosing mesoscopic faults are the primary rocks associated with the brittle fault system of the turtleback. These rocks and anastomosing fault zones are exceptionally well exposed. Where they are found together, they tend to display particular associations which suggest a given sequence of development (Fig. 4-6). The degree of development and thickness of each rock type, however, vary widely across the turtleback, and most places do not exhibit the entire range of fault rocks. These rocks are locally and variably mineralized.

Fault gouge

A thin (<1 cm -10 cm) layer of clay-rich fault gouge occurs at the surface of faults #1 and #2 wherever these faults consist of single, discrete, sliding surfaces (Fig. 4-7A). This gouge displays a prominent "P" foliation (Rutter, 1987) which is asymmetric with respect to the principal sliding surface. Although few orientation data presently exist for the orientations of the "P" foliations, they typically dip approximately eastwards. Backscattered SEM images of this foliation show that it is defined by a penetrative compositional layering which is overprinted by extension fractures (Fig. 4-7B). The gouge contains inclusions of both the footwall and hangingwall.
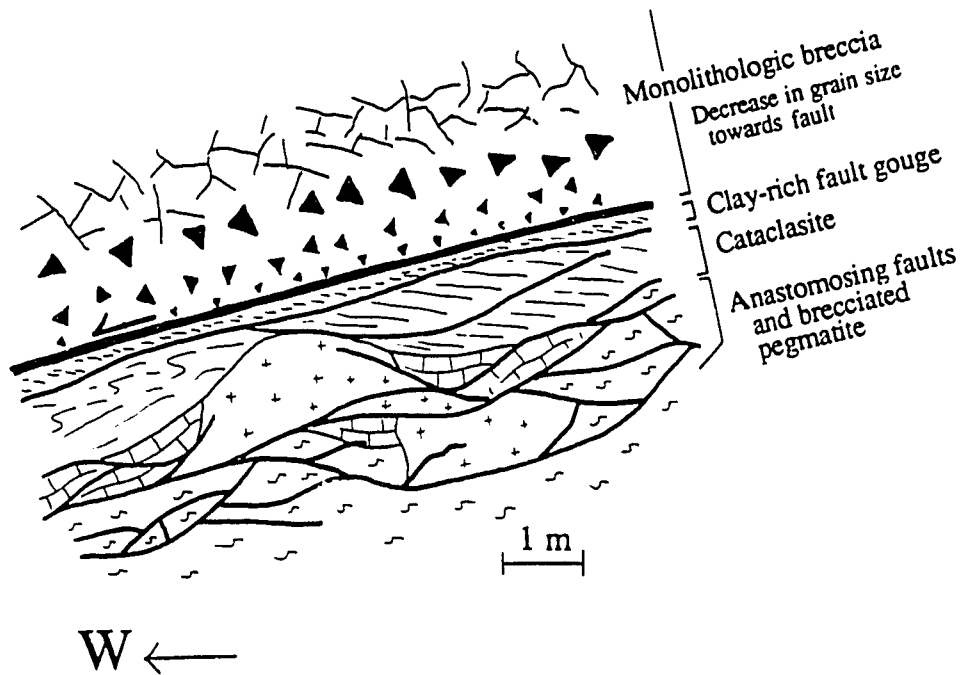
Figure 4-6. Generalized diagram which illustrates fault rocks of Badwater Turtleback. Turtleback fault itself is shown as heavy black line. Scale is approximate.
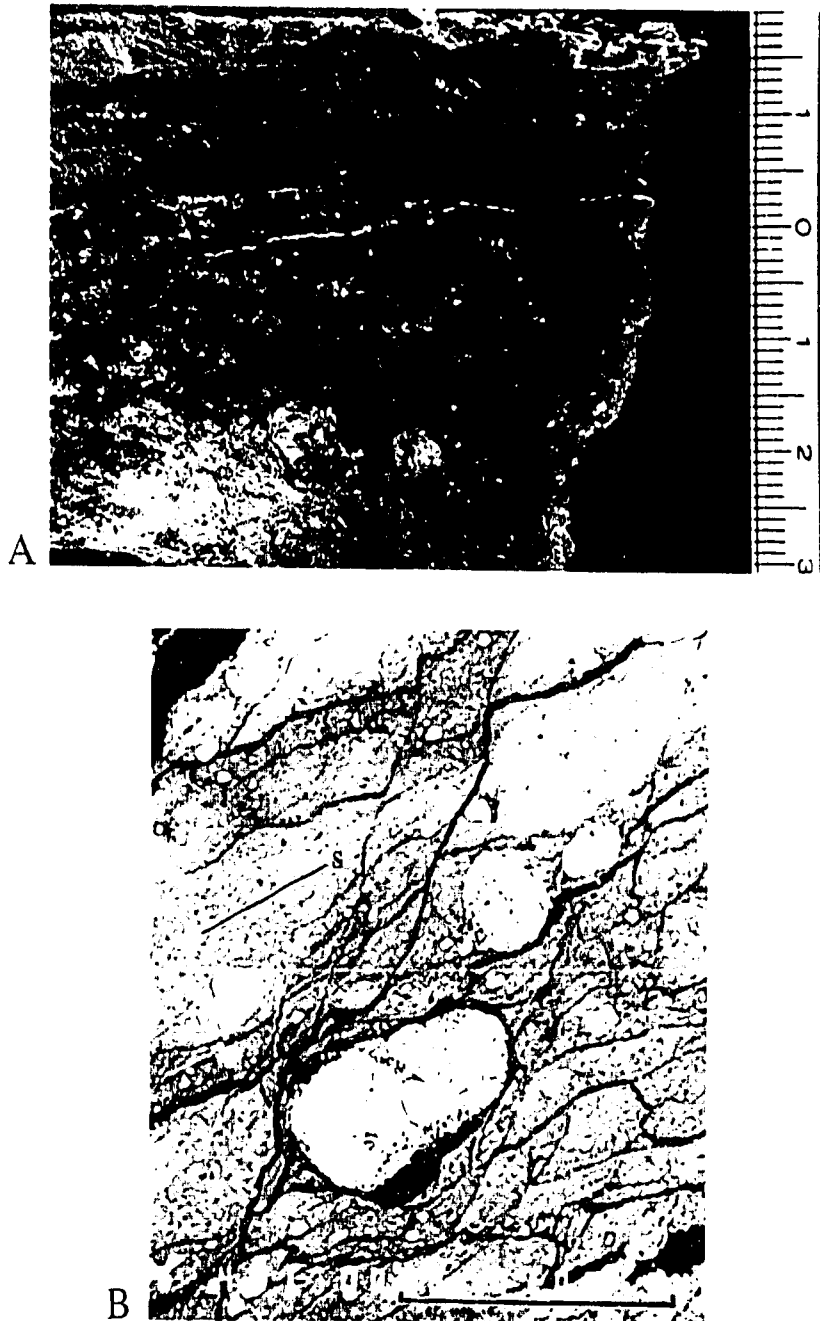
Figure 4-7. Clay-rich fault gouge from Badwater Turtleback fault. 4-7A: clay-rich fault gouge (rust-colored) and nonfoliated cataclasite (greenish). Note that gouge locally displays a distinct foliation. Motion on fault is top-to-left. 4-7B: SEM backscattered photograph of clay-rich fault gouge of 4-7A. Note that fractures overprint a faint, but penetrative compositional foliation, labelled "s". Motion on Turtleback fault is top-to-right. Scale bar = 0.1mm.

Cataclasite

The term "cataclasite" is used here to describe fine-grained fault rock which contains a relatively low percentage of clay minerals. The cataclasite may or may not contain visible inclusions. Where it does contain inclusions, the inclusions 1) float within the fine-grained matrix, and 2) are fractured at the mm scale. The cataclasite on the Badwater Turtleback consists of both foliated and nonfoliated varieties. It lies directly beneath clay-rich fault gouge in most localities but also occurs locally in places which do not exhibit gouge.

Similar to the gouge, the cataclasite shows evidence for extreme mobility as it locally invades fractures into the overlying hangingwall (Fig. 4-8A). This mobility is probably the cause of large thickness variations of the cataclasite along short distances of the fault zone. Figure 4-8B shows that the cataclasite can vary in thickness from only 4 cm to greater than 50 cm in less than 4 m. Adjacent to some major thickness changes, such as in figure 4-8C, the cataclasite displays rootless fold hinges.

Breccia

The Badwater Turtleback displays both poly- and monolithologic breccias. Polylithologic breccias occur along many high- and low-angle faults in the footwall, but only locally along the Badwater Turtleback fault. Monolithologic breccias occur adjacent to the Badwater Turtleback fault in both its hangingwall and footwall. These monolithologic breccias are shattered, but otherwise intact, rock; they contain very little matrix material and their clasts typically interlock with each other.

In the footwall, monolithologic breccias are penetratively fractured at a scale of less than 1 cm (Fig. 4-9A). These breccias grade into foliated and nonfoliated cataclasites, upwards towards the Turtleback fault and/or outcrop-scale shear fractures
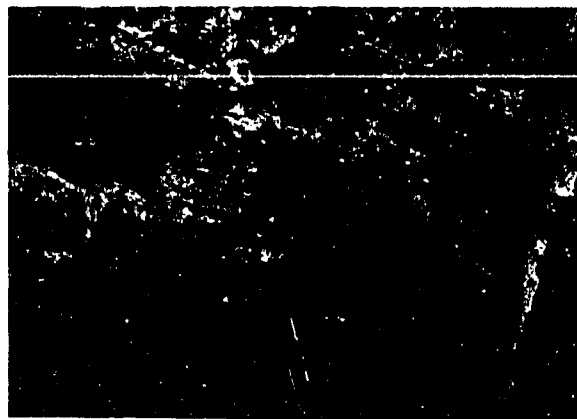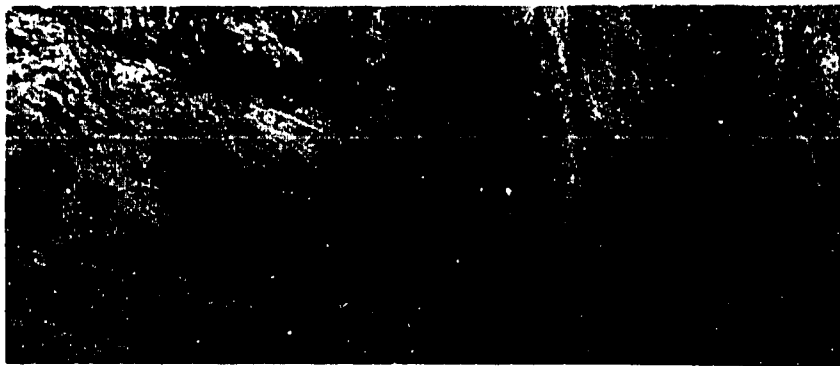
Figure 4-8. Photographs of cataclasite. 4-8A: Cataclasite and fault gouge intruding brecciated rocks in hangingwall of fault #2. 4-8B: Variation in thickness of cataclasite along turtleback fault. Bottom of cataclasite is marked by a dashed line. 4-8C: Detached isoclinal fold hinge in mobilized cataclasite. Principal slip surface on Turtleback fault is marked on photograph.

and locally downwards into outcrop-scale shear fractures. Fractures locally display iron oxide mineralization and staining. Pegmatite is by far the most common rock type to exhibit this style of brecciation.

In the hangingwall, monolithologic breccias exhibit a variety of clast sizes which tend to be larger than clasts in the footwall. From 0 to about 20 cm above the fault, non-foliated cataclasite grades into fine-grained breccia, which over a distance of 0 to about 100 cm from the fault, grades into coarse-grained breccias. Clasts in these coarser breccias tend to be randomly, but penetratively fractured at scales of less than 10 cm (Fig. 4-9B). With increasing distance from the fault, these breccias become increasingly intact. Hangingwall volcanic rocks typically display this style of brecciation in places where the Turtleback fault is a discrete, single surface.

Zones of anastomosing faults

Zones of anastomosing small-scale faults (<5 m in length) are found locally subjacent to fault gouge and cataclasite along the Turtleback fault (Fig. 4-10). As these zones are best developed within well-foliated rocks they may be a well-foliated equivilent of the brecciated pegmatite. Faults within these zones locally cut overlying fault rocks and bend into the Turtleback fault itself. Figure 4-5B shows a plot of 50 such faults beneath the Turtleback fault at the mouth of Nose Canyon. Most of these faults dip to the northwest, but show a complete range within that quadrant. Rare striations on these fault surfaces indicate both dip- and strike-parallel motions.

Mineralization

The Badwater Turtleback faults locally host mineralization which was not the focus of this study (Fig. 4-11). The mineralization includes iron-oxide, barite, and
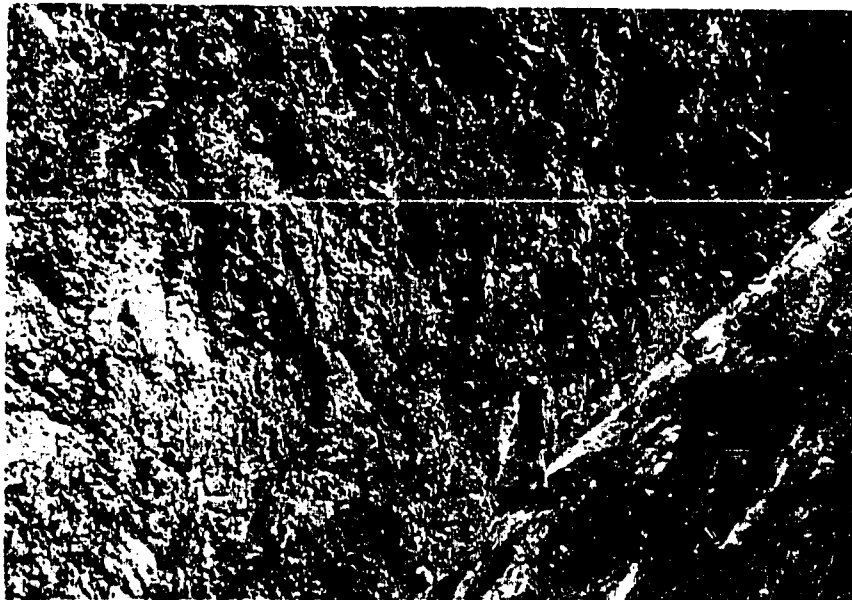
Figure 4-9. Monolithologic breccias. 4-9A: Brecciated pegmatite in footwall. 4-9B: Brecciated dioritic rock in hangingwall. Striations, which run parallel to red pencil, are parallel to the dip of the fault.

Figure 4-10. Zone of anastomosing, small-scale faults beneath Turtleback fault. Turtleback fault is prominent surface marked by black arrow. Note other prominent fault surface above pack.
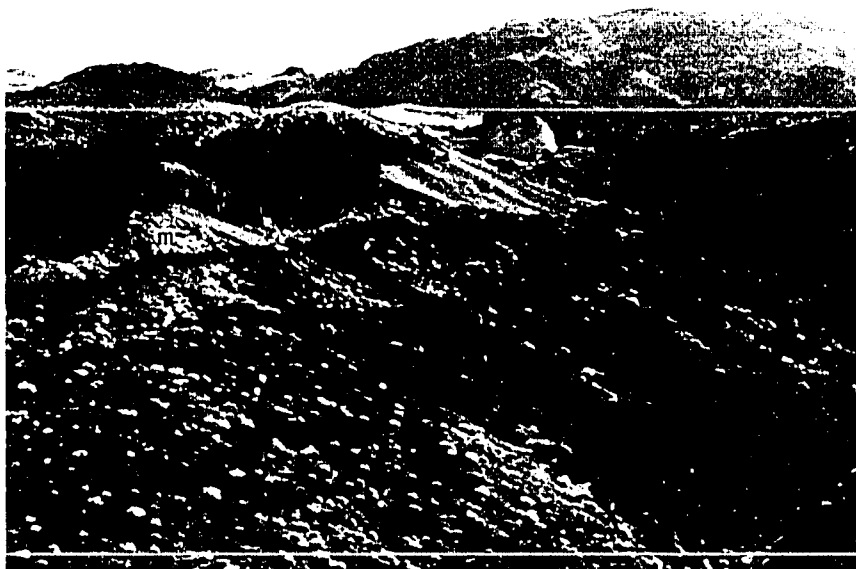
Figure 4-11. Iron-oxide and barite mineralization along Turtleback fault #1. Mineralization is black ledge, marked "m", immediately beneath fault.

possibly massive tourmaline (Steve Byrnes, 1989, personal communication) similar to the deposits subjacent to the Amargosa fault near Ashford Mill (Byrnes, 1989). Similar mineralization also occurs along numerous high-angle faults. The Turtleback faults also locally contain abundant fibrous gypsum.

Gravitational reactivation of Turtleback fault system

The monolithologic breccias in the hangingwall are distinctive rock types in that individual blocks are pervasively fractured, but fragments show little or no evidence for rotation or movement relative to each other. These breccias resemble the crackle- and jigsaw-breccia facies of Yarnold and Lombard (1989) for large rock-avalanche deposits. They also resemble other known nearby rock avalanche or landslide deposits in the Amargosa Chaos (Topping, 1990), Titus Canyon area (Reynolds, 1969), and Shadow Valley basin (Davis et. al, 1991). While presence of these breccias alone may not require such gravitational sliding, they have a specific spatial relationship with the turtleback fault surfaces. This relationship, combined with fault kinematics, argues that gravitational sliding occurred on different parts of the Turtleback fault system after the surfaces had rotated to low angles and ceased seismogenic movements.

These findings of gravitational slip along the Turtleback faults follow Drewes, 1959 who initially proposed a gravitational origin for all three turtlebacks. They differ from Drewes (1959), however, in that the surfaces originated as rooted, tectonic faults. Evidence that these faults were originally tectonic consists of the abundant mineralization, continuity of these faults into areas of intact bedrock, and the segmented nature of fault #2.

Within the context of gravitational sliding, the hangingwall of the Badwater Turtleback fault can be described as unsupported, potentially unsupported, or

supported, depending on how deeply the bounding fault roots into the valley floor (Fig. 4-12). Unsupported hangingwall exists as klippen where the bounding fault surface is free in all directions. Potentially unsupported hangingwall occurs along the rangefront above fault #2 where it is cut off by fault #3 at shallow depths; normal slip on fault #3 periodically exposes the bottom of fault #2 and removes the hangingwall support. Subsequent erosion can bury the fault and make it appear to be rooted. Supported hangingwall lies above sections of faults which root deeply into the valley floor, typically because the fault lies deep within the rangefront.

Figure 4-13 shows the nature of the Turtleback hangingwall as it relates spatially to the various Turtleback faults and hangingwall monolithologic breccia. In general, unsupported and potentially unsupported hangingwall contains monolithologic breccia while supported hangingwall contains little or no monolithologic breccia. This correlation of breccias which are typical of known gravitational slides, with faults that may permit such sliding, suggests that those faults did act as surfaces for gravitational slip. Furthermore, unsupported and potentially unsupported hangingwall typically overlies a single, well-defined fault surface with abundant clay-rich fault gouge. By contrast, supported hangingwall overlies faults which are locally discontinuous and/or poorly defined and contain little or no clay-rich fault gouge. Gravitational sliding probably provided the clay-rich gouge (Yarnold and Lombard, 1989) and modified the preexisting Turtleback faults to their present well-defined surfaces. These relationships between breccias and the hangingwall are mostly independent of rock type as brecciation affects all types of rocks that are found in the hangingwall except for fanglomerate. The fanglomerate, however, is still unconsolidated sediment which could probably respond ductilely to gravitational sliding by intergranular adjustments rather than pervasive fracturing.
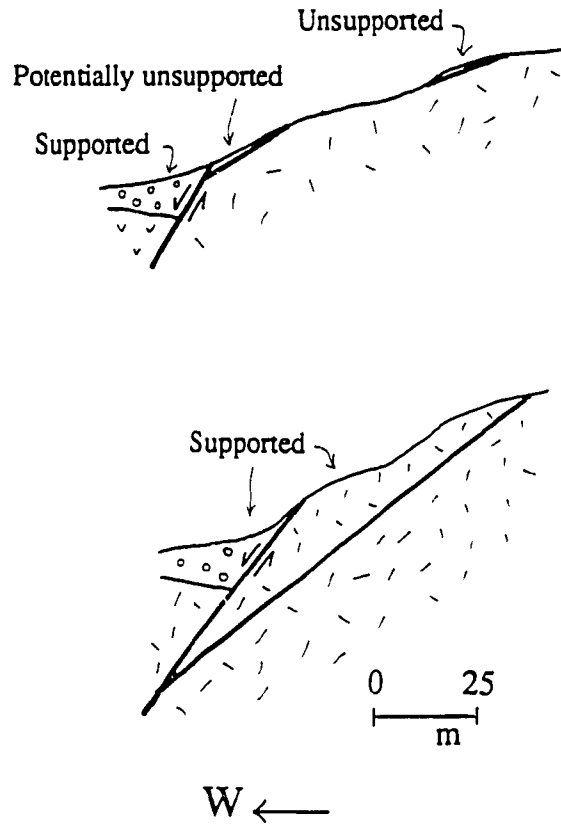
Figure 4-12. Examples of unsupported, potentially unsupported, and supported hangingwall. Scale is approximate.
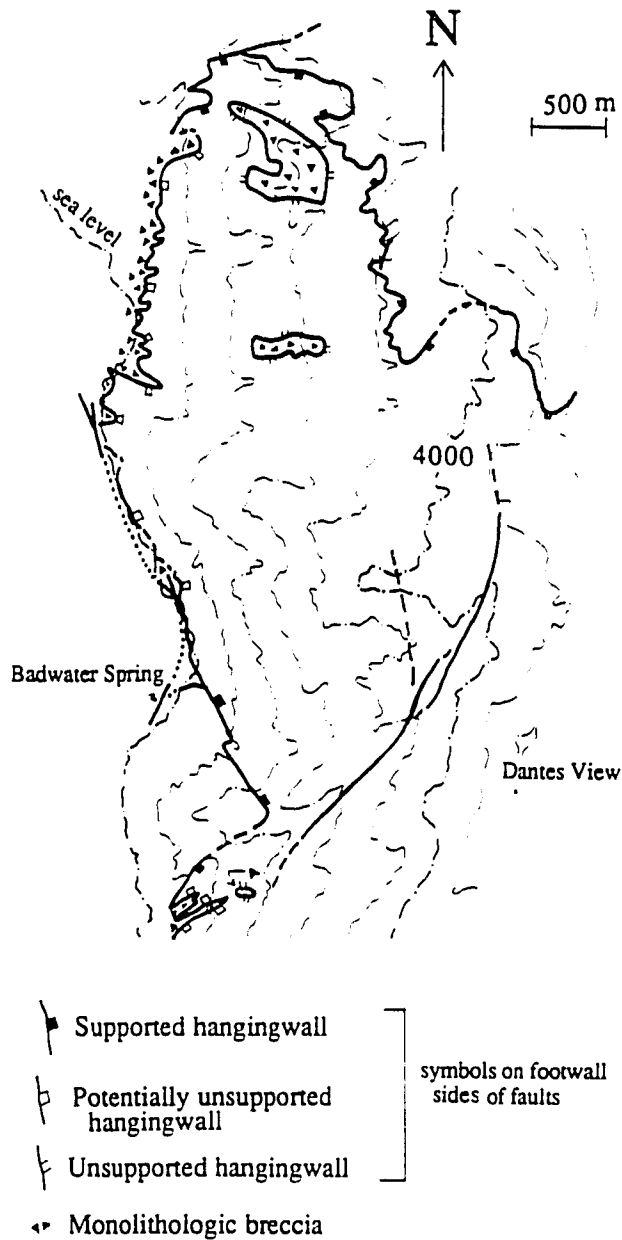
Figure 4-13. Map of Badwater Turtleback fault system showing locations of unsupported, potentially unsupported, and supported hangingwall, and distribution of monolithologic breccias in hangingwall. Fanglomerate, which probably would not display brecciation, occupies the hangingwall along the northern half of the southern segment of fault #2. Note that the symbols used to designate the style of hangingwall support are shown on the *footwall* side of the faults.

Gravitational sliding also explains the apparent two-stage slip history of the turtleback faults. The southern and middle segments of fault #2 both give evidence for right-lateral oblique- followed by dip-parallel motion. Furthermore, high-angle faults which cut the footwalls of faults #1 and #2 (see discussion of these faults in chapter four) and major faults elsewhere along the Black Mountains front also exhibit abundant evidence for oblique-slip (Wills, 1989; Struthers, 1990). Given the overall right-lateral setting of the Death Valley region (Burchfiel and Stewart, 1966; Wright, 1989), such right-lateral oblique-slip should be predicted on north- and northwest-trending faults. Therefore, late-stage dip-parallel motion on these major faults was probably not tectonic, but instead, gravitational.

Model for gravitational sliding

Faults #1 and #2 both dip westward at relatively low angles and are "stranded" at the earth's surface by later faulting. Therefore, both these faults are seismically inactive. Both faults, however, display evidence for later gravitational sliding. Given evidence that these faults rotated from initially high angles (Miller, 1991b) it is likely that gravitational sliding took place on the fault surfaces after they rotated to angles which were too gentle for continued seismogenic slip.

Figure 4-14 displays a four stage evolution of these surfaces. Stages C and D resemble the model by Drewes (1959). At the first stage, A, a high-angle fault (fault #1) slips seismogenically, but rotates to lower angles with continued extension. At the second stage, B, it stops moving seismogenically and is cut off by fault #2. At stage C, uplift in the footwall of fault #2 removes the support for the hangingwall of fault #1 and allows gravitational sliding. At stage D, gravitational sliding buries fault #1 and makes it appear rooted. Continued uplift on fault #2 may cause further sliding.
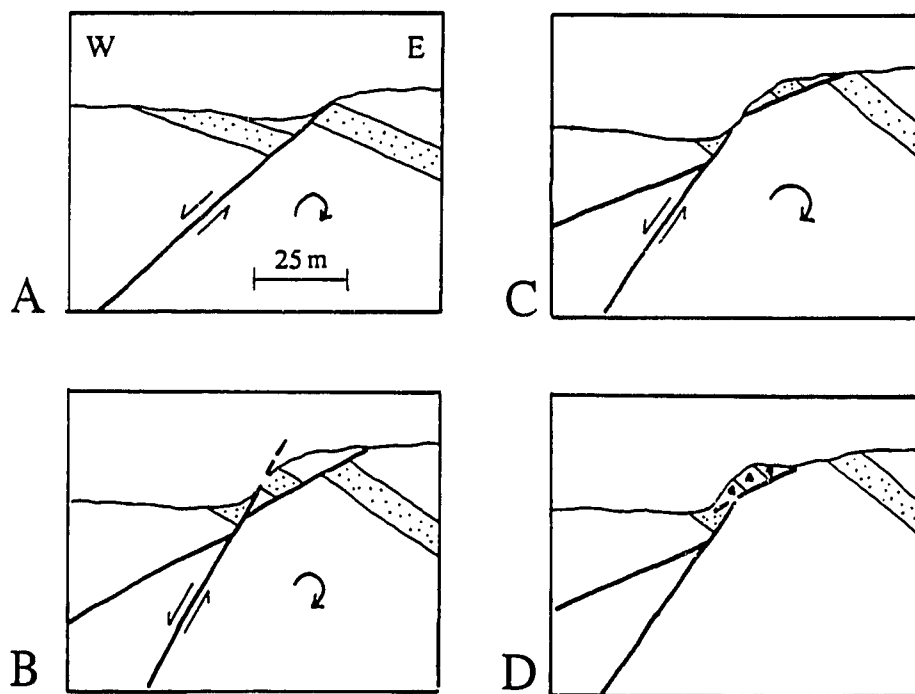
Figure 4-14. Model for abandonment and reactivation of fault surfaces in a rotational setting. 4-14A: Extensional faulting leads to rotation of fault to a lower angle. 4-14B: Initial fault stops moving as a result of rotation and becomes offset along later, higher angle fault. 4-14C: Continued slip along later fault uplifts and exposes bottom of early fault. 4-14D: Unsupported hangingwall slides along early fault and buries its trace. Scale, shown on 4-14A, is approximate.

A gravitational cause of late stages of slip on the turtleback faults has several important implications. First, these faults could mistakenly be considered to be rooted normal faults only because they disappear into the floor of Death Valley. Numerous other low-angle normal faults are treated solely as tectonic features because they disappear into their respective valley floors. Second, this model for gravitational sliding provides a mechanism to explain apparent late-stage activity on a seismically inactive fault. It also suggests that stranded low-angle fault segments may be significant geologic hazards. Finally, coarse-grained monolithologic breccias, which are prevalent throughout the Basin and Range, may provide a tool to identify other landslide deposit surfaces which are now treated as tectonically significant fault zones.

Summary and Conclusions

The Badwater Turtleback fault system consists of three temporally and spatially distinct fault surfaces which show a decrease in dip angle, and an increase in age, eastward. This geometry, combined with moderately to steeply dipping hangingwall rocks, suggests that the fault system, and its footwall, rotated a minimum of 37° eastwards or southeastwards during extension. Restoration of the footwall by this amount indicates that ductile strain in the footwall occurred on a zone that dipped at least 43° westward. Because uplift and denudation along surfaces which dip at these angles necessarily approximates the amount of horizontal extension, this geometry of the Badwater Turtleback is most consistent with low to moderate amounts of extension in the Death Valley region.

This geometry, however, does not preclude large-scale extension in the Death Valley region because (1) more segments of the Badwater Turtleback fault, which would allow proportionately more transport, may still be identified, and (2) the

Badwater Turtleback is a relatively small feature that may not accurately represent the entire region. Furthermore, the dip of the mylonitic shear zone may have decreased with depth as suggested by Holm et al. (1992). A different fault system which would allow more extension at this location, however, has not been identified, nor is there any direct evidence of a listric geometry to the shear zone. Future studies in the Black Mountains concerning depths and styles of mylonitization, their transition into the brittle field, and the geometries of other low-angle faults should further elucidate the problem.

The distribution of distinctive monolithologic breccias with respect to the local settings of the various turtleback faults, combined with fault kinematic data, suggests that these faults provided surfaces for gravitational sliding. This sliding occurred after the faults had rotated to low angles and ceased moving seismically.

Chapter Five

GEOMETRIC EVOLUTION OF THE BADWATER TURTLEBACK, ITS RELATIONSHIP TO THE COPPER CANYON AND MORMON POINT TURTLEBACKS, AND IMPLICATIONS FOR EXTENSION IN THE DEATH VALLEY REGION

Introduction

Low-angle normal (detachment) faults and kinematically related footwall mylonite zones are hallmarks of metamorphic core complexes in extensional regions. While they clearly play important roles in crustal extension, the associations of mid-crustal with upper crustal rocks raise questions regarding the scales at which these systems operate; their low dip angles raise questions regarding their initial geometries and subsequent geometrical evolutions.

The present-day debate over the magnitude of extension in the Death Valley region highlights these two problems of crustal extension. Those workers who favor large magnitude (>300%) extension favor transport on a single, regional-scale, detachment system (Hamilton, 1988; Wernicke et. al, 1988; Holm et al., 1992). By contrast, other workers prefer large amounts of localized extension within the Black Mountains block only; they argue for much lower magnitudes of extension throughout the region. These workers suggest that tectonic transport took place on several independent, locally developed, shear zones (Wright et. al, 1991). Similarly, important contrasts in the geometrical evolution of the system(s) exist between these two different extensional models for Death Valley. Although recent work by both groups suggests that the presently low-angle fault surfaces initiated at high angles, they differ on the specific mechanism of rotation. Those models which call for large-

magnitude extension typically invoke some form of the "rolling hinge" model of Hamilton (1988) whereby normal faults initiate at steep angles but rotate to lower angles because of isostatic effects on the denuding footwall. By this model, the footwall migrates in the direction of hangingwall transport. Those models which require lesser amounts of extension suggest that rotation occurred by isostatic adjustments without a migrating footwall (King and Ellis, 1990), or by concurrent slip on several normal faults which produced a domino effect (Miller, 1991b).

The three turtlebacks of the Black Mountains are a necessary focus of this debate because they provide the principal surfaces of transport on the east side of Death Valley (Fig. 5-1). Each turtleback consists of a core of mylonitic rocks separated from an upper plate of brittlely faulted volcanic and sedimentary rocks by a low-angle normal fault zone. Accordingly, models which call for large-scale extension regard them as fundamentally the same system which evolved according to the rolling hinge model of Hamilton (1988) while the more conservative models regard them as separate, independently evolving systems.

The Badwater Turtleback displays exceptionally well-exposed relations in its lower plate and bounding fault system which help constrain its geometric evolution. These relations, combined with geochronologic work by Holm et al. (1992), and mapping by Drewes (1963), Otton (1974; 1977), and Pavlis (unpublished), on the Copper Canyon and Mormon Point turtlebacks farther south, suggest that the Badwater turtleback experienced an early period of isostatically-induced rotation followed by domino-style rotation. Significantly, all three turtlebacks behaved independently during both episodes of rotation.
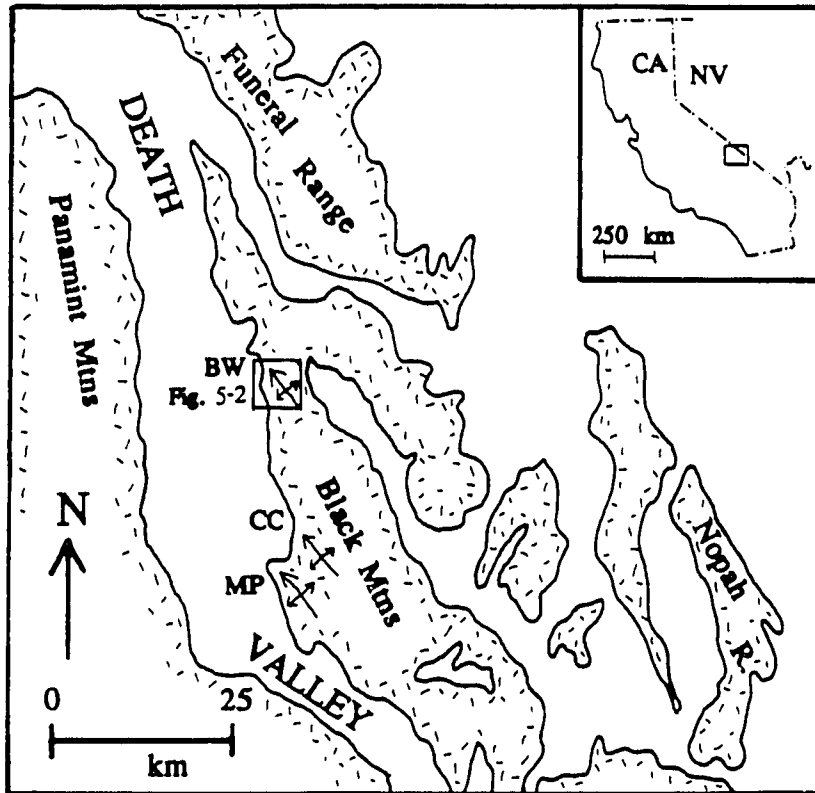
Figure 5-1. Map of Death Valley region. Locations are as follows: BW, Badwater Turtleback; CC, Copper Canyon Turtleback; MP, Mormon Point Turtleback.

Badwater Turtleback fault system

The Badwater Turtleback fault system consists of at least three distinct west-dipping fault surfaces. Furthermore, at least one episode of earlier fault motion must be inferred from structural and geochronologic relations. All these faults decrease in age and increase in dip westward (Figs. 5-2A, 2B). For the purpose of identification, the visible faults are labeled from oldest to youngest as faults #1, #2, and #3; the inferred fault(s) is here called "fault #0". Slip on fault #0 took place on either an older surface which was later reactivated as fault #1, or on an entirely different surface.

Spatial and temporal relationships of faults #1, #2, and #3 are described by Miller (1991b) who referred to them as the "low-angle segment, frontal segment, and active segment" respectively. Because of the outstanding exposure on the Turtleback, the age relationships and geometries of faults #1 and #2 are clear. Fault #2, for example, must postdate fault #1 because it truncates fault #1 on the north wall of Natural Bridge Canyon and because it contains mylonitic rocks in its hangingwall near Badwater Spring (Figs. 5-2A, 2B). Fault #3, however, which is potentially active, is expressed solely as fault scarps in Quaternary alluvium and a prominent fault-line scarp at the front of the range. Other relationships, summarized by Miller (1991b), indicate that it post-dates the other faults.

The presence of fault #0 is required from relations on the east edge of the Badwater Turtleback, near the crest of the Black Mountains. There, fault #1 cuts volcanic rock in both its hangingwall and footwall. Near Dantes View, the footwall rocks have an age of 6.3 Ma (Fleck, 1970). Holm et al. (1992), however, reported an Ar age on biotite from the mylonitic rocks of 13.6 Ma. These ages indicate a significant time gap between ductile deformation and slip on the present-day fault system. Because the mylonites exhibit structural evidence for deformation which led

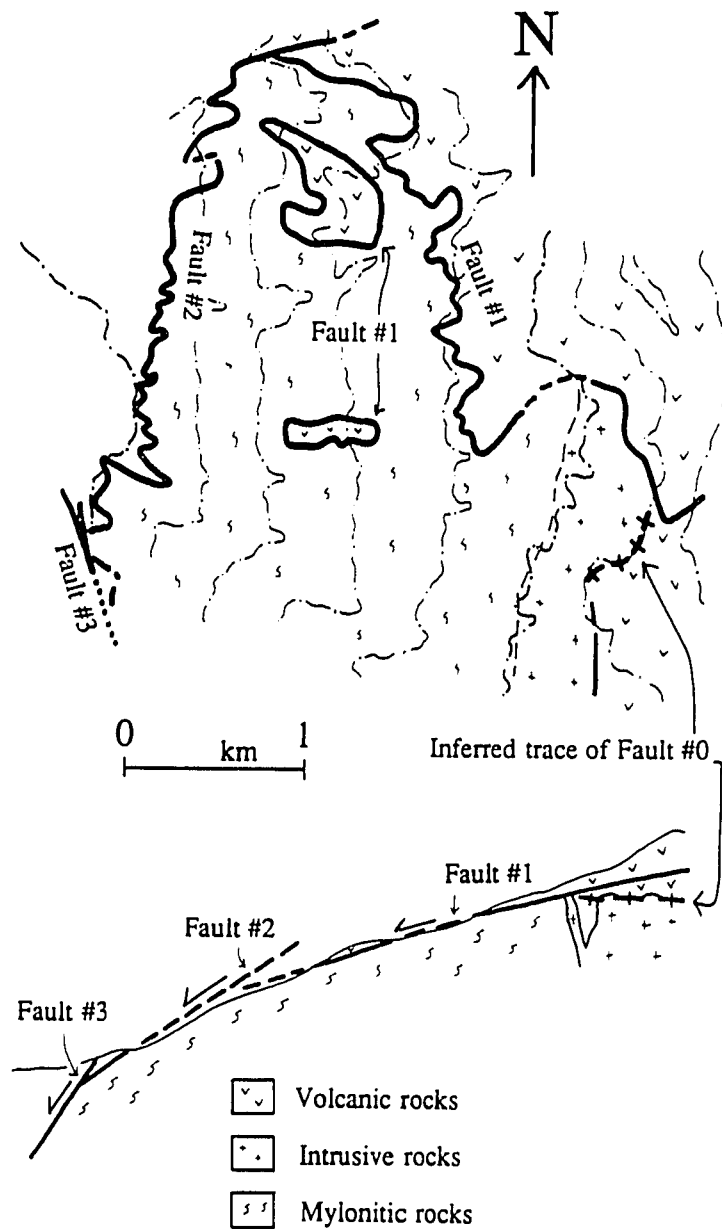**Figure 5-2.** Generalized map and cross-section of Badwater Turtleback showing geometry of fault system. 5-2A, Generalized map. 5-2B, Generalized cross-section. Direct evidence of fault #0 was eroded from the footwall of fault #1 at about 6 Ma, but its presence must be inferred as discussed in text. The fault is shown schematically at the contact of Tertiary volcanic and intusive rocks of the footwall.

directly to brittle faulting (Miller, 1992 and Chapter 2), an earlier fault(s) must have existed prior to fault #1. Furthermore, the footwall volcanic rocks lie depositionally on mylonitic and intrusive rocks of the footwall. Therefore, the mylonites must have been at or near the earth's surface by 6.3 Ma.

Although fault #0 was eroded from the footwall of fault #1 prior to eruption of the volcanic rocks, it appears as a dashed line at the contact of the volcanic and underlying intrusive and metamorphic rocks on figures 2A and 2B. Holm et al. (1992) and Asmerom et. al (1990) interpret this contact as their "Black Mountains detachment" and show it as continuous with fault #1. Hamilton (1988) also interprets the contact as a fault but places is well below exposures of footwall mylonites. While the presence of an actual fault at this contact would permit the interpretation that the mylonites were still at some depth after 6.3 Ma, the existence of fault #0 is still required by the geochronology. The "Black Mountains detachment" could in fact *be* fault #0. The irregular nature of the contact beneath the volcanic rocks, and mapping by Drewes (1963) near Dantes View, however, suggest that, in the northern Black Mountains, the contact is depositional.

Badwater Turtleback antiform

One of the most noticeable features about the Badwater Turtleback is its broad, convex-upwards shape. This shape is a product of two things: 1) fault surfaces of the Turtleback fault system which get progressively older and shallower to the east, and 2) a broad antiformal geometry to the underlying metamorphic rocks. This antiform trends N20E, approximately perpendicular to the direction of transport as defined by various kinematic indicators combined with stretching lineations and outcrop-scale fold axes (see chapter two).

Because the antiform trends roughly normal to the predominant lineation direction and most outcrop-scale fold axes, its geometry is defined by the plunge *angles* of these features instead of the plunge directions. Specifically, at low elevations, lineations and fold axes tend to plunge relatively steeply northwestward while at higher elevations, they tend to plunge gently northwestward or southeastward Because of these changes in plunge angles, the folds and lineations must have been gently folded by the antiform (Fig. 5-3A, 3B). Furthermore, lithologic contacts define a "half-antiform" in that they run nearly parallel to the ground surface which gets less steep with increasing elevation (Figs. 5-3B, 3C). Foliation itself, howe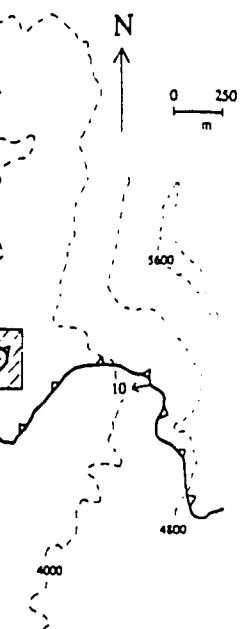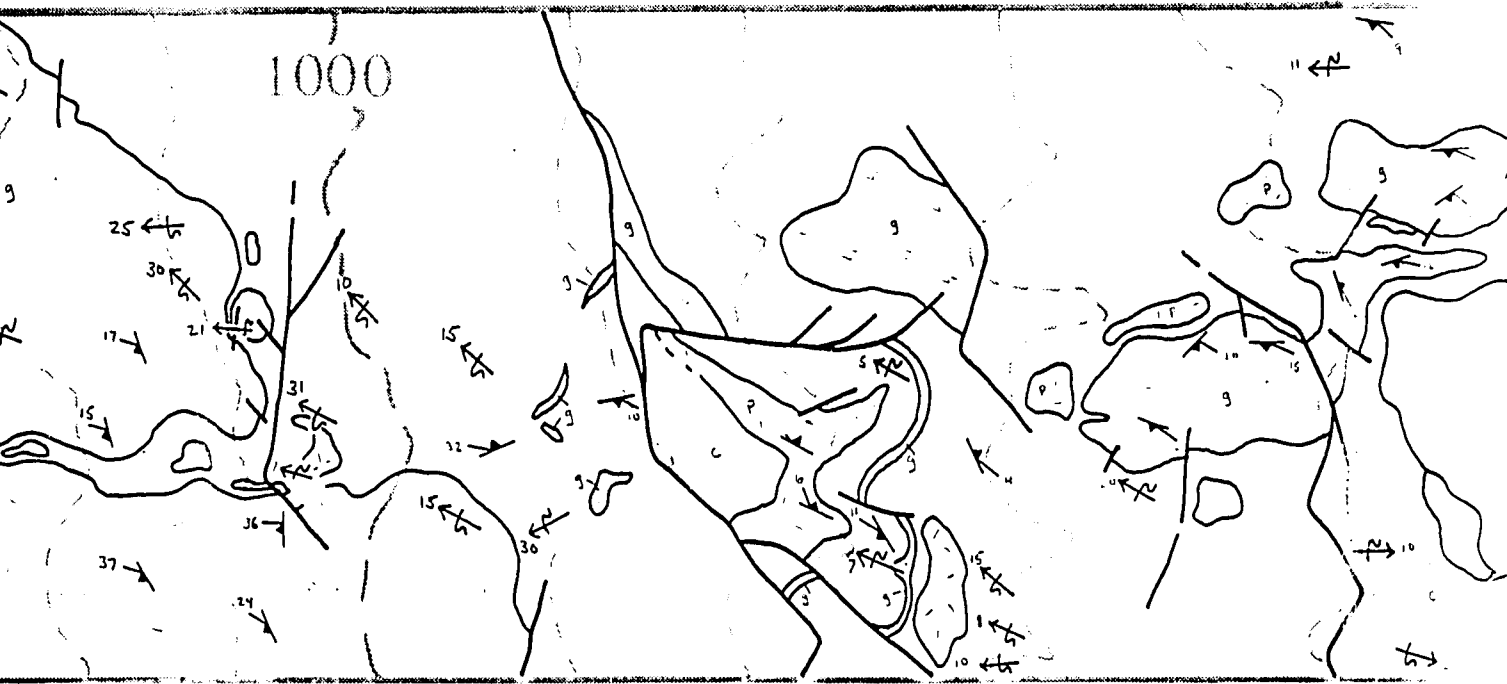ver, does not readily define the antiform (Fig. 5-4) because it tends to be folded about the northwest-trending axes of figure 5-3B.

Copper Canyon and Mormon Point turtlebacks

The Copper Canyon and Mormon Point turtlebacks also display antiformal geometries which resemble that on the Badwater Turtleback. While both turtlebacks are bounded by approximately planar brittle faults (Otton, 1977; Pavlis, in press; Miller, unpublished mapping on Copper Canyon Turtleback), Otton (1974; 1977) showed that foliation in marble tectonite dipped less steeply northwestward with increasing elevation at the Copper Canyon Turtleback. At Mormon Point, Pavlis found that the predominant foliation actually dips southeastward at higher elevations (T. Pavlis, 1991, personal communication). These observations therefore indicate that all three turtlebacks are antiformal about axes that trend roughly N20°E, as well as the obvious northwest trend indicated by Drewes (1963) and most workers since then.

Figure 5-3. Simplified strip map and cross section of Badwater Turtleback. Calcite and dolomite marbles are grouped together as "mylonitic carbonate" and only large bodies of pegmatite are shown. 5-3A shows northern half of Badwater Turtleback and locations of 5-3B,C. 5-3B, Simplified map drawn in east-west orientation, oblique, rather than normal to axis of antiform. The map illustrates how plunges of lineations and fold axes define the turtleback antiform. Fig. 5-3C, simplified cross section, shows that lithologic contacts also define the antiform. Sense-of-shear arrows are drawn schematically to emphasize that lineations and fold axes of 5-3B define the antiform as well.

1000

N

0 250
m

A

C

1000'

sea level

5600

4800

4000

2000

A'

— 3000'

— 2000'

— 1000'

— sea level

3000

A'

3000'

2000'

1000'

sea level

← ←	z fold
←	s fold
← 14	Strike and dip direction of foliation; trend and plunge of stretc
P	Pegmatite
▨ c_2	carbonate structurally above gneiss
S S	Quartzofeldspathic gneiss
c	Calcite and Dolomite marble

$-$ A'

0   200
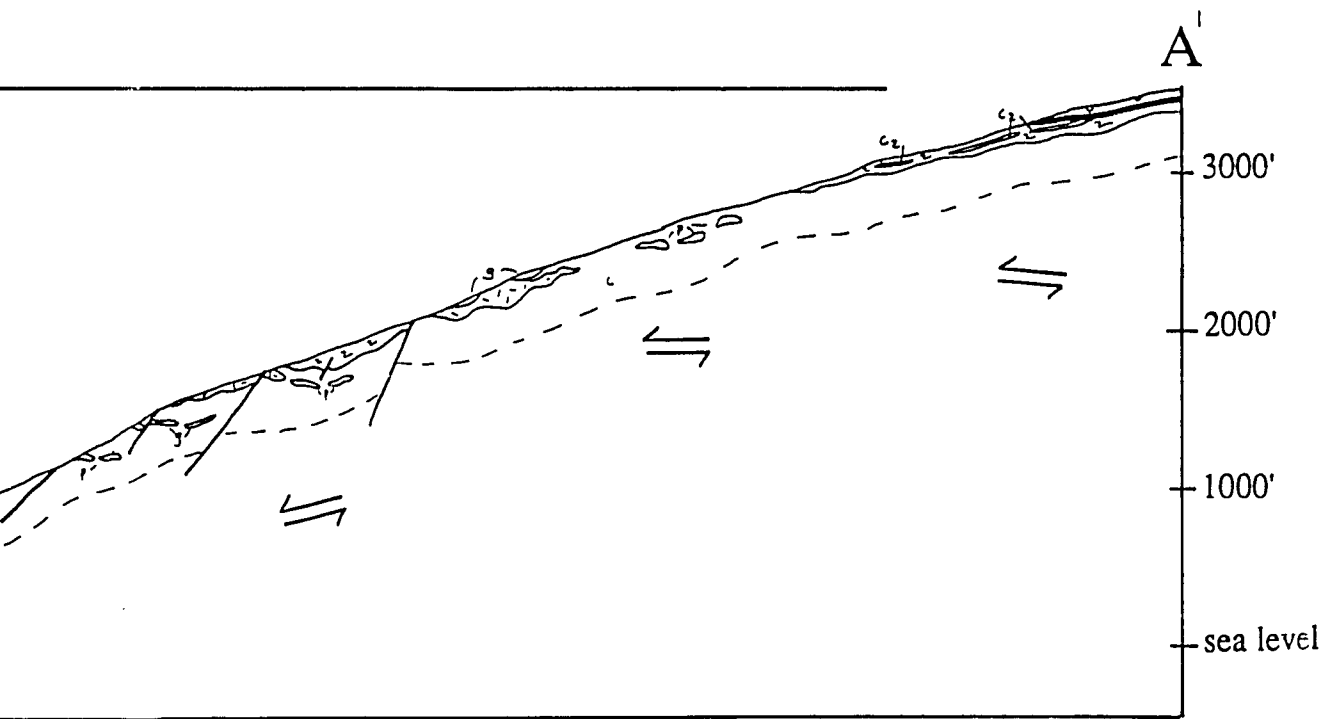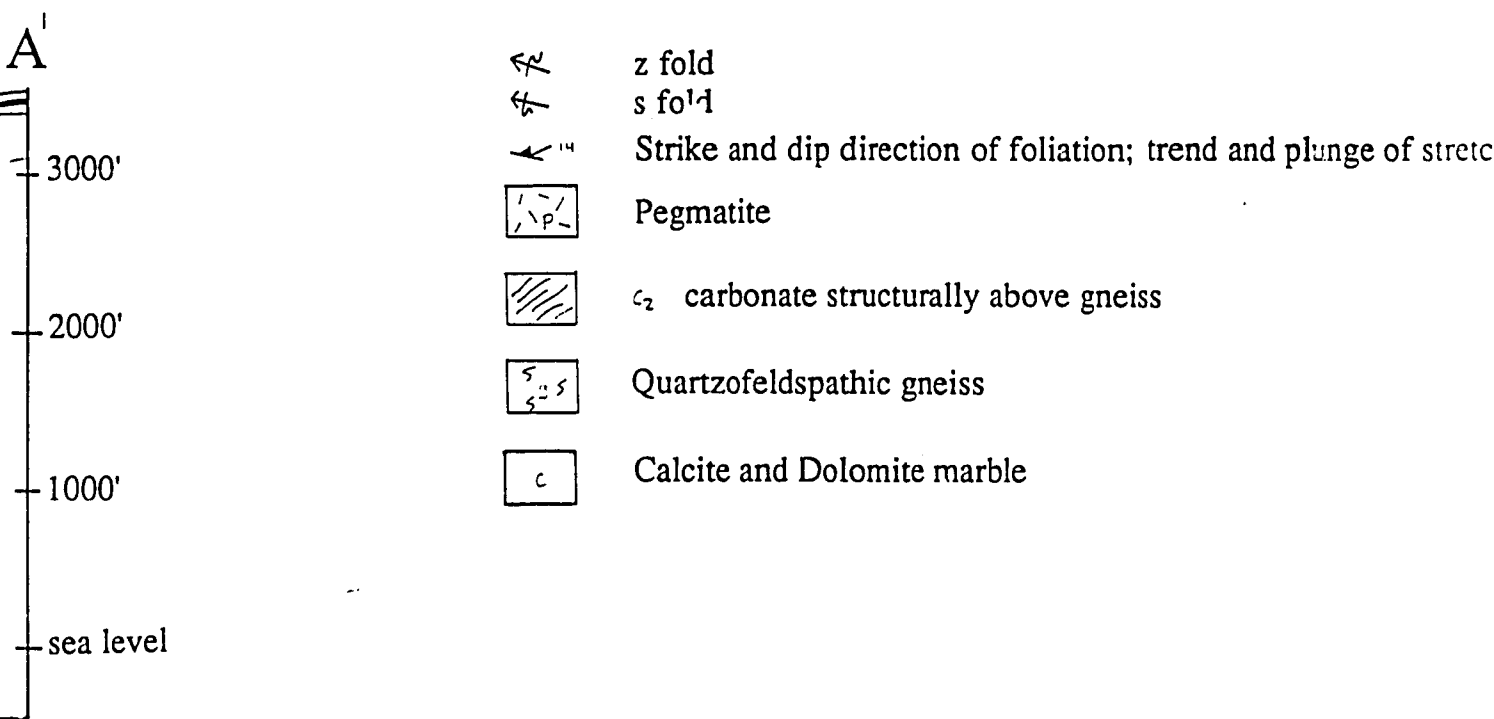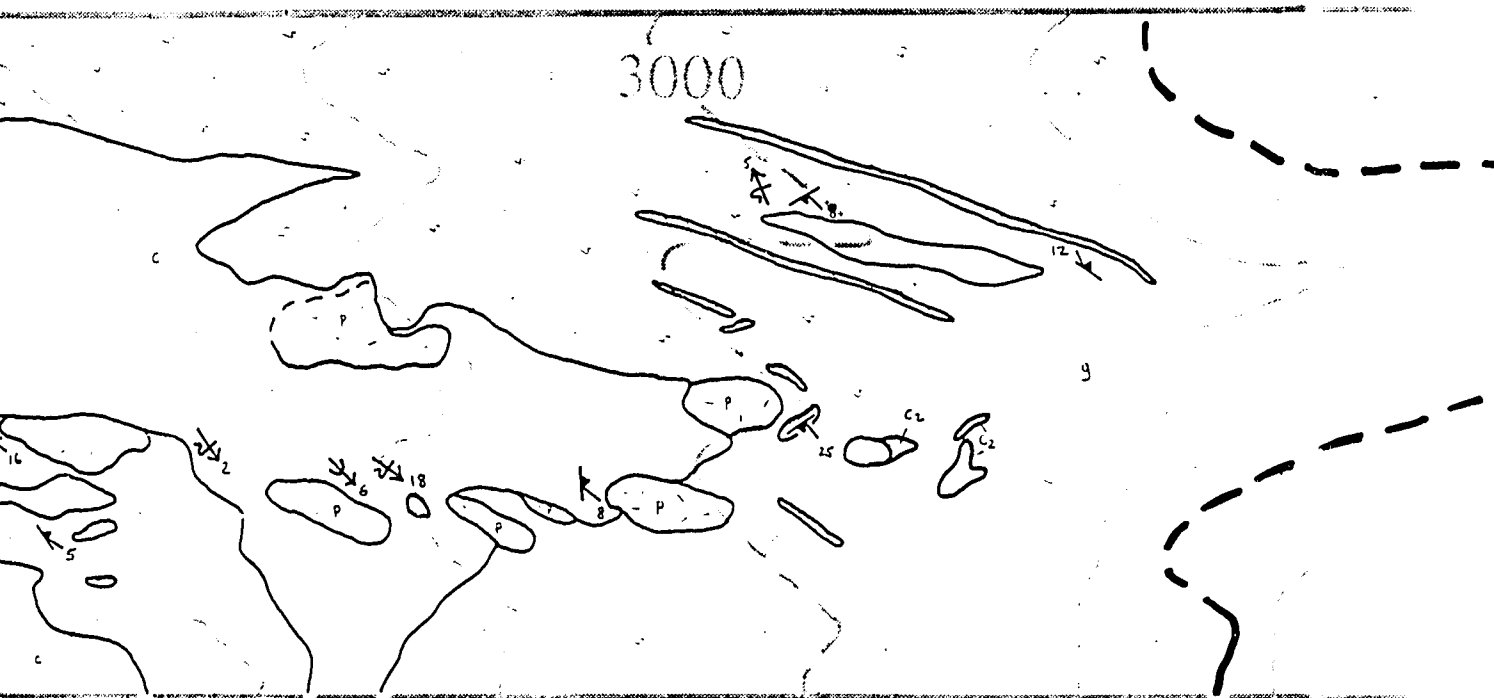
m
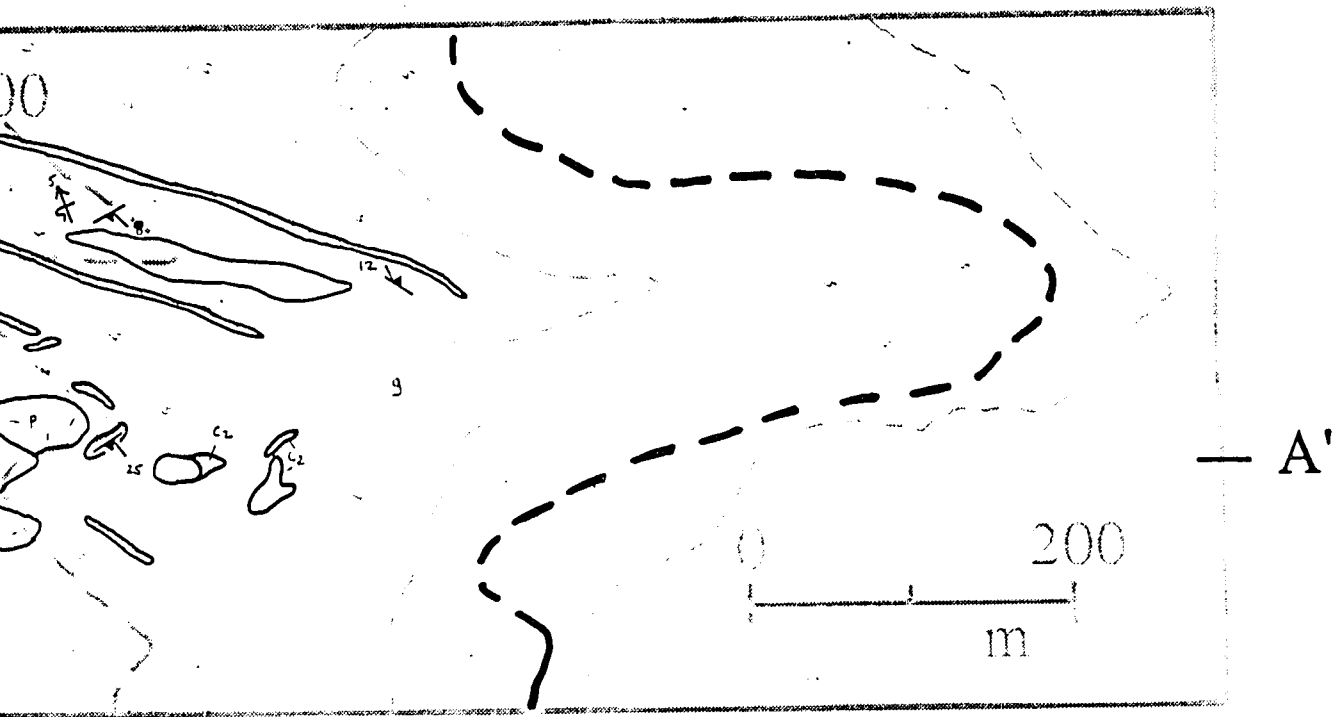
ld
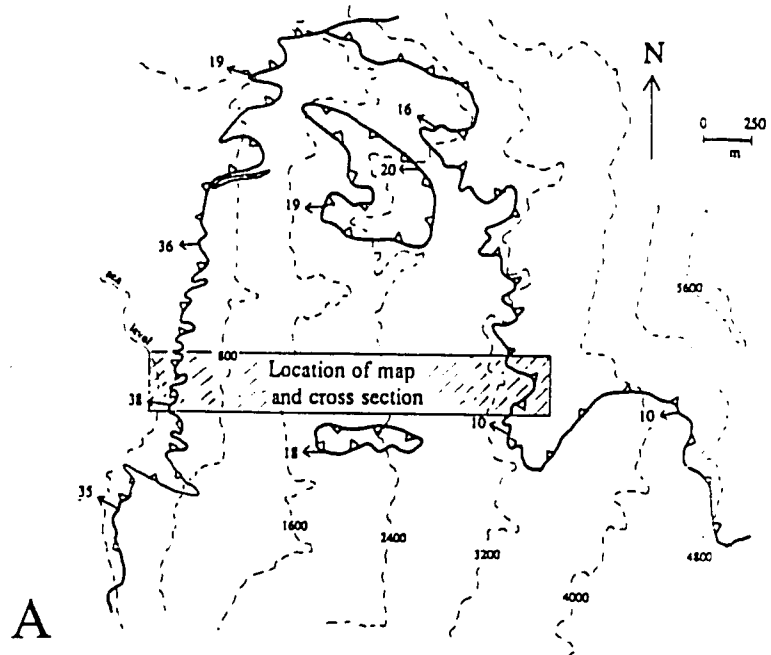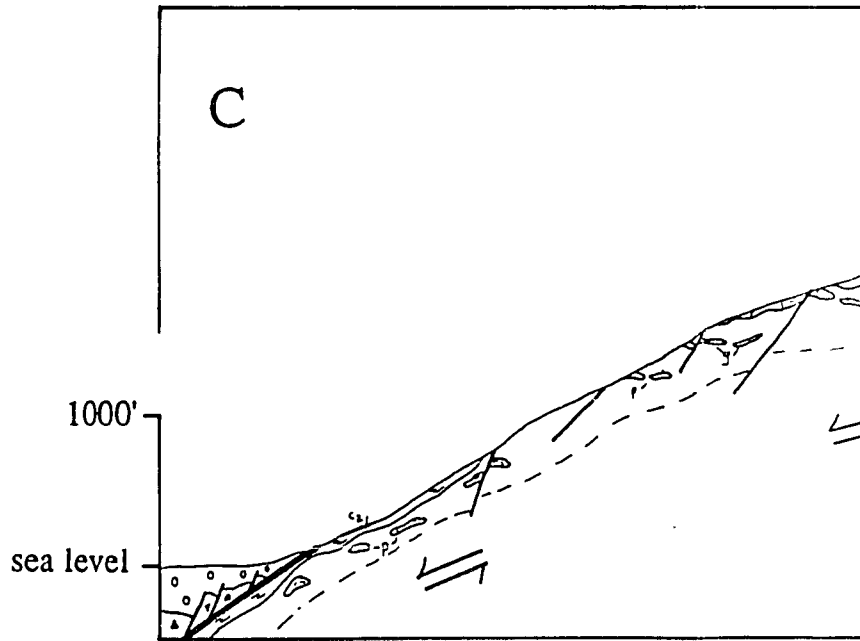
ke and dip direction of foliation; trend and plunge of stretching lineation

matite

carbonate structurally above gneiss
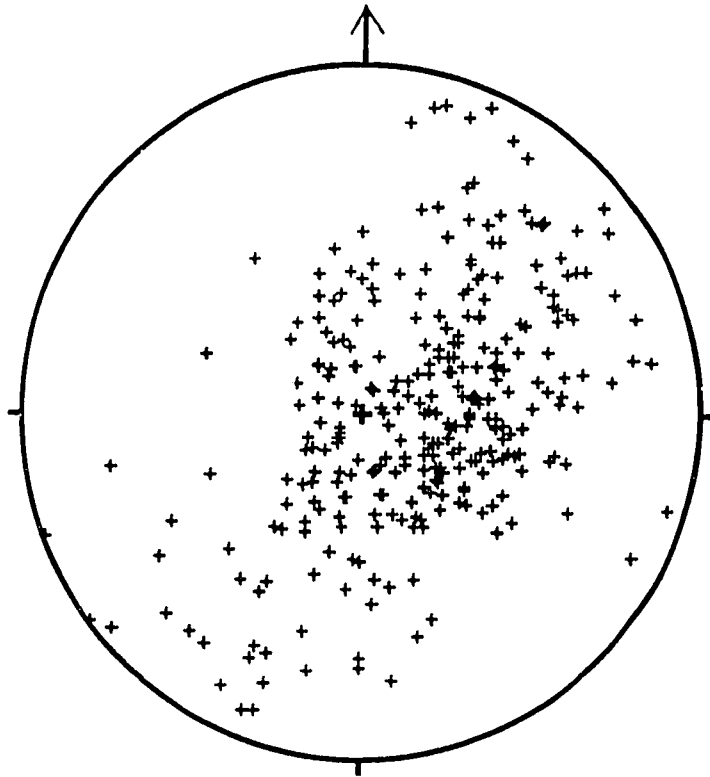
rtzofeldspathic gneiss

cite and Dolomite marble

Figure 5-4. Stereographic projection of mylonitic foliation in footwall of Badwater Turtleback. Because of NW-trending folds, foliation itself does not define the turtleback antiform.

Discussion

Many workers explain similar antiforms in metamorphic core complexes as products of isostasy. By these models, unloading of the footwall by both erosion and continued slip on the fault causes the fault and footwall to rotate to shallower dips in the upper crust; below only a few km, the fault retains its initially steep angle (Buck, 1988; Hamilton, 1988; King and Ellis, 1990). With continued slip on the fault system, the increasingly lower angle sections of the fault become abandoned and are replaced by newer, high-angle sections (Fig. 5-5). Such rotation actually folds the fault and footwall under the same upper crustal conditions as the brittle faulting and may produce compressive stresses in the footwall that overprint, but are subparallel to the extension direction (Bartley et al., 1990).

A major difference between models which call on isostatic adjustments to rotate faults to lower angles is that some models call for a "rolling hinge" while others do not. In the rolling hinge model (Hamilton, 1988; Wernicke and Axen, 1987), the transition zone from the gently dipping, upper crustal fault, to the more steeply dipping shear zone below marks the "hinge" (Fig. 5-5). As extension progresses, the footwall migrates in the direction of transport and causes the hinge to roll forward. Behind the hinge, inactive parts of the fault system lie stranded at low angles. By contrast, King and Ellis (1990), recently concluded that localized uplift on the order of 10 km or more could cause isostatically induced rotation without migration of the footwall. Significantly, such uplift and rotation does not require large amounts of horizontal extension.

Holm et al. (1992) used argon geochronology to argue that the rolling hinge model applies to Death Valley. They found that, along their inferred "Black Mountains detachment", the southeastern Black Mountains had cooled below about 300°C before
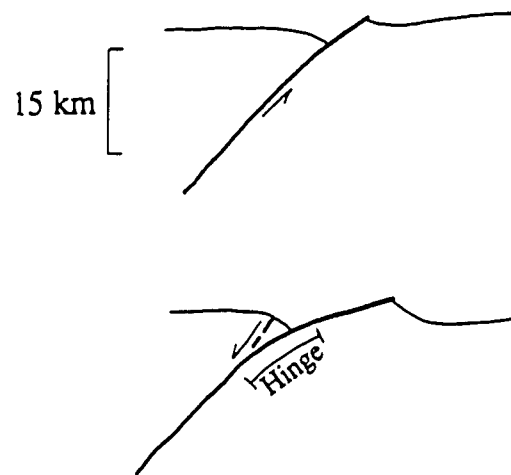
Figure 5-5. Rotation of initially high-angle fault to lower angles and subsequent replacement by a new high-angle fault using the isostatic models of Buck (1988) and King and Ellis (1990).

200 Ma, the Mormon Point area from 8.1 to 8.4 Ma, the Copper Canyon area from 6.7 to 7.0 Ma, and the Badwater Turtleback from 12.7 to 13.4 Ma. Well to the east of the inferred detachment fault, they found a 9.8 Ma biotite age in the Greenwater Range. Holm et al. (1992) suggested that, with the exception of the Badwater Turtleback, these ages indicate a northwest trend in progressively younger cooling ages. By their model, each age marks a different position of the 300°C isotherm in a single northwestwardly migrating footwall. They suggest that the Badwater Turtleback has anomalously old ages because it was initially at shallower crustal levels but was later dropped to lower levels along a splay of the detachment system.

A single detachment fault, which migrates northwestward according to the rolling hinge model, however, fails to explain the antiformal shape of all three turtlebacks. Such a migrating footwall should leave the remnants of the hinge only at the last site of activity; older, stranded sections of the detachment and underlying mylonites should be gently dipping and roughly planar. Because each turtleback exhibits the antiformal geometry, they must have evolved independently of each other, akin to the non-migrating model of King and Ellis (1990). Furthermore, the trend in the data presented by Holm et al. (1992) is tenuous at best. It relies on four points, one of which significantly predates Tertiary extension and another which conflicts with the trend. In fact, because the different ages cluster in different parts of the Black Mountains, the geochronology by Holm et al. (1992) supports the interpretation that the turtlebacks do not fit the rolling hinge model, but are instead separate systems.

Geometric evolution of Badwater turtleback

The isostatic flexure model of King and Ellis (1990) explains the antiformal shapes of the Badwater and other turtlebacks, but it fails to explain the later cross-

cutting planar faults which make up the presently observed Badwater Turtleback fault system. Miller (1991) suggested that these brittle fault surfaces rotated domino-style to their present low angles. Such rotation must have occurred after deposition of the 6.3 Ma volcanic rocks and therefore after the turtleback received its antiformal geometry. Because the fault systems at Mormon Point and Copper Canyon were also active during this time, all three probably acted in concert to rotate the fault surfaces, and their footwalls, to lower angles.

Figure 5-6 illustrates a general model for the geometric evolution of the Badwater Turtleback. It employs an early period of isostatically-induced rotation followed by a later period of predominantly domino-style rotation. This model uses the geochronology by Holm et al. (1992) but follows the suggestion by Wright et al. (1991) that different fault zones of the Black Mountains are distinct features rather than outcrops of the same detachment system.

At approximately 13 Ma, rocks of the Badwater Turtleback, in the footwall of fault #0, passed through the 300°C isotherm; shear zones at Mormon Point and Copper Canyon were probably not yet active, although Pavlis (1991) reported evidence for deformation during intrusion of the Willow Spring pluton at about 10.6 Ma. With continued slip on fault #0, these rocks were brought into the upper crust where they rotated to lower angles according to the model by King and Ellis (1990). By approximately 8 Ma and 7 Ma, the Mormon Point and Copper Canyon shear zones, respectively, had carried those footwall rocks through the 300°C isotherm, and were beginning to form their antiformal geometries. At 6.3 Ma or earlier, eruption of volcanic rocks onto the footwall of the Badwater Turtleback marked the cessation of this episode of slip on fault #0. Reactivation of fault #0 as fault #1, or the
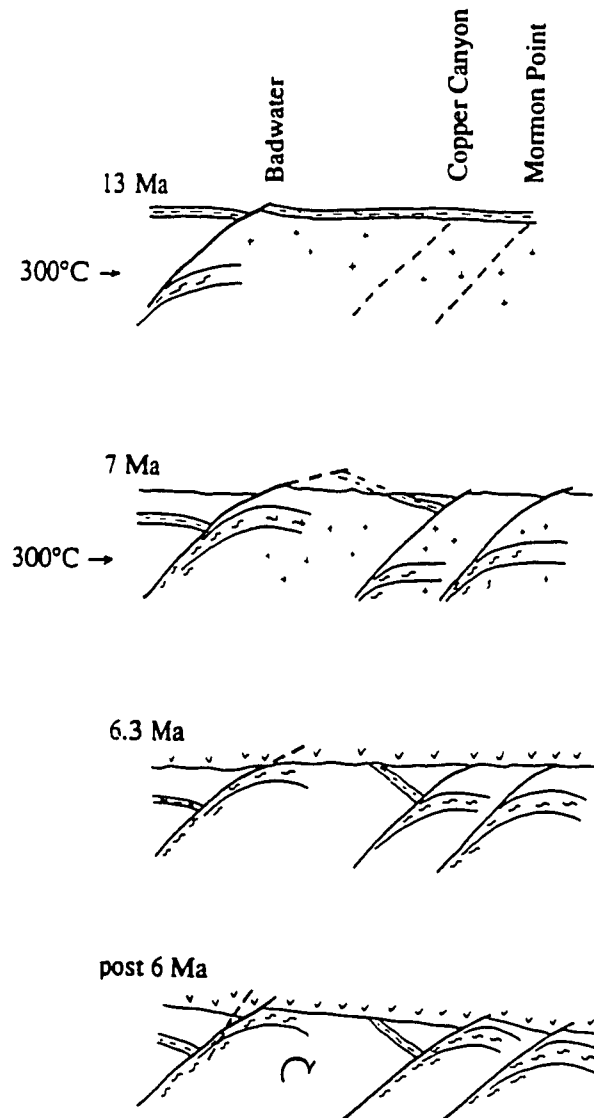
Figure 5-6. Generalized geometric evolution of the Badwater Turtleback and its relationship to the Copper Canyon and Mormon Point Turtlebacks. Fault #1 is drawn so that it reactivates fault #0. This model contains several simplifications for illustrative purposes only: top layer with dashed lines does not represent a specific unit but is drawn only to help illustrate the model; continuous lines in footwalls of each turtleback do not represent specific rocks but instead show approximate outlines of the turtleback shapes: Volcanic rocks are greatly simplified. Volcanism was concurrent with much of the extension in the Black Mountains so in many places significantly predates the 6.3 Ma age shown on this figure (Wright et al., 1991). Furthermore, the contact of the volcanic rocks with the turtlebacks is shown everywhere as depositional although it is faulted in many places.

development of fault #1 as an entirely new surface, accompanied by movement on the
fault systems at the Mormon Point and Copper Canyon turtlebacks, marked the onset
of domino-style rotation on the Badwater Turtleback. With continued extension, these
faults rotated to lower angles and were replaced by later, higher angle faults.

Conclusions

The antiformal geometry of footwall mylonites, bounded by a system of
planar, low-angle normal faults, suggests that the Badwater Turtleback experienced
two different modes of rotation. An early period of isostatically induced rotation
formed the turtleback antiform prior to significant uplift on the Copper Canyon and
Mormon Point turtlebacks farther south. A later period of domino-style faulting,
concurrent with slip on the other turtlebacks, formed the later planar faults and caused
them to rotate to low angles. Because all three turtlebacks exhibit antiformal
geometries and are cut by later, distinct planar faults, they are not part of the same
detachment system, but instead, separate features with similar geometrical histories.

These conclusions are in accord with arguments for localized extension within
the Black Mountains block; they conflict with arguments for large magnitudes of
regional extension along a single evolving detachment system. Future work which
emphasizes the nature of the earliest brittle faults on the three turtlebacks may help
clarify the transition from one mode of rotation to another.

REFERENCES

Applegate, J.D.R., Walker, J.D., and Hodges, K.V., 1992, Late Cretaceous extensional unroofing in the Funeral Mountains metamorphic core complex, California: Geology, v. 20, p. 519-522.

Asmerom, Y., Snow, J.K., Holm, D.K., Jacobsen, S.B., Wernicke, B.P., and Lux, D.R., 1990, Rapid uplift and crustal growth in extensional environments: An isotopic study from the Deaht Valley region, California: Geology, v. 18, p. 227-230.

Bartley, J.M., Fletcher, J.M., and Glazner, A.F., 1990, Tertiary extension and contraction of lower-plate rocks in the central Mojave metamorphic core complex, southern California: Tectonics, v. 9, p. 521-534.

Boyer, S.E., and Allison, M.L., 1987, Estimates of extension in the Basin and Range Province: Geological Society of America Abstracts with Programs, v. 19, p. 597.

Boyer, S.E., and Hossack, J.R., 1992, Structural features and emplacement of surficial gravity-slide sheets, northern Idaho-Wyoming thrust belt, in Link, P.K., Kuntz, M.A., and Platt, L.B., eds., Regional Geology of Eastern Idaho and Western Wyoming: Geological Society of America Memoir 179, p. 197-213.

Buck, W.R., 1988, Flexural rotation of normal faults: Tectonics, v. 7, p. 959-973.

Burchfiel, B.C., and Stewart, J.H., 1966, "Pull-apart" origin of the central segment of Death Valley, California: Geological Society of America Bulletin, v. 77, p. 439-442.

Byrnes, S., 1989, A reconnaissance study of brittle deformation along the frontal faults of the Black Mountains, Death Valley, California, M.S. thesis, University of New Orleans, 81p.

Cemen, I., Drake, R., and Wright, L.A., 1982, Stratigraphy and chronology of the Tertiary sedimentary and volcanic units at the southeastern end of the Funeral Mountains, Death Valley region, California, in J.D., Cooper, B.W. Troxel, and L.A. Wright, eds., Geology og selected aras in the San Bernardino Mountains, western Mojave Desert, and southern Great Basin, California, Geological Society of America Field trip guidebook and volume, Anaheim, California meeting, p. 77-88.

Cemen, I., Wright, L.A., Drake, R.E., and Johnson, F.C., Cenozoic sedimentation and sequence of deformational events at the southeastern end of the Furnace Creek strike-slip fault zone, Death Valley, California, in K.T. Biddle and N. Christie-Blick, eds., Society of Economic Paleontologists and Mineralogists Special Publication 37, 127-141, 1985.

Cichanski, M.A., Stratigraphy and structure of the upper plate of the Badwater Turtleback, Death Valley, California, University of Washington, Department of Geological Sciences Senior thesis, 23p., 1990.

Curry, H.D., 1938, "Turtleback" fault surfaces in Death Valley, California: Geological Society of America Bulletin, v. 49, p. 1875.

Curry, H.D., 1954, Turtlebacks in the central Black Mountains, Death Valley, California, in Jahns, R.H., ed., Geology of southern California: California Division of Mines Bulletin 170, chapter 4, p.53-59.

Davis, G.A., Parke, M., Bishop, K., Fowler,T.K., and Friedmann, S.J., 1991, Grand scale detachment and emplacement of gravity-driven slide sheets into a Miocene terrestrial basin, eastern Mojave Desert, California: Geological Society of America Abstracts with Programs, v. 23 p. 467.

Davis, G.H., 1980, Structural characteristics of metamorphic core complexes, southern Arizona, in Crittenen, M.D., Jr., Coney, P.J., and Davis, G.H., eds., Cordilleran metamorphic core complexes, Geological Society of America Memoir 153, p. 35-78.

Davis, G.H., 1983, Shear zone model for the origin of metamorphic core complexes: Geology, v. 11, p. 342-347.

Drewes, H., 1959, Turtleback faults of Death Valley, California, a reinterpretation: Geological Society of America Bulletin, v. 70, p. 1497-1508.

Drewes, H., 1963, Geology of the Funeral Peak Quadrangle, California, on the eastern flank of Death Valley: United States Geological Survey Professional Paper 413, 78p.

Ellis, M.A., and Trexler, J.H., 1991, Basin-margin development in pull-apart settings: An example from Death Valley, California: Geological Society of America Abstracts with Programs, v. 23, p. 82.

Evans, B., Fredrich, J.T., and Wong, T. -F., 1990, The brittle-ductile transition in rocks: American Geophysical Union Monograph 56, p. 1-20.

Fleck, R.J., 1970, Age and tectonic significance of volcanic rocks, Death Valley area, California: Geological Society of America Bulletin, v. 81, p. 2807-2816.

Goods, S.H., and Brown, L.M., 1979, The nucleation of cavities by plastic deformation: Acta Metallurgica, v. 27, p. 1-15.

Hamilton, W.D., 1988, Detachment faulting in the Death Valley region, California and Nevada: U.S. Geological Survey Bulletin 1790, p. 51-85.

Heard, H.C., 1960, Transition from brittle fracture to ductile flow in Sonhofen limestone as a function of temperature, confining pressure and interstitial fluid pressure, in D.T. Griggs and J. Handin, Rock Deformation: Geological Society of America Memoir 79, p. 193-226.

Hodges, K.V., Walker, J.D., and Wernicke, B.P., 1987, Footwall structural evolution of the Tucki Mountain detachment system, Death Valley region, southeastern California, in Coward, M.P., et al., eds., Continental extensional tectonics: London, Geological Society, p. 393-408.

Hodges, K.V., and Walker, J.D., 1990, Petrologic constraints on the unroofing history of the Funeral Mountains metamorphic core complex, California: Journal of Geophysical Research, v. 95, p. 8437-8445.

Holm, D.K., Snow, J.K., and Lux, D.R., 1992, Thermal and barometric constraints on the intrusive and unroofing history of the Black Mountains: Implications for timing, initial dip, and kinematics of detachment faulting in the Death Valley region, California: Tectonics, v. 11, p. 507-522.

Holm, D.K., and Wernicke, B.P., 1990, Black Mountains crustal section, Death Valley extended terrain, California: Geology, v. 18, p. 520-523.

Hunt C.B., and Mabey, D.R., 1966, Stratigraphy and structure, Death Valley, California: U.S. Geological Survey Professional Paper 494-A, 165 p.

Jackson, J.A., and White, N.J., 1989, Normal faulting in the upper continental crust: observations from regions of active extension: Journal of Structural Geology, v. 11, p. 15-36.

Johnson, R.A., and Loy, K.L., 1992, Seismic reflection evidence of seismogenic low-angle faulting in southeastern Arizona: Geology, v. 20, p. 596-600.

Keener, C., Serpa, L.F., and Pavlis, T.L., 1990, Late Cenozoic faultingf at Mormon Point Turtleback, Death Valley, California (Abs.); Geol. Soc. America Abs. with Programs, v. 22, p. 34.

King, G., and Ellis, M., 1990, The origin of large local uplift in extensional regions: Nature, v. 348, p. 689-693.

Lister, G.S. and Davis, G.A., 1989, The origin of metamorphic core complexes and detachment faults formed during Tertiary continental extension in the northern Colorado River region, U.S.A.: Journal of Structural Geology, v. 11, p. 65-94.

Miller, E.L., Gans, P.B., and Garling, J., 1983, The Snake Range decollement: An exumed mid-Tertiary brittle-ductile transition: Tectonics, v. 2, p. 239-263.

Miller, M.G., 1990, The Badwater Turtleback fault, Black Mountains, Death Valley, CA: Its geometry and lower plate deformation (Abs.): Geol. Soc. America Abs. with Programs, v. 22, p. 68-69.

Miller, M.G., 1991a, Field evidence for syntectonic intrusive origin of mylonitic rocks in the footwall of a metamorphic core complex, Badwater Turtleback, Death Valley, CA: Geological Society of America Abstracts with Programs, v. 23, p. 189.

Miller, M.G., 1991b, High-angle origin of the currently low-angle Badwater Turtleback fault, Death Valley, California: Geology, v. 19, p. 372-375.

Miller, M.G., 1992, Brittle faulting induced by ductile deformation of a rheologically stratified rock sequence, Badwater Turtleback, Death Valley, California: Geological Society of America Bulletin, v. 104, p. 1376-1385.

Moores, E.M., 1966, Mio-Pliocene sediments, gravity slides, and their tectonic significance, east-central Nevada: Geological Society of America Bulletin, v. 77, p. 88-98.

Otton, J.K., 1976, Geologic features of the central Black Mountains, California, *in* B.W. Troxel and L.A. Wright, eds., Geologic features of Death Valley, California Division of Mines and Geology Special Report 106, p. 27-33.

Otton, J.K., 1977, Geology of the central Black Mountains, Death Valley, California: The turtleback terrane, Ph.D. dissertation, Pennsylvania State University, University Park, 155p.

Pavlis, T.L., 1991, Exposures of the floor of a Miocene, syn-tectonic pluton, Death Valley, California: The turtleback terrane: Geological Society of America Abstracts with Programs, v. 23, p. 189.

Pavlis, T.L., Serpa, L.F., and Keener, C., in press, Role of seismogenic processes in fault rock development at Mormon Point Turtleback, Death Valley, California: Geology.

Ramsay, J.G., and Huber, M.I.,1983, The Techniques of Modern Structural Geology, Volume 1, Strain Analysis. Academic Press, New York, 307p.

Rehrig, W.A., and Reynolds, S.J., 1980, Geologic and geochronologic reconnaissance of a northwest-trending zone of metamorphic core complexes in southern Arizona, *in* Crittenen, M.D., Jr., Coney, P.J., and Davis, G.H., eds., Cordilleran metamorphic core complexes, Geological Society of America Memoir 153, p. 131-158.

Reynolds, M.W., 1969, Stratigraphy and structural geology of the Titus and Titanothere Canyons area, Death Valley, California, Ph.D. dissertation, Berkeley, University of California, 310p.

Scholz, C.H., 1988, The brittle-plastic transition and the depth of seismic faulting: Geologische Rundschau, v. 77, p. 319-328.

Sibson, R.H., 1977, Fault rocks and fault mechanisms: Geological Society of London Journal, v. 133, p. 191-213.

Simpson, C., and DePaor, D.G., in press, Strain and kinematic analysis in general shear zones: Journal of Structural Geology.

Smith, D.L., 1992, History and kinematics of Cenozoic extension in the northern Toiyabe Range, Lander County, Nevada: Geological Society of America Bulletin, v. 104, p. 789-801.

Stewart, J.H., 1983, Extensional tectonics in the Death Valley area, California: Transport of the Panamint Range structural block 80 km northwestward: Geology, v. 11, p. 153-157.

Struthers, J., 1990, Evidence for right-lateral oblique slip on the Black Mountains range front: Desolation Canyon, Death Valley, California, Department of Geological Sciences senior thesis, University of Washington, 24p.

Suppe, J., 1985, Principles of Structural Geology. Prentice-Hall, Englewood Cliffs, New Jersey, 537 p.

Topping, D.J., 1990, Large landslides and Miocene extension in the Amargosa Chaos Basin, soiuthern Death Valley, California: EOS, v. 71, p. 1612.

Tullis, J., and Yund, R.A., 1985, Dynamic recrystallization of feldspar: A mechanism for ductile shear zone formation: Geology, v. 13, p. 238-241.

Tullis, J., Snoke, A.W., and Todd, V.R., 1982, Significance and petrogenesis of mylonitic rocks: Geology, v. 10, p. 227-230.

Turner, F.J., and Weiss, L.E., 1963, Structural Analysis of Metamorphic Tectonites. McGraw-Hill, New York, 545 p.

Wernicke, B., 1981, Low-angle normal faults in the Basin and Range Province-- Nappe tectonics in an extending orogen: Nature, v. 291, p. 645-648.

Wenicke, B.P. and Axen, G.J., 1988, On the role of isostasy in the evolution of normal fault systems: Geology, v. 16, p. 858-861.

Wernicke, B.P. Axen, G.J., and Snow, J.K., 1988, Basin and Range extensional tectonics at the latitude of Las Vegas, Nevada: Geol. Soc. America Bull., v. 100, p. 1738-1757.

Whitney, D.L., Hirschmann, M., and Miller, M.G., in press, Zincian ilmenite from a pelitic schist, Death Valley, California: Canadian Mineralogist.

Wills, C.J., 1989, A neotectonic tour of the Death Valley fault zone: California Geology, v. 42, p. 195-200.

Wright, L.A., 1989, Overview of the role of strike-slip and normal faulting in the Neogene history of the region northeast of Death Valley, California--Nevada: in Late Cenozoic evolution of the Southern Great Basin, Open File 89-1, edited by M. Ellis, p. 1-12.

Wright, L.A., Otten, J., and Troxel, B.W., 1974, Turtleback surfaces of Death Valley viewed as phenomena of extension: Geology, v. 2, p. 53-54.

Wright, L.A., Serpa, L., and Troxel, B.W., 1987, Tectono-chronologic model for wrench fault related crustal extension, Death Valley area, California: Geological Society of America Abstracts with Programs, v. 19, p. 898-899.

Wright, L.A., and Troxel, B.W., 1973, Shallow-fault interpretation of Basin and Range structure, southwestern Great Basin, in de Jong, K.A., and Scholten, R., eds., Gravity and Tectonics: New York, John Wiley and Sons, p. 397-407.

Wright, L.A., and Troxel, B.W., 1984, Geology of the North 1/2 Confidence Hills 15' Quadrangle, Inyo County, California, scale 1:24,000, California Division of Mines and Geology, Map Sheet 34, 31 p.

Wright, L.A., Troxel, B.W., Burchfiel, B.C., Chapman, R., and Labotka, T., 1981, Geologic cross section from the Sierra Nevada to the Las Vegas Valley, eastern California to southern Nevada: Geol. Soc. America Map and Chart Series MC-28M.

Wright, L.A., Thompson, R.A., Troxel, B.W., Pavlis, T.L., DeWitt, E.H., Otton, J.K., Ellis, M.A., Miller, M.G., and Serpa, L.F., 1991, in press, Cenozoic Magmatic and tectonic evolution of the east-central Death Valley region, California: paper and field guide for GSA field trip, San Diego, CA.

Yarnold, J.C., and Lombard, J.P., 1989, A facies model for large rock-avalanche deposits formed in dry climates: in I.P. Colburn, P.L., Abbott, and J. Minch, eds., Conglomerates in basin analysis: A symposium dedicated to A.O. Woodford: Pacific Section, Society of Economic Paleontologists and Mineralogists, v 62, p. 9-31.

VITA

Martin Gregg Miller
Born January 19, 1960, Cincinnati, Ohio
Married Julie Margaret Bryant August 2, 1986

BA Colorado College, Geology, June, 1982.

M.S. University of Washington, Geological Sciences, June, 1987.
  Thesis: Deformation near Lillooet, British Columbia: Implications for the slip history of the Yalakom fault.

Ph.D. University of Washington, Geological Sciences, December, 1992.
  Dissertation: Structural and kinematic evolution of the Badwater Turtleback fault, Death Valley, California.